

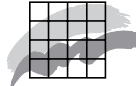


National Environmental Research Institute
University of Aarhus · Denmark

Research Notes from NERI No. 240, 2007

Impacts of Climate Change on Air Pollution Levels in the Northern Hemisphere

[Blank page]



National Environmental Research Institute
University of Aarhus · Denmark

Research Notes from NERI No. 240, 2007

Impacts of Climate Change on Air Pollution Levels in the Northern Hemisphere

Gitte Hedegaard Brandt

Data sheet

Series title and no.:	Research Notes from NERI No. 240
Title:	Impacts of Climate Change on Air Pollution Levels in the Northern Hemisphere
Author:	Gitte Brandt Hedegaard
Department:	Department of Atmospheric Environment
Publisher:	National Environmental Research Institute © University of Aarhus - Denmark
URL:	http://www.neri.dk
Year of publication:	August 2007
Referee:	Jørgen Brandt
Financial support:	No external financial support
Please cite as:	Hedegaard, G. B. 2007: Impacts of Climate Change on Air pollution levels in the northern hemisphere. National Environmental Research Institute, University of Aarhus. Denmark 103pp. – Research Notes from NERI No. 240 http://www.dmu.dk/Pub/AR240.pdf
	Reproduction permitted provided the source is explicitly acknowledged
Abstract:	<p>The fate of a selected number of chemical species is inspected with respect to climate change. The coupled Atmosphere-Ocean General Circulation Model ECHAM4-OPYC3 is providing future meteorology for the Chemical long-range Transport Model DEHM-REGINA. Three selected periods (1990s, 2040s and 2090s) are inspected. The 1990s are used as a control and validation period. In this decade the model results are tested against similar model simulations with MM5 meteorology and against observation from the EMEP monitoring sites in Europe. In the validation the emissions are held constant at the 1990 level in all simulations in order to separate out the effects from climate change. The overall performance of the ECHAM4-OPYC3 setup as meteorological input to the DEHM-REGINA model is acceptable according to the ranking method. It is concluded that running a chemical long-range transport model on data from a "free run" climate model is scientifically sound!</p> <p>The absolute dominating impact from climate change on a large number of chemical species is found to be the predicted temperature increase. The temperature is by the ECHAM4-OPYC3 model predicted to increase 2-3 Kelvin on a global average with local maxima in the Arctic of 11 Kelvin. As a consequence of this temperature increase, the temperature dependent biogenic emission of isoprene is predicted to increase significantly in concentration over land in the DEHM-REGINA chemistry-transport model. This leads to an increase in the ozone production and in the number of free OH radicals. This again leads to a significant change in the typical life times of many species, since the hydroxyl radicals are participating in a large number of chemical reactions. It is e.g. found that more sulphate will be present in the future over the already polluted areas and this increase can be explained by an enhancement in the conversion of sulphur to sulphate.</p>
Keywords:	Climate change, Air quality, Biogenic VOC emissions, Isoprene, Temperature change
Layout:	Gitte Brandt Hedegaard
ISSN (electronic):	1399-9346
Number of pages:	103
Internet version:	The report is available in electronic format (pdf) at NERI's website http://www.dmu.dk/Pub/AR240.pdf
Supplementary notes:	This report was originally submitted as a Master Thesis.

Contents

Abstract 5

Sammenfatning 6

Introduction 8

- 1.1 Objectives of this study 8
- 1.2 Structure of this thesis 8

2 Climate and air pollution modelling 9

- 2.1 Modelling the climate system 9
- 2.2 Modelling the transport and chemistry of the atmosphere 9
- 2.3 State of the art in combined air pollution and climate modelling 9

3 Model descriptions 10

- 3.1 The atmosphere-ocean general circulation model, ECHAM4-OPYC3 10
- 3.2 The chemical transport model, DEHM-REGINA 10

4 Experimental design 11

- 4.1 Meteorological parameters and modifications 11
- 4.2 Temporal and spatial interpolations 11

5 Validation of the experimental method for the period 1990-1999 12

- 5.1 Statistical methodology 12
- 5.2 Validation results for the control period 1990-1999 12
- 5.3 Ranking results 12
- 5.4 t-test results for the validation period 1990-1999 12
- 5.5 t-test results for the period 1990-1999, 2040-2049 and 2090-2099 12
- 5.6 Summary and discussion 12

6 Results and discussion 13

- 6.1 Changes in meteorology calculated by the ECHAM4-OPYC3 13
- 6.2 Changes in air pollution levels calculated by DEHM-REGINA 13
- 6.3 Summary and discussion 13

7 Summary, conclusions and future perspectives 14

- 7.1 Summary and conclusions 14
- 7.2 future and conclusions 14

8 Acknowledgement 15

National Environmental Research Institute

Abstract

The fate of a selected number of chemical species is inspected with respect to climate change. The coupled Atmosphere-Ocean General Circulation Model ECHAM4-OPYC3 is providing future meteorology for the Chemical long-range Transport Model DEHM-REGINA. In order to separate out the effect from climate change the anthropogenic emissions are held constant at 1990 level in all simulations with exception of the validation simulations. Three selected periods (1990's, 2040's and 2090's) are inspected.

The 1990's is used as a control and validation period. In this decade an evaluation of the output from the DEHM-REGINA model with ECHAM4-OPYC3 meteorology input data is carried out. The model results are tested against similar model simulations with MM5 meteorology and against observation from the EMEP monitoring sites in Europe.

The test results from the control period show that the overall mean values and standard deviations are similar for the two simulations, however the model setup with climate input data fails to predict correctly with respect to the timing of the variability in the data as expected. The overall performance of the ECHAM4-OPY3 setup as meteorological input to the DEHM-REGINA model is acceptable according to the ranking method. It is concluded that running a chemical long-range transport model on data from a "free run" climate model is scientifically sound!

From the model runs for the three decades, it is found that the trend detected in the evolution of the chemical species, is the same between the 1990 decade and the 2040 decade and between the 2040 decade and the 2090 decade, respectively.

The absolute dominating impact from climate change on a large number of chemical species, is found to be the predicted temperature increase. The temperature is by the ECHAM4-OPYC3 model predicted to increase 2-3 Kelvin on a global average with local maxima in the Arctic of 11 Kelvin. As a consequence of this temperature increase, the temperature dependent biogenic emission of isoprene is predicted to increase significantly in concentration over land in the DEHM-REGINA chemistry-transport model. This leads to an increase in the ozone production and in the number of free *OH* radicals.

This again leads to a significant change in the typical life times of many species, since the hydroxyl radicals participating in a large number of chemical reactions. It is e.g. found that more sulphate will be present in the future over the already polluted areas and this increase can be explained by an enhancement in the conversion of sulphur to sulphate.

Sammenfatning

I denne rapport er fordelingen og niveauerne i atmosfæren for nogle udvalgte kemiske stoffer studeret under et fremtidigt ændret klima. Der er anvendt en koblet atmosfære-ocean generel cirkulationsmodel (ECHAM4-OPYC3) til at simulere en fremtidig meteorologisk situation for det 21. århundrede. Dette meteorologiscenarium er dernæst brugt som input til DMU's kemiske transport model DEHM-REGINA, udviklet ved Afdeling for Atmosfærisk Miljø. Ændringer i atmosfærens kemiske sammensætning blev studeret repræsenterende tre udvalgte perioder (1990'erne, 2040'erne og 2090'erne). I disse simuleringer er de menneskeskabte emissioner fastholdt på et konstant 1990-niveau for at udskille og dernæst studere effekten af et ændret klima, hvorved 1990'erne blev brugt som kontrolperiode for modelsystemet.

Modelresultaterne er dels testet mod korresponderende simuleringer baseret på input fra meteorologimodellen MM5 og dels mod observationer fra det europæiske EMEP målenetværk. Testresultaterne viser, at de to måder at modellere på er lige gode med hensyn til forudsigelser af de generelle middelværdier og standard afvigelser ved sammenligning mellem målinger og modelforudsigelser. Konklusionen er, at det er videnskabeligt forsvarligt at køre en kemisk transportmodel (som DEHM-REGINA) baseret på meteorologidata fra en "fri" kørsel af en klimamodel.

Den globale middeltemperatur i det 21. århundrede er forudsagt til at stige 3 °C i følge ECHAM4-OPYC3 simuleringerne af klimaets udvikling. Denne temperaturstigning har vist sig at spille en dominerende rolle med hensyn til effekter fra et ændret klima på luftforureningen. Som en konsekvens af temperaturstigning øges de stærkt temperaturafhængige naturlige emissioner af isopren betydeligt over land. Dette fører til en øget produktion af ozon og frie hydroxyl radikaler, som igen vil øge den kemiske produktionsrate. For eksempel indikerer disse modelstudier, at der vil være mere sulfat tilstede i en fremtidig atmosfære over de områder, som allerede er forurenede af svovldioxid og sulfat. Ændringen kan forklare med en øget omdannelse af svovldioxid til sulfat pga. tilstedeværelsen af flere hydroxyl radikaler.

Rapporten er baseret på et specialestudie udarbejdet i 2006 i samarbejde med Københavns Universitet, Danmarks Meteorologiske Institut og Danmarks Miljøundersøgelser.

1 Introduction

Within the latest decade there has been a growing interest in the effects of climate change on the future air pollution levels. It is well known that the composition of the atmosphere will change due to changes in anthropogenic emissions. From climate modelling studies it is predicted that some meteorological parameters will change in the future both due to the natural variability and due to the man-made changes of the composition of the atmosphere. A general temperature increase is expected in the future [Houghton, 2001]. This temperature increase will effect many if not all other meteorological parameters and since the distribution of air pollution is highly dependent on the meteorology, it could be hypothesized, that the air pollution levels and distribution even with unchanged emissions will be changed in a warmer climate. To estimate how and how much the climatic effect alone will have on the air pollution in the future requires computer models. These climate effects are especially very computer demanding to study, if one wishes to include as many meteorological and chemical processes as possible.

Until now, a great number of sensitivity studies of the effect from specific meteorological parameters on air pollution distribution has been carried out (see e.g. Zlatev and Brandt [2005]). In these studies for example the temperature alone has been altered to suit different temperature scenarios. Sensitivity studies makes it possible to get at rough overview of, which and how large the effect of a specific meteorological parameter will have on the air pollution in the future. However, to include all effects of a changing climate much more complicated modelling tools are needed.

In this thesis the hemispheric chemical long-range transport model DEHM-REGINA (Danish Eulerian Hemispheric Model - REGIONal high resolutioN Air pollution model) is used to investigate the future air pollution levels and distribution in the northern hemisphere with special emphasis on Europe and Arctics. The coupled Atmosphere-Ocean General Circulation Model ECHAM4-OPYC3 is providing 21'st century meteorology and part of the 20'th century based on the IPCC SRES A2 scenario [Nakicenovic et al., 2000] every 6 hour as input to the chemical long-range transport model DEHM-REGINA. In order to save computing time the experiment is focused on three decades instead of simulating the 21'st century in one continuous run. The three periods are; 1990-1999, 2040-2049 and 2090-2099. In order to test the validity of the methods and to produce results, five simulations have been made (cf table 5.1). The first two of these are used to test the scientific foundation of this experiments: One simulation is based on MM5 [Grell et al., 1995] meteorology and one simulation is based on ECHAM4-OPYC3 [Stendel et al., 2002] meteorology. Both simulations are carried out for the period 1990-1999 and is forced with the real emissions for this period. The basic idea behind these two simulations is to test the model results against measurements of air pollution in the 1990's. If the overall mean values and other statistics are similar for the two simulations, it

can be concluded that running a chemical long-range transport model on data from a "free run" climate model is scientifically sound!

After this evaluation three simulations with constant 1990 emissions are made in order to separate out the effects on air pollution from climate change only. The meteorology in these three simulations are all based on ECHAM4-OPYC3 and the time periods are the 1990's, the 2040's and the 2090's, which are assumed to represent the changes in the 21'st century.

1.1 Objectives of this study

"A changed future climate will have an impact on future levels and distribution of air pollution concentrations and depositions of chemical species in the northern hemisphere". This is the main hypothesis of this thesis. To test this hypothesis several questions have to be answered first.

There are two main steps in this experiment. First of all the following hypothesis is assumed: "The Atmosphere-Ocean General Circulation Model ECHAM4-OPYC3 is able to provide a realistic and consistent picture of the meteorological key parameters applied in the air pollution model". On the basis of this assumption the first step in this investigation is to justify that it does make sense to drive an air pollution model with data from a "free run" climate model. From knowledge of the air pollution chemistry and climate change it should be identified, which meteorological parameters are changing with a changed climate and furthermore which of these will effect the pollution levels and distribution in the future.

Nearly all processes involved in the chemical composition of the atmosphere are dependent on the weather and thereby also on climate change. Atmospheric transport and transport patterns including the horizontal and vertical mixing is directly determined by the different weather parameters as e.g. wind, convection, mixing properties in the ABL, solar radiation, temperature, and heat fluxes, etc. The atmospheric chemical reactions and photolysis rates are determined e.g. by the humidity, global radiation as function of the cloud cover and type, temperature, albedo, etc. Furthermore, the precipitation frequency and amount and the surface properties have great influence on the wet and dry deposition levels. At last there are several parameters that have a large influence on the emissions, as e.g. the temperature dependence of natural emissions of volatile organic compounds (VOC's) and the temperature dependence of anthropogenic emissions from domestic heating, power consumption, etc. Natural emissions of NO_x also depends on the weather, e.g. from lightning or from soil.

Some air pollution parameters will presumably be more suitable as a basis for testing the impacts from climate change on air pollution and these should be identified before moving on to the next step in this experiment.

After the methods and performance of the model setup has been validated we continue with the second step in this experiment. Since the chemical long-range transport model DEHM-REGINA used in this experiment includes the chemistry of 63 chemical species, there is a great amount of data to analyze from the output of these simulations. To investigate all chemical species and all their ancillary processes is far beyond the scope of this thesis. Therefore eight important chemical species is chosen and analyzed with respect to the key meteorological parameters. Interesting questions raised in this connection is; "What impact do the projected temperature increase have on the air pollution levels?", "What is the impact of changing

precipitation levels and frequencies on the air pollution concentrations and depositions?" etc....

The number of specific hypotheses that can be tested and questions that can be answered using the single-way coupled GCM-CTM model system setup in this thesis is huge. Many of these specific hypotheses can only be answered by running the chemistry-transport model DEHM-REGINA a large number of times to do scenario- or sensitivity studies. The main objectives of this thesis is therefore limited to test the following two hypothesis:

"A changed future climate will have an impact on future levels and distribution of air pollution concentrations and depositions of chemical species in the northern hemisphere"

"The Atmosphere-Ocean General Circulation Model ECHAM4-OPYC3 is able to provide a realistic and consistent picture of the meteorological key parameters applied in the air pollution model"

and finally the objective:

"to identify some of the most important processes involved in the impacts from global change on air pollution levels and distribution "

1.2 Structure of this thesis

A short introduction to the climate system and chemical transport modelling followed by a state of the art within the combined field of climate and air pollution modelling is summarized in chapter 2. This is followed by a description of the models used in this work (Chapter 3) and a description of the EMEP monitoring network (Chapter 3), which the results in this analysis is evaluated against. In chapter 4 the method of coupling the models is documented. Finally the validation of the method (chapter 5) and the results and discussion of the fate of the selected species is provided in chapter 6. The conclusions and suggestions to future work is summarized in chapter 7.

2 Climate and air pollution modelling

In order to construct the results of this thesis, data from both a global climate model and data from a long-range chemical transport model has been used. In the following two sections, a short introduction to these two modelling areas will be given. The numerical methods used in these two modelling fields and the physical parametrization of the two model types are different because of the difference in scale in time and motion of the parameters. The numerical methods and the physical parameterizations have to be relatively simple in a global climate model compared to a chemical transport model since a climate model has to run relatively fast on the computer while maintaining a description of all the important processes going on in the atmosphere, ocean and cryosphere. On the other hand the numerical methods in an air pollution model need to be quite comprehensive in order to resolve the very sharp gradients both in time and space of the concentrations of the chemical species. In comparison a climate model cannot account for that many details, if its purpose is to predict climate. Because of limited computer capacity and limited knowledge of some of the physical processes going on in the climate, parameterizations are needed. Finally there is the chemistry module, which for the same reasons mentioned above is kept simple (if not non-existent) in a climate model and of course is rather sophisticated in a chemical transport model. Also the resolution of the two types of models differs in general. The resolution both in time and space is usually lower in a climate model compared to a chemical transport model due to computer capacity.

2.1 Modelling the climate system

The climate system is a very complicated system, which not only depends on several spheres but also on their mutual interactions. For example the oceans of the world play just as an important role as the atmosphere in the total climate system. The cryosphere, biosphere and geosphere are other examples of semi-closed systems, which together with the atmosphere and hydrosphere contribute to defining the climate system of the earth. An example of the interactions between spheres could be the heat exchange between air and water. Warm sea water will naturally warm up the above lying air when an air mass passes over the sea surface. Also the evaporation of the warm sea water into the colder air is an example of an exchange process. The sensible and latent heat flux is only some of the processes working as exchange processes in the climate system.

Basically the dynamics of the earth is driven by the uneven distribution of incoming solar radiation. This means that the atmosphere and surface of the earth receive an uneven amount

of energy at different places. This energy gives rise to transport of heat from the equator to the poles and during this energy transport exchange processes between air masses, water masses and the land surface takes place. Heat exchange will trigger chemical processes, which leads to a change in the chemical composition of the involved air or water. This can give rise to other more physical effects, such as changed greenhouse effect or changed albedo. Also a changed chemical composition can lead to changes in the various ecosystems of the earth and again these changes can feedback on the chemistry and climate. Photochemical reactions are another type of chemistry going on in the climate system. The ultraviolet radiation interacts with the chemical compounds in the climate system. This again gives rise to a change in the chemical composition of the atmosphere and so on.... As I have tried to illustrate above there are many complicated processes going on in the climate system. In attempting to model all these processes one have to keep in mind that the scale of time and motion of all these processes are highly variable. A climate model has to take into account both the synoptic scale weather pattern systems and the microphysics of the clouds. At the same time it has to account for example for both the millennium-scale Thermohaline Circulation (TC) in the ocean and the chemical reactions going on in the ozone budget.

It is well known that the climate interact on a global scale, which means that a climate model also has to be a global model - a model covering the entire earth geographically.

These above mentioned demands to a climate model are impossible to fulfil simultaneously. First of all, the computer capacity today is still not large enough to run a complete model of the climate system in a reasonable period of time. Secondly science cannot yet describe all physical and chemical processes correctly. Even though scientists today are able to describe many advanced processes in great detail, it doesn't necessarily mean that it is possible to model the processes. Many processes are described by continuous functions, which need to be discretized in order to solve the equations. Also the often relatively low resolution of a climate model introduces sub-grid-scale phenomena which needs to be approximated by parameterizations. This means that when trying to model the climate system a lot of assumptions and approximations are made, which inevitably will be followed by uncertainties in the model results.

Today a large variety of climate models are used to study the different issues of the climate system. The types of climate model varies from the very simple zero dimensional radiative balancing models to the quite complicated general circulations model. The type of model chosen do not only depend on the available computer capacity, it is rather a dependency of, which kind of climatic issue one wants to study. For example simple models are used to study specific processes of the atmosphere. Simple models have the advantage of keeping the demands to computer capacity down and thereby having a relatively short simulation time. This feature makes them an excellent tool when one wishes to simulate very long periods of time. The simple models are also useful, when one wishes to study the effect of a particular process in the atmosphere, since the number of included processes are limited in a simple model and therefore makes it possible to isolate the individual effects. On the contrary the three dimensional general circulation models are very useful when one wishes to study the full climate system, however the high computing time of such a comprehensive model limits the study period to usually one or a couple of centuries.

In this thesis a general atmosphere-ocean circulation model is used. The development of these models originates from the numerical weather prediction models, which were introduced in the 1920's by Richardson [1922] [Trenberth, 1992]. The first development of what today is

called a general circulation *climate* model was introduced during the 1950's by e.g. Charney et al. [1950] and Smagorinsky et al. [1965] [McGuffie and Henderson-Sellers, 2001]. During the 1980's the climate modelling field expanded significantly and e.g. Manabe and Wetherald can be mentioned as some of scientists in the front of the climate modelling community during the 1980's and 1990's [McGuffie and Henderson-Sellers, 2001]. Because of the high dependency of computer capacity, the field of climate modelling have closely followed the development of computers through the last five decades [McGuffie and Henderson-Sellers, 2001].

Today a wide range of coupled climate general circulation models exist and on a regular basis model intercomparison projects are carried out. In the intercomparison projects both the performance and the results of the models are evaluated. The Coupled Model Intercomparison Project (CMIP) is an example of a project where the results of up to 20 coupled climate model are compared [Meehl et al., 2000], [Lambert and Boer, 2001]. The CMIP project was split into two subprojects where the ability of the models to simulate the current climate and ability of the models to react to a specific external suppressed forcing (e.g. a 1% per year CO_2 increase) were tested. Also the Intergovernmental Panel on Climate Change (IPCC) have included chapters on model evaluation in each of its reports. Latest in the 2001 report the intercomparison results of up to 34 different models are compared (for a full list of the compared models see p. 478 Houghton [2001]). One of these models is the ECHAM4-OPYC3 model (used in the work of this thesis) from which it e.g. is concluded that the model simulates the trend of global warming of the 20'st century quite well [Houghton, 2001].

2.2 Modelling the transport and chemistry of the atmosphere

In the atmosphere a great number of physical and chemical processes takes place. If one wishes to study the air pollution levels and distribution in the atmosphere, a very comprehensive model is needed. The concentration levels and distributions of chemical species like gases, liquids and particles are dependent on transport, deposition, emissions, chemical reactions and photochemistry in the atmosphere. This means that in order to describe the fate of only one single chemical specie a large number of chemical reactions need to be calculated and at the same time the transport and deposition, which are highly dependent on meteorology and concentration of the respective species need to be derived. This means the prediction of one single specie demands the derivation of the weather in the domain of interest and the concentration of several interacting exchange species. From this, it is clear that to set up models which purpose is to describe the fate of maybe ten species, quickly ends up including a very large number of chemical species and reactions.

In the field of atmosphere chemistry modelling different types of models are represented. The most advanced models present today are the regional Eulerian full three dimensional chemistry transport models. The full three dimensional models give the most realistic presentation of the transport of chemical species and they are able to simulate a full concentration field of the included chemical compounds [Seinfeld and Pandis, 1998]. There are two types atmospheric transport models; Eulerian and Lagrangian models. However, today almost all three dimensional chemical transport models are based on the Eulerian approach.

The advances of the regional three dimensional Eulerian models is that they can provide relatively high resolution data over a limited area (e.g. Europe), however they demand suitable boundary conditions. The regional models have an typical horizontal resolution of 10-50 km

and is integrated in time over periods from a few days and up to a few years. The regional models are also used to make air pollution forecasts or to study the fate of chemical compounds under a specific meteorological event.

Unfortunately, the demands to computing capacity and the computing time increases with increased complexity and resolution of a given model and therefore also simpler chemical models have been developed. The simplest chemical models are the so-called zero dimensional box models, where the concentration is constant in space and therefore only depend on time. These models are suitable for studying very complex chemical systems or for studying chemical systems where equilibrium is achieved on times scales much shorter than those for transport [Brasseur and Madronich, 1992]. In between the zero dimensional and the three dimensional models also one and two dimensional models exist. They are mainly used for sensitivity studies, simulations over very long time periods or e.g. latitude-altitude distribution studies (uniform distribution along the latitudes are assumed) [Seinfeld and Pandis, 1998], [Brasseur and Madronich, 1992].

Presently, the state of the art within regional air pollution modelling in Europe can be divided into two main categories of models: The first type is the full three-dimensional Eulerian chemistry transport models covering domains from Europe to the northern hemisphere. These models include comprehensive descriptions of all involved chemical/physical processes and includes 50-80 chemical species. The models typically runs with a resolution of 10-50 km and includes approximately 20 vertical levels. Examples of these models are the EMEP model in Norway [<http://www.emep.int>, 2006], the MATCH model in Sweden [Andersson et al., 2006], the Polair3D in France [Mallet and Sportisse, 2004] and the EURAD model in Germany [Ebel et al., 2001]. The DEHM-REGINA model used in this thesis work also belongs to this class of models.

The second type of models, which are widely used is a little bit more simple version of the 3D Eulerian chemistry transport model. These models are different first and foremost in the vertical discretization, where typically three layers are included and not the 20 layers like in the 3D comprehensive models described above. The vertical exchange is here parameterized quite simple into a mixed layer, a reservoir layer and a free troposphere layer. Typically the chemical scheme is based on the CBM-IV scheme where the number of chemical species is around 35. Also processes like deposition and emissions are more simple parameterized in these models. The advantage is much lower computing time. The disadvantage is of course the less good performance of the models compared to measurements. Examples of the more simple Eulerian models are the REM3 model in Germany [Stern et al., 2003], the LOTOS-EUROS model in the Netherlands [Schaap et al., 2005], the CHIMERE model in France [Schmidt et al., 2001] and the DEOM model in Denmark [Brandt et al., 2001a], [Brandt et al., 2001b]. All the mentioned models are only examples and there exists, of course, many more models in the world.

Also intercomparisons projects has been performed within the field of chemical transport modelling. For example as part of the European Tracer EXperiment (ETEX) carried out in 1994, the performance of 28 models were compared based on the data obtained during the experiment [Mosca et al., 1997]. In this intercomparison project the DREAM model developed at National Environmental Research Institute (NERI) participated [Brandt, 1998]. Another example is the intercomparison of five ozone forecast system based on German monitoring data from the summer of 1999 [Tilmes et al., 2002]. Here the performance of the DEOM model also developed at NERI was evaluated against other models [Brandt et al., 2001a],

[Brandt et al., 2001b]. The DEHM-REGINA model has roots in both the DREAM and the DEOM models. Most recently the long-term prediction of ozone simulated with seven regional models has been compared [van Loon et al., 2006]. One of the models in this project is the DEHM-REGINA model which are used in this thesis.

2.3 State of the art in combined air pollution and climate modelling

In the last decade several studies of how the air pollution levels are changing in the future has been made. Changes in the emission levels is the most obvious and direct player, which inherently will change the air pollution levels in the future. As an example Bach et al. [2006] have evaluated the health and economy benefits and drawbacks from different emission scenarios, using the atmospheric chemical-transport model DEHM-REGINA coupled with an economy cost-benefit model. These investigation was carried out as a part of the "Assessment of the effectiveness of European air quality policies and measures" [Bach et al., 2006]. This type of emission reduction scenarios is an example of a group of experiments carried out which does not account for changes in the pollution level and distribution due to a changed climate, since meteorology typically is taken from a "base" year (e.g. 2000). In these kind of experiments, the emissions are changed, but the meteorology is kept constant, meaning that the same meteorological data is used both for the base scenario and for the emission reduction scenario.

Prather et al. [2003] evaluated the surface distribution and seasonality of ozone in the 21'st century based on the results from the Intergovernmental Panel on Climate Change (IPCC) Third Assessment Report (TAR) [Houghton, 2001] by comparing the results from 10 different models. The emissions in all these 10 simulations were based on the IPCC preliminary SRES A2 scenario [Nakicenovic et al., 2000] which by then was the only anthropogenic emission scenario analyzed with fully chemistry models [Prather and Ehhalt, 2001]. As Meteorological input some of these model used assimilated winds and others used winds from climate models. The spatial resolution of the models varied widely. For most of the models the meteorology was resolved at a six hour or even smaller time-step [Prather et al., 2003]. Prather et al. [2003] found a tendency to an upward shift of the base-line levels of O_3 . The largest shift was found in the summer season in the northern mid-latitudes and this is worrisome, since it coincides with the area where the largest regional cases of ozone pollution are present already [Prather et al., 2003]. However these projections do not include the response from the climate system and as noted in the TAR [Prather and Ehhalt, 2001]; the natural ecosystems and their emissions of ozone precursors are expected to be altered in the future [Prather et al., 2003]. Also changes in the physical climate itself, such as for example changes in temperature, humidity and the dynamics are expected to alter the global pollution distribution [Prather et al., 2003]. But these effects are the here mentioned model simulations not able to account for because of the lack of 21'st century meteorology input and the missing feedback link to the climate.

Hogrefe et al. [2004] used a regional model centered over the eastern United States and showed that the effect from a changed climate may contribute as equal to the air pollution levels in the future as the effects from changed emissions and growing intercontinental transport. However because they only studied a limited area the results obtained are very dependent on

the boundary conditions applied to the model. Generally it is a problem using limited area models covering only a small area when studying a larger scale phenomena.

To account for the direct role of changes in the climate Johnson et al. [2001] simulated the period 1990-2100 with a 3-D Atmosphere-Ocean-Chemistry Model. They made two simulations; a control experiment with fixed greenhouse gases at a pre-industrial level and a climate change experiment which has greenhouse gases evolving in accordance to IPCC's SRES A2 scenario [Nakicenovic et al., 2000]. Johnson et al. [2001] found that the impact of climate change decreases the net production of ozone with approximately 120 Tg/yr in the troposphere. By photochemistry ozone is split into $O(^1D)$ which results in a loss of ozone due to the chemical process $O(^1D)+H_2O \rightarrow 2OH$. This loss contributes to a large decrease in ozone and at the same time, the input of ozone at the top of the model domain increases less. Here it should be kept in mind, that the vertical resolution of the Chemistry Transport Model (CTM) used, is very poor (only 9 layers from the surface to the 100 hPa pressure level). This means, that this model simulation is not able to treat feedbacks from and to the stratospheric ozone correctly. Johnson et al. [2001] also found, that there is an indication that the current estimates of buildup of methane may be greatly overestimated. However there are several uncertainties connected to this experiment. For example the role of climate change on the natural emissions and the fact that the vertical and horizontal resolution of the model is poor were not accounted for in these simulations [Johnson et al., 2001].

Zlatev and Brandt [2005] used the Unified Danish Eulerian Model (UNI-DEM) to do sensitivity studies of the pollution levels in Europe due to climate change. In these experiments the emission and meteorology were kept constant except for some key meteorological parameters which were tuned to suited the IPCC SRES A2 scenario [Nakicenovic et al., 2000]. Zlatev and Brandt [2005] found among other results that these key meteorological parameters (temperature level+diurnal+seasonal variation, humidity and precipitation) are increasing the number of days in Europe, which exceed the permitted threshold value for ozone with respect to human health.

In parallel with the work carried out in this thesis Murazaki and Hess [2006] have examined the United States air quality with respect to the tropospheric ozone. They divide the tropospheric ozone into two contributions, namely the background ozone and the ozone produced from precursors locally emitted. Murazaki and Hess [2006] found that over the western United States (more remote regions with low NO_x emissions) the changes in the two contributions cancels out, whereas over the eastern United States (denser populated and higher NO_x emissions) the future expected decrease in background ozone is far smaller than the expected increase in locally produced ozone. This investigation was carried out by a time-sliced experiment using the NCAR climate system model (CSM) 1.0 [Boville and Gent, 1988] as meteorology input to the global chemical transport model MOZART-2 [Horowitz, 2003], [Murazaki and Hess, 2006]. The climate simulation was forced with the IPCC SRES A1 scenario [Nakicenovic et al., 2000] and it provides future meteorology to the chemical transport model MOZART-2 every 3 hours. The two time periods investigated was each 11 years long and consisted of the period 1990-2000 and the future period 2090-2100. In both simulations the emissions (both anthropogenic and biogenic) were kept at a constant 1997 level in order to separate the effects of climate change on the future surface ozone concentration.

As stated, the work of Murazaki and Hess [2006] was carried out in parallel with this work. When they published their results this year, the model experiments, simulations and statistical tests in this thesis work were already carried out!

Murazaki and Hess [2006] used the same basic methodology testing the results for two decades (1990's and 2090's) as used in this study. However, they only studied a limited area (United States), they only had ozone in focus and they also kept the natural emissions constant which is in contrast to this study.

3 Model descriptions

This section contains a short summary of the numerical, physical and chemical characteristics of the chemical long-range transport model DEHM-REGINA and the climate model ECHAM4-OPYC3, which have been used to construct the data of this thesis.

A chemical long-range transport model needs meteorological input data. In this work a prediction of the impacts of climate change on the air pollution levels in the future is desired. Therefore the chemical long-range transport model simulation is based on predicted climate data instead of the normally applied past or present-day meteorology obtained from a numerical weather forecast model.

In this experiment we use the results from the coupled atmosphere-ocean general circulation model ECHAM4-OPYC3, which has been forced with emissions according to the IPCC SRES A2 scenario. Section 3.1 describes this climate model and the main characteristics of the simulated meteorology found in studies using the model. Subsequently the chemical long-range transport model will be described. In chapter 4 a description of the model setup of this particular experiment can be found.

3.1 The atmosphere-ocean general circulation model, ECHAM4-OPYC3

As the name ECHAM4-OPYC3 indicates, this general circulation model consist of an atmosphere (ECHAM4) and an ocean component (OPYC3), respectively.

The atmosphere component (ECHAM4) is vertically discretized in a hybrid-sigma coordinate system and it consists of 19 layers extending up to the pressure level of 10 hPa. The prognostic variables are vorticity, divergence, logarithm of surface pressure, temperature, specific humidity and the mixing ratio of total cloud water. Apart from the water components of these prognostic variables, they are all represented by spherical harmonics with a triangular truncation at wave number 42 (T42). This gives a horizontal resolution of approximately $2.8^{\circ} \times 2.8^{\circ}$. The time step for the dynamics and the physics is 24 minutes and the radiation time step is 2 hours. Both seasonal and diurnal cycles in solar forcing are simulated [Roeckner et al., 1999].

The concentrations of greenhouse gases and halocarbons as well as the surface sulphur emissions are prescribed in the model according to the IPCC SRES A2 scenario. The tropospheric sulphur concentrations is calculated interactively within the atmosphere model by including a simplified sulphur model. This sulphur model is driven by the surface emissions from the SRES A2 scenario and by internally calculated processes such as sulphur chemistry, transport

and deposition (for further details see Roeckner et al. [1999]). With respect to the experiment carried out in this thesis, the inclusion of a sulphur model in the ECHAM4-OPYC3 model, only acts to improve the description of global radiation and therefore the weather parameters used as input to the chemical transport model DEHM. The sulphur and sulphate levels studied in the final results from this experiment is solely generated in the chemical long-range transport model, and are therefore only indirectly (through meteorology) affected by the sulphur concentration model in the ECHAM4-OPYC3 described here!

The transport of water vapor, cloud water and chemical constituents is calculated with a semi-Lagrangian scheme following Williamson and Rasch [1994]. For further details about horizontal diffusion, turbulent fluxes, drag associated with orographic gravity waves, the soil associated processes, cumulus convection, and the stratiform cloud water equation, see Roeckner et al. [1996]. The solar radiation is parameterized according to Fouquart and Bonnel [1980] and with some modification the long wave radiation scheme follows Morcrette et al. [1986]. The modifications of the long-wave radiation parametrization consists of the inclusion of some additional greenhouse gases and the 14.6 μ meter band of ozone. Also the water vapor continuum, the single scattering properties and the effective radius of cloud droplets and ice crystals has been revised (for further details see Roeckner et al. [1996]).

The ocean component of the AOGCM is an extended version (level 3) of the OPYC model [Oberhuber, 1993]. The ocean model consists of three submodels. These submodels are; an interior ocean, a surface mixed layer and a sea ice component. Vertically the model is divided into 11 layers and poleward of 36° the horizontal resolution is truncated at T42, which is identical to the atmosphere model. For lower latitudes (equatorward of 36° latitude) the meridional resolution is gradually decreased to 0.5° at the equator [Roeckner et al., 1999]. For details about the dynamics of the three submodels see Roeckner et al. [1999].

The coupling of the three oceanic submodels are done quasi-synchronously and they exchange information once a day. The atmosphere model provides daily-averaged surface fluxes of momentum, heat and fresh water to the ocean model, which returns daily-averages of the sea surface temperatures (SST) and daily-averages of the ice- momentum and concentration and the ice and snow thicknesses. The model also includes annual mean flux corrections for heat and fresh water. Unfortunately these flux corrections, beside correcting the fluxes annually, also results in a warm bias in the initial state, because of the way the flux corrections are constructed (cf. Stendel et al. [2002] and Roeckner et al. [1999]). This warm bias is approximately 0.3 Kelvin [Personal correspondence with Martin Stendel, DMI, 2006], [Cubasch et al., 1995]. This should be kept in mind when the final results from the chemical transport model DEHM are analyzed.

3.1.1 Forcings/A2 Scenario

The meteorological data used in this thesis is the result from a 240 year long time-dependent ECHAM4-OPYC3 simulation. The simulation is only forced with respect to the concentrations of greenhouse gases, halocarbons and sulphur. The concentrations are in the period 1860-1990 derived from observations and for the period 1990-2100, they are prescribed according to the IPCC SRES A2 scenario. The emissions following the A2 scenario is given every ten year and are linearly interpolated between the decade values. Furthermore, the tropospheric ozone distribution is allowed to vary as a result of prescribed concentrations of anthropogenic precursor gases (CH_4 , NO_x , CO) and stratospheric O_3 and NO_x whose

concentrations are given for 1860, 1985 and 2050. Intermediate values are then calculated by linear interpolation, and from 2050 and forth the concentration is held constant at the 2050 level [Roelofs and Lelieveld, 1995].

The A2 scenario is in the IPCC's special report on emission scenarios described as follows:

"The A2 storyline and scenario family describes a very heterogeneous world. The underlying theme is self-reliance and preservation of local identities. Fertility patterns across regions converge very slowly, which results in high population growth. Economic development is primarily regionally oriented and per capita economic growth and technological change are more fragmented and slower than in other storylines" (cite from Nakicenovic et al. [2000]).

The A2 scenario is compared to the other scenario families having the largest populations. The adaption of new technologies is rather slow compared to for example the A1 scenarios. The economy gap between now-industrialized and developing parts of the world will remain unchanged in contrast to the A1 and B1 scenarios, where the income gap will be smaller in the termination of the 2100'st century. Environmental restrictions is only carried out regionally. In summary the A2 scenario describes a world with limited cooperation and an unstabilized population growth [Nakicenovic et al., 2000].

3.1.2 ECHAM4-OPYC3 simulations of the climate of the 21'st century

In the period 1990-2100 the total forcing from all greenhouse gases results in an increase in radiation from 2 W/m^2 to 8.1 W/m^2 in the ECHAM4-OPYC3 simulation used in this thesis work. The increase in forcing with respect to pre-industrial levels is similar to the old IS92a scenario, however approximately 2.5 W/m^2 larger than the increase in the same period for the IPCC SRES B2 scenario, which assumes an unchanged population growth and a regionally limited ecological development [Nakicenovic et al., 2000].

Sulphur emissions are projected to increase by 50% until the 2030's, whereafter they gradually decrease to present day level in year 2100 [Stendel et al., 2002].

The global average temperature is found to increase by 2-3 K during the 21'st century, which is in good agreement with previous studies [Stendel et al., 2002]. There are large seasonal and regional differences in this warming with values up to 11 Kelvin in the winter in the Canadian and Siberian Arctic. For annual means, the largest increase is projected over Greenland and the subpolar regions of Asia, North America and Europe. In these areas the annual increase exceeds 6 Kelvin [Stendel et al., 2002].

In good agreement with other studies both the diurnal temperature range decreases and the warming over land is significantly larger compared to the warming over the ocean [Stendel et al., 2002]. The sea ice in the Arctic is estimated to retreat by approximately 40%. Particularly, over the Barents Sea, the sea ice is predicted to vanish completely by the end of the century.

The globally averaged precipitation only changes slightly. However, there are huge regional and seasonal differences. Winter precipitation over the temperate and Arctic regions increases by 10-50%, whereas the precipitation generally decreases over the subtropics and mid-latitudes, which is good in agreement with other studies. However, the Sahel area differ from these observations, more rain is projected in this region in the summertime [Stendel et al., 2002].

These authors also find that the hydrological cycle is enhanced. An increase in evaporation is found together with a decrease in precipitation over the oceans, leading to an excess of water over the continents and thereby an enhancement of the hydrological cycle.

Finally concerning the mean sea level pressure this ECHAM4-OPYC3 simulation results in a shift towards a higher NAO index [Stendel et al., 2002]. Both the Icelandic low and the Azores high are slightly enhanced making the differences larger and thereby the NAO index more positive.

3.2 The chemical transport model, DEHM-REGINA

After the meteorology from ECHAM4-OPYC3 has been provided, one very important assumption has to be made: It is assumed that the ECHAM4-OPYC3 simulation provides a realistic and consistent picture of the weather in the 21st century for meteorological input to the long-range transport model the Danish Eulerian Hemispheric Model DEHM-REGINA (REGional high resolution Air pollution model).

The DEHM model has been under development during the last 15 years at the National Environmental Research Institute NERI (cf. [Christensen, 1993], [Christensen, 1997], [Frohn et al., 2002b], [Frohn et al., 2003] and [Frohn, 2004]). The original version of the model is a DEHM-sulphur version [Christensen, 1997], which includes SO_2 , SO_4 and heavy metals. After that a mercury [Christensen et al., 2004], a CO_2 [Geels, 2003], a POP [Hansen et al., 2004], [Hansen, 2006] and the here used version of the model DEHM-REGINA [Frohn, 2004] were developed. For general documentation and validation of the model performance see Christensen [1997], Frohn [2004], Brandt et al. [2005], Geels et al. [2004], van Loon et al. [2004], and van Loon et al. [2006].

The DEHM model is a terrain-following model based on a set of coupled 3D-advection-diffusion equations. Figure 3.1 shows a schematic representation of the DEHM model system as it is today. In the middle level three boxes with different meteorological options are shown. These are meteorology based on the MM5 weather forecast model [Grell et al., 1995], the Eta weather forecast model [Nikovic et al., 1998] and finally the climate model ECHAM4-OPYC3 used in this experiment [Stendel et al., 2002], [Roeckner et al., 1999].

The DEHM-REGINA model is a full 3D Eulerian model covering the entire northern hemisphere and it includes several nesting options, which are available within the mother domain (northern hemisphere) (see figure 3.2). The purpose of the DEHM-REGINA model is to describe the chemical reactions going on in the troposphere [Frohn, 2004].

In the following sections the physical parameterizations, the chemistry and the numerical methods of the DEHM-REGINA model will be summarized. This is followed by a description of the emissions data used in the DEHM-REGINA model. And finally an overview of the EMEP measuring network, which the simulated data of the 1990's is validated against, is presented.

3.2.1 Model domain

Horizontally the mother domain of the DEHM-REGINA model covers the majority of the northern hemisphere with a resolution of 150 km x 150 km (see figure 3.2). The mother

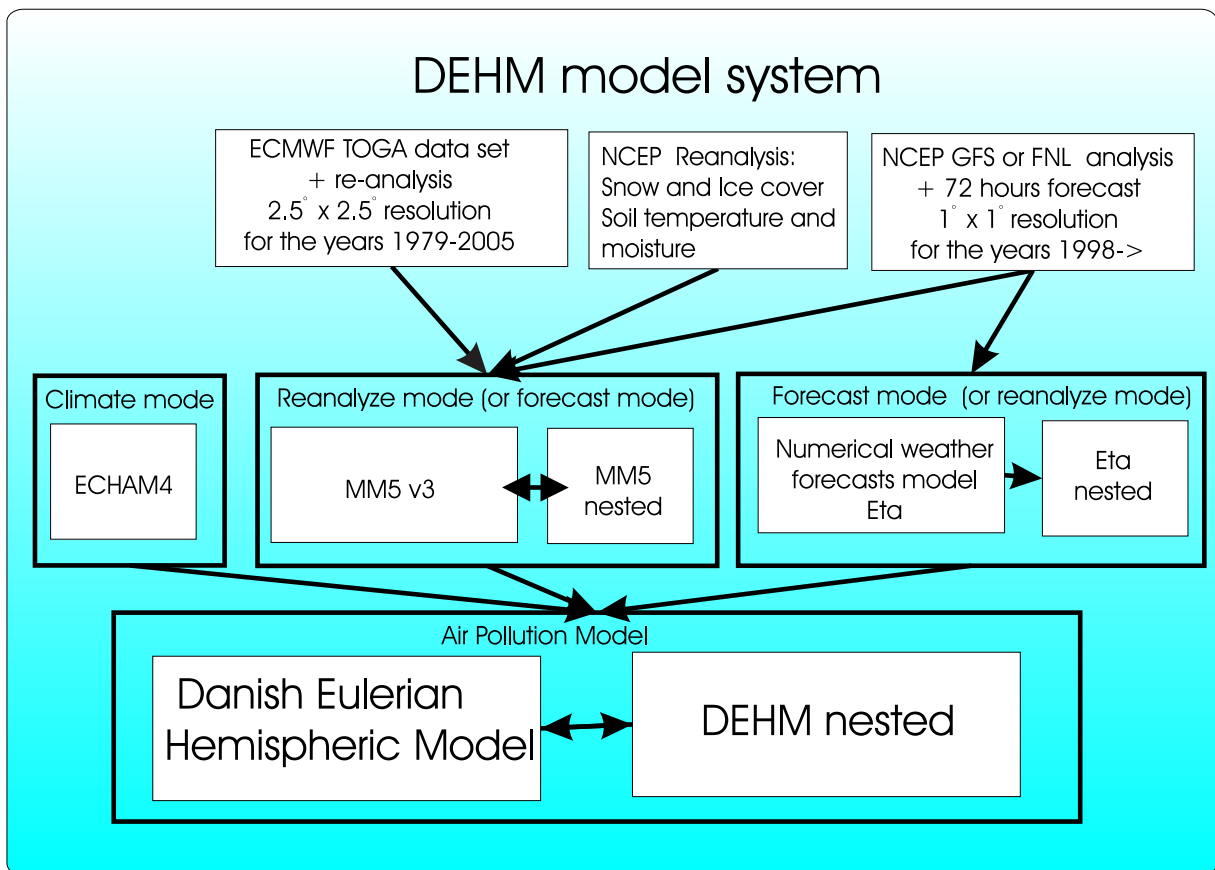


Figure 3.1: The DEHM model system (courtesy of Dr. J.H. Christensen, NERI).

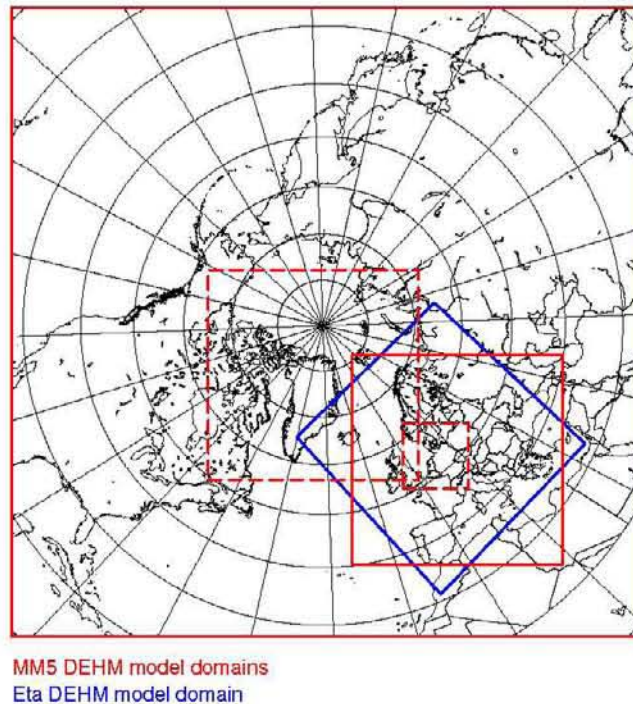


Figure 3.2: DEHM-REGINA model domains (courtesy of Dr. J.H. Christensen, NERI).

domain is the only domain used in this experiment, however the model are also set up, so it can run with two different nest options. These two nests are covering Europe (or the Arctic) and northern Europe, having a resolution of 50 km x 50 km and 16.7 km x 16.7 km, respectively. Since the meteorological data used in this experiment originates from a global climate model and therefore has a quite low spatial resolution, it do not make sense to run the DEHM-REGINA model with the two nested options here.

If one wishes to run the model in one of the two nested modes, it would be more reasonably to use high resolution meteorology from a regional climate model like for example the HIRHAM model [Hesselbjerg Christensen et al., 1996]. For instance at the Swedish Meteorological and Hydrological Institute (SMHI) Langner et al. [2005] has done a similar experiment. Langner et al. [2005] used the meteorological data from the regional atmospherical climate model version 1 (RCAv1) of the Rossby center, as input to the regional chemistry/transport/deposition model MATCH.

Vertically the DEHM-REGINA model contains 20 irregular distributed layers from the surface to the 100 hPa pressure level. The resolution is highest close to the surface. Ranging from approximately 50 meters between the layers in the boundary layer, to having approximately 2000 meters between the layers at the top of the domain (see table 4.1 p. 28 Frohn [2004]).

3.2.2 The physical parameterizations

The governing equation of the DEHM-REGINA model is the continuity equation:

$$\begin{aligned} \frac{\partial c_i}{\partial t} = & - \left(u \frac{\partial c_i}{\partial x} + v \frac{\partial c_i}{\partial y} + \dot{\sigma} \frac{\partial c_i}{\partial \sigma} \right) + K_x \frac{\partial^2 c_i}{\partial x^2} + K_y \frac{\partial^2 c_i}{\partial y^2} + \frac{\partial}{\partial \sigma} \left(K_\sigma \frac{\partial c_i}{\partial \sigma} \right) \\ & + E_i(x, y, \sigma, t) - \Lambda_i c_i + Q_i(c_1, c_2, \dots, c_q) \text{ where } i = 1, 2, \dots, q \end{aligned} \quad (3.1)$$

For details about the derivation of the equation and the transformation into σ -coordinates see chapter 4 in Frohn [2004] or alternatively chapter 2.4 in Brandt [1998]. The first three terms of the right-hand-side of the equation describes the advection, the next three terms expresses the diffusion, which are derived from Reynolds decomposition [Holton, 1992],[Seinfeld and Pandis, 1998] and K-theory of first order [Seinfeld and Pandis, 1998]. The last three terms on the right hand side of equation 3.1 originates from the addition of production and loss terms. The production terms includes chemical production in the atmosphere and emissions. The loss term consist of removal due to chemistry, scavenging (uptake of chemical components in water droplets) and subsequent wet deposition [Frohn, 2004]. These five contributions from the loss and production terms are included in the three last terms in equation 3.1. E_i describes the emissions of the i^{th} chemical component, $\Lambda_i c_i$ is the wet scavenging of the component i and finally Q_i represent the chemical production and loss of the different components.

Equation 3.1 describes in principle the concentration c_i at all scales included in the DEHM-REGINA model. However, it is not possible to calculate an exact solution to this continuity equation. Therefore numerical discretization, integration and physical parameterizations are needed. Since dispersion is a sub-grid-scale phenomena, it is necessary to parameterize dispersion, e.g. by using K-theory of first order (for further details see Frohn [2004] and Christensen [1997]).

Also the process of dry deposition is a quantity, which needs parameterizations, since there is no exact theory describing this physical process. The dry deposition module used in this version of the DEHM-REGINA model is based on the resistance method and is similar to the dry deposition module of the EMEP model (for details and documentation see Simpson et al. [2003]). Dry deposition is applied as a lower boundary condition to the vertical dispersion when solved in the model.

Wet deposition is yet a physical process, which cannot be described precisely and therefore needs to be parameterized. In the DEHM-REGINA model the wet deposition is parameterized by a scavenging ratio formulation, where the scavenging is divided into two contributions. The first contribution is the in-cloud scavenging, which represents the uptake in droplets inside a cloud. The second contribution originates from precipitation events and is uptake in droplets below the cloud base. The wet deposition is of cause very dependent on the precipitation frequency and amount. These parameters are not calculated directly in the DEHM-REGINA model, instead the used values for precipitation are taken directly from the chosen meteorological input model; MM5, ETA or ECHAM-OPYC3 (cf. figure 3.1). Details about the specific parameterization of the in-cloud and below-cloud scavenging can be found in Christensen [1995] and Frohn [2004]. The DEHM-REGINA model also includes information on different land use categories.

3.2.3 Chemistry

The chemical scheme of the DEHM-REGINA model is an explicit scheme and it is based on the scheme of the EMEP model [Frohn, 2004], [Brandt et al., 2005]. The DEHM-REGINA chemical scheme includes the chemistry of 63 different chemical compounds. These 63 chemical species participates in a great number of chemical processes, however it is not possible to include them all. The present DEHM-REGINA model version includes 120 important chemical reactions [Frohn, 2004], [Brandt et al., 2005]. The model includes e.g SO_x , NO_x , O_3 , CO , NH_x , many VOC 's and primary and secondary particles ($PM_{2.5}$, PM_{10} , $SeaSalt$, SO_4 , NO_3 , NH_4) [Brandt et al., 2005]. For a full list of all the chemical species see p.41 in Frohn [2004] and for details about the chemical reactions and the reaction rates see table 5.2-5.10 in Frohn [2004] (After the work of Frohn [2004] has finished, 5 additionally chemical species has been added to the DEHM-REGINA model, these species are; $PM_{2.5}$, PM_{10} , TSP , $Seasalt$ and $Smoke$).

3.2.4 Numerical methods

The governing equation of the chemical transport model is the continuity equation (cf. equation 3.1). In order to solve this equation numerical methods are needed. Since the model here includes both advection processes in the atmosphere and chemical reactions, the time scale for the different processes included in the model are highly variable. This problem is solved by dividing the model into five submodels in order to separate the very different time scales and to solve the submodels using different numerical methods. The five submodels are listed below (cf. table 3.1). The splitting procedure used in the present model is a non-symmetric splitting procedure based on the ideas of McRae et al. [1984] [Frohn, 2004].

Now for each time step in the total DEHM-REGINA model five subsequent procedures are carried out. These five procedures are the solving of the respective equation in each submodel in the same order as they are listed in table 3.1 (for further details see Frohn et al. [2002b] and Frohn [2004]). This procedure optimizes the accuracy and stability of the whole model. The demands to accuracy and stability of the numerical methods used to solve the different submodels varies! This splitting of the model into submodels enables the possibility of using different numerical temporal and spatial algorithms for solving the different terms of continuity equation 3.1 and furthermore sub-time-steps can be introduced in the chemistry submodel in order to cope with the large variability in time scales.

In the two right columns of table 3.1 the methods chosen for the numerical spatial discretization and the temporal integration used for the individual submodels are listed. When choosing a numerical scheme one has to compromise between high accuracy and reasonably low computing time. The accuracy of the physical parametrization determines the need for accuracy of the numerical scheme. If a physical process is very simple parameterized, some computing time can be saved by choosing a low accuracy numerical schemes. On the other hand physical properties, which has been very accurate described, needs to be solved with a high accuracy scheme [Frohn, 2004]. This is the case for the horizontal advection, where the modified version of the Accurate Space Derivatives (ASD) scheme has been used [Frohn et al., 2002b]. The advection of a chemical compound has a large impact on the resulting calculated concentration. Therefore it becomes very important in a chemical transport model like the DEHM-REGINA model to describe the process of advection very accurate [Frohn,

Submodel	Type	Equation term	Spatial scheme	Temporal scheme
1	3D advection	$\frac{\partial c_i}{\partial t} = - \left(u \frac{\partial c_i}{\partial x} + v \frac{\partial c_i}{\partial y} + \dot{\sigma} \frac{\partial c_i}{\partial \sigma} \right)$	Horizontal: modified ASD Vertical: Finite elements	Taylor series expansion
2	x-direction dispersion	$\frac{\partial c_i}{\partial t} = K_x \frac{\partial^2 c_i}{\partial x^2}$	Finite elements	Crank-Nicolson method
3	y-direction dispersion	$\frac{\partial c_i}{\partial t} = K_y \frac{\partial^2 c_i}{\partial y^2}$	Finite elements	Crank-Nicolson method
4	vertical dispersion	$\frac{\partial c_i}{\partial t} = \frac{\partial}{\partial \sigma} \left(K_\sigma \frac{\partial c_i}{\partial \sigma} \right)$	Finite elements	Crank-Nicolson method
5	chemistry, emissions and wet deposition	$\frac{\partial c_i}{\partial t} = E_i(x, y, \sigma, t) - \Lambda_i c_i + Q_i(c_1, c_2, \dots, c_q)$	Changes in mixing ratios due to chemical reactions	EBI method and Two-step method

Table 3.1: The DEHM-REGINA model is split into 5 submodels in order to optimize the numerical solutions. Basically it is the continuity equation of the model, which has been split into five subterms. The subterms are solved with different numerical methods in space and time. The first and second column shows the number of the submodel and the respective physical process. In the center column the ancillary term of the continuity equation can be seen and finally the two right columns shows the spatial and temporal numerical schemes used in the DEHM-REGINA model for solving the submodels (for further details see Christensen [1993], Frohn et al. [2002b] and Geels et al. [2004])

2004], [Peters et al., 1995].

Higher order schemes like the ASD scheme has the disadvantages of introducing high frequency computational noise and oscillations. In order to reduce this noise and oscillations a Forester filter have been used [Forester, 1977]. In order to avoid negative concentrations a Bartnicki filter is used [Bartnicki, 1989]. For further details about the filtering procedure of the DEHM-REGINA model see Frohn et al. [2002b] and Frohn [2004].

As can be seen from table 3.1 the vertical advection and the dispersion is discretized using the finite element scheme [Pepper et al., 1979], [Frohn et al., 2002b] and [Christensen, 1995]. The finite element scheme has an lower accuracy than the ASD scheme, but saves computing time and is acceptable with respect to the accuracy concerning these parameters [Frohn, 2004].

To solve the horizontal and vertical advection in time the Taylor serie expansion method has been used [Frohn et al., 2002b], [Frohn, 2004]. The length of the time step is controlled by the Courant-Friedrich-Levy (CFL) stability criterion. Dispersion is solved numerical in time using the Crank-Nicolson method [Geels et al., 2004].

Submodel 5 consists of the chemistry, emissions and wet deposition. In this submodel, for each full model time step (defined by the advection) the changes in mixing ratios is calculated due to chemical reactions [Frohn, 2004]. However the time step in the chemistry submodel is subdivided into smaller sub-time steps in order resolve the chemistry better. The mixing ratio fields is extracted, whenever the time spent in submodel 5 (chemistry submodel) equals the advection time step [Frohn, 2004]. To solve the equations numerical with respect to time two different methods has been used in this submodel. For the first two time steps the Euler Backward Iterative (EBI) method [Hertel et al., 1993] has been used. The following time steps has been solved using the two-step method [Verwer et al., 1996]. Two time resolving methods has been employed, since the latter is far more accurate, however this methods requires two initial fields in order to get started [Frohn, 2004].

The present and earlier versions of the performance of DEHM-REGINA model has been widely tested [Christensen, 1993], [Christensen, 1995], [Christensen, 1997], [Frohn et al., 2002a], [Frohn et al., 2002b], [Frohn et al., 2003], [Frohn, 2004], [Brandt et al., 2001a], [Brandt et al., 2001b] and [Geels et al., 2004]. The DEHM-REGINA model has participated in several model inter-comparison projects which results can be seen in van Loon et al. [2004] and van Loon et al. [2006]

3.2.5 Emission data

The anthropogenic emissions used in the present version of the DEHM-REGINA model consist of a combined set of data. The emission of the primary pollutants consist of data from the Global Inventory Activity (GEIA) [Graedel et al., 1993], the Emission Database for Global Atmospheric Research (EDGAR) [Olivier et al., 1996] and finally data from the European Monitoring Evaluation Programme (EMEP) [Vestreng, 2001] for Europe. The emissions are released in the model similar to the emission release in the EMEP-model [Simpson et al., 2003]. The emission data is divided into 10 different emission types (se table 4.2 in Simpson et al. [2003]), which vertically is released in different specified levels of the model. Temporally the emission are differentiated according to estimated factors. For further details see Simpson et al. [2003].

3.2.6 EMEP measuring network

In order to validate the model performance with ECHAM4-OPYC3 meteorology, comparisons has been made with earlier simulations using MM5 meteorology and with observations (cf. chapter 5). The observations used for this validation originates from the EMEP measuring network. The EMEP measurement programme includes a large number of chemical components [Hjellbrekke, 2000]. The location of the specific measuring sites are shown in figure 3.3. Not all measuring sites are measuring all the validated chemical components all the time, for details about the measurement period and frequency of the individual components see Hjellbrekke [2000].

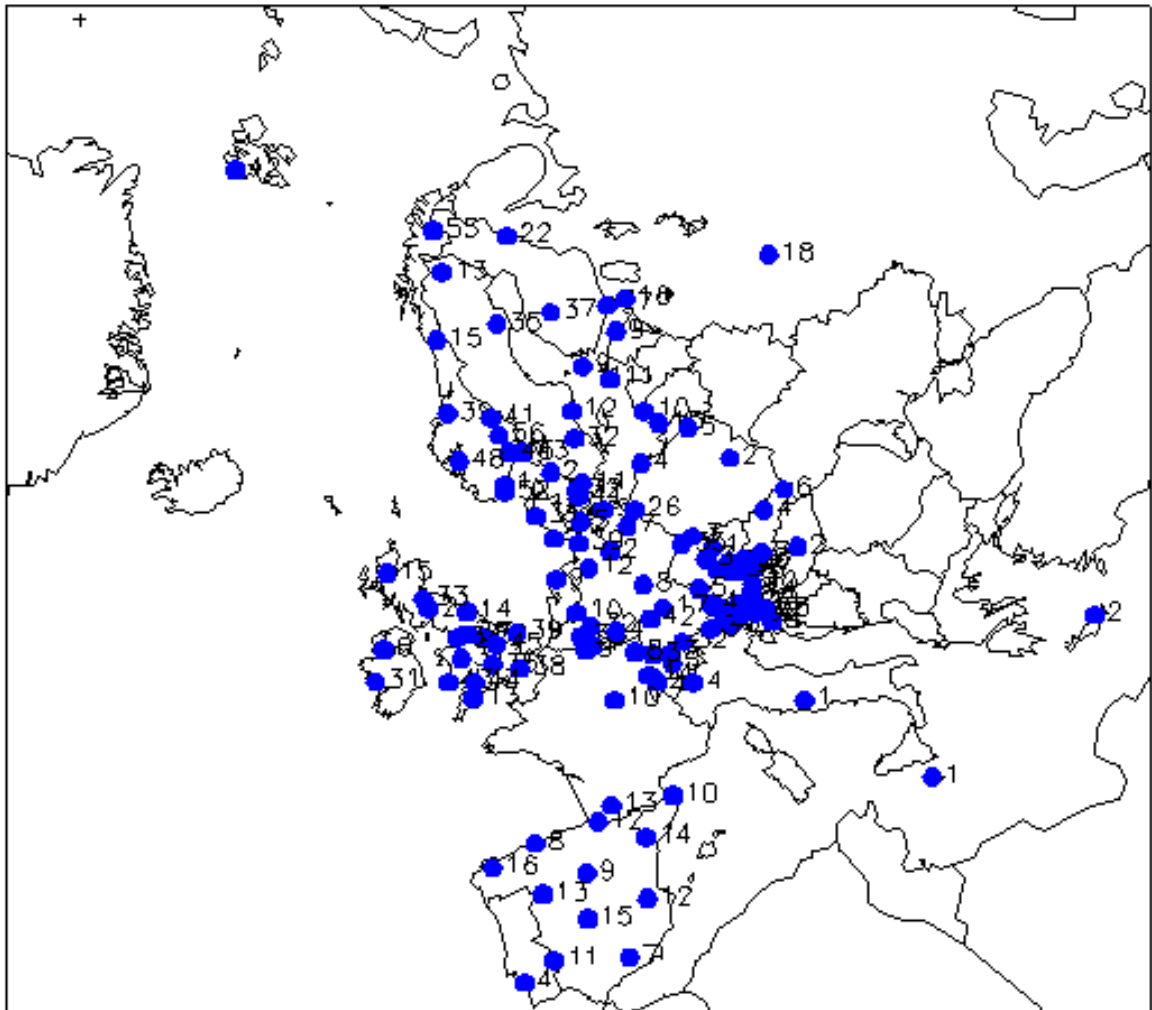


Figure 3.3: The EMEP measurement network 2001 [www.emep.int]

4 Experimental design

The model set up is rather straight forward. The ECHAM4-OPYC3 provides a number of meteorological parameters (see table 4.1) and these are used as input meteorology to the DEHM-REGINA model, which is described in section 3.2. However there are several changes, which have to be made before the data from ECHAM4-OPYC3 climate model can be implemented as meteorological data in the DEHM-REGINA model. First of all the climate data have a much lower spatial and temporal resolution than the chemical long-range transport model. This means that interpolations have to be made in order to use the ECHAM4-OPYC3 data as meteorological input to the DEHM-REGINA model.

4.1 Meteorological parameters and modifications

Since the climate simulation of the ECHAM4-OPYC3 model already were carried out, when the work of this master thesis began, there wasn't any choice of which output parameters should be saved from the climate simulation. The parameters, which were saved, when the climate simulation was carried out and therefore were available for this experiment is listed in table 4.1.

Compared to what is usually done, when the DEHM-REGINA model is run with meteorology from a weather prediction model (e.g. MM5), the only missing parameter was the turbulent kinetic energy TKE. In the present version of the model the turbulent kinetic energy is used to calculate the mixing height. Since TKE is missing from the ECHAM4-OPYC3 data set another parametrization of the mixing height has been used. This calculation of the mixing height is based on a simple energy balance equation for the internal boundary layer (for further details see Christensen [1997]). The mixing height parametrization has been used before in earlier versions of the DEHM-REGINA model [Christensen, 1997] and it is documented to perform quite well [Brandt, 1998].

Also the vertical velocity are calculated in DEHM-REGINA model instead of interpolate it from the ECHAM4-OPYC3 layers. The vertical velocity is derived from the u and v velocities, using the continuity equation. By this method mass-conservation is ensured, which is very important in a chemistry model like DEHM-REGINA.

4.2 Temporal and spatial interpolations

The ECHAM4-OPYC3 provides data every six hour with a horizontal resolution of approximately 300 km x 300 km ($2.8^\circ \times 2.8^\circ$). Vertically the ECHAM4-OPYC3 model version consists

3D	2D
Geopotential height	Surface pressure P_0
Temperature T	Snow depth
Wind speed u	Stratiform and convective precipitation
wind speed v	Sensibel and latent heat flux
Relative Humidity RH	MSLP
	Cloud water
	Surface geopotential (orography)
	Friction velocity u_*
	10 meter wind u_{10} and v_{10}
	2 meter temperature
	2 meter dew point temperature
	Surface temperature
	Albedo
	Sea ice

Table 4.1: ECHAM4-OPYC3 parameters provided as meteorology input for the DEHM-REGINA model.

of 19 irregular located layers extending from surface to the 10 hPa level. DEHM-REGINA on the other hand includes 20 irregular distributed layers. The upper layer is located at the 100 hPa pressure level. DEHM-REGINA has a much higher vertical resolution than the ECHAM4-OPYC3 model near the surface.

The differences in both temporal and spatial resolution results in the necessity of interpolation in time and space. The temporal resolution of the meteorological data is interpolated to temporal resolution of the advection term and the horizontal resolution gets interpolated to suite the DEHM-REGINA grid resolution of 150 km x 150 km. Also vertically a interpolation is carried out (except σ which are derived through the continuity equation) in order to construct a higher resolution of the ECHAM4-OPYC3 data, which the DEHM-REGINA model needs in the boundary layer.

Of cause these interpolations introduces some errors, however these errors are considered acceptable compared to other uncertainties in the model. Since much chemistry and depositions is going on in the boundary layer and the resolution of the climate data is poor compared to normal weather prediction data, especially the lack of vertical resolution in the lowest layers is expected to introduce uncertainties.

Interpolation of the 360 day long ECHAM4-OPYC3 year

A year in the ECHAM4-OPYC3 model is only 360 days long. ECHAM4-OPYC3 still contains the yearly variability in solar radiation, but the earth is travelling a little bit faster around the sun than in reality. In order to compare the data from the ECHAM4-OPYC3-DEHM-REGINA simulation with MM5-DEHM-REGINA simulation and with observations in the validation, interpolations has been made.

According to PRUDENCE project [www.prudence.dmi.dk], which also is based on ECHAM4-OPYC3 data, the most appropriate way of extending the ECHAM4-OPYC3 year to actual time is carried out by the following method;

* addition of an extra day in May, July, August, October and December.

* addition of an extra day in February in leap years.

These new extra days should be inserted between day 15 and day 16.

In this model setup an average value of the already existing day 15 and 16 has been added between day 15 and 16 in all the 31-day long months. In the leap years an average value for day 29+30 in February has been calculated and introduced as day 29. For the rest of the years an average value of February day 28+29+30 has been calculated and introduced as February day 28. This procedure is carried out in order to get a continuous and realistic data set. Since the final analysis is based upon at least annual averaged data, this correcting procedure are not expected to matter much in the final results! However it is necessary in order to compare the different simulations with measurements.

5 Validation of the experimental method for the period 1990-1999

In this chapter a DEHM-REGINA model simulation based on ECHAM4-OPYC3 meteorology is compared to a simulation based on MM5 meteorology and to observations. Both simulations are performed with the same variable emissions (1990-1999), which means that the differences reflected in the model output from the two simulations, solely are due to the differences in the input meteorology. Since the output from a climate model does not reflect the real meteorology, this validation is necessary in order to test, if it is possible at all to use data from a "free run" climate model as meteorological input data to the DEHM-REGINA model.

In order to validate data from the simulations carried out in this thesis, several statistical parameters has been calculated and some statistical tests have been performed. The validation period is 1990-1999 and two DEHM-REGINA simulations with different meteorology and variable emissions has been carried out (cf. the green area in table 5.1). After the performance of the model has been validated, it is interesting to test if there are any changes in mean values predicted for the same area (Europe, EMEP sites) between the three decades 1990-1999, 2040-2049 and 2090-2099 with ECHAM4-OPYC3 meteorology and constant emissions (in table 5.1 marked with red).

In the following section (5.1) some general theory on the statistical methods used in this thesis is summarized. Section 5.2 presents the validation results of the measured and predicted selected chemical species. This selection of species is dependent on the available observed data, since the model results in this analysis is compared with measurements. In the next step in the analysis a t-test is performed to test if the model run on climate data contains any biases. Specie for specie it is tested if there are any significant differences between

Emissions	constant	variable	variable
Model	ECHAM4-OPYC3	ECHAM4-OPYC3	MM5
1990's	X	X	X
2040's	X		
2090's	X		

Table 5.1: For this experiment 5 model simulations of the chemical transport model DEHM-REGINA with different emission scenarios and different input meteorology has been carried out. For the validation of the model setup, two simulations with variable emissions has been carried out (marked with green) and for the prediction of the impact of climate change on air pollution levels and distributions three simulations has been carried out (marked with red)

the the two simulations (DEHM-REGINA with MM5 meteorology vs DEHM-REGINA with ECHAM4-OPYC3 meteorology, preserved emissions). From this test, any possible biases in the DEHM-REGINA ECHAM4-OPYC3 simulation should be located, since the performance of the DEHM-REGINA MM5 simulation already is known from earlier studies DEHM-REGINA model (see Christensen [1997], Frohn [2004], Brandt et al. [2005], Geels et al. [2004], van Loon et al. [2004], and van Loon et al. [2006]). Finally the last section (5.6) of this chapter contains an analysis of the predicted results for the two future decades 2040's and 2090's at the locations of the measurement stations. This last step is solely carried out to connect the validation, which is based on the results at some specific sites in Europe (EMEP measuring sites), to the next chapter, where the prediction at the total northern hemisphere is investigated (cf. 6).

5.1 Statistical methodology

The comparison of data has been performed by inspection of measures for the averages and the variability of the data. The statistical parameters calculated here are the mean (\bar{P}) and the fractional bias (FB), which represents the average values, the correlation coefficient (\hat{r}), which represents the variability in the data series [Brandt, 1998] and finally the normalized mean square error ($NMSE$), which represent both the averages and variability of the data.

5.1.1 Statistical formulas

If P is the predicted value, the mean is defined by

$$\bar{P} = \frac{1}{N} \sum_{i=1}^N P_i \quad (5.1)$$

where N is the total number of predicted values in each data series Taylor [1997].

The fractional bias is defined as in Brandt [1998]

$$FB = 2 \frac{\bar{P} - \bar{O}}{\bar{P} + \bar{O}} \quad (5.2)$$

In equation (5.2) P refers to the predicted value (of the DEHM-REGINA ECHAM4-OPYC3 simulation and the DEHM-REGINA MM5 simulation) and O refers to the observed value.

As mentioned above, the correlation coefficient (\hat{r}) and the normalized mean square error ($NMSE$) are calculated to give an estimate of how well the model simulates the variability of the data compared to measurements.

The correlation coefficient is given as the covariance between the two series of deviation from their respective means, divided by their respective standard deviations [Brandt, 1998]

$$\hat{r} = \frac{\sum_{i=1}^N (O_i - \bar{O})(P_i - \bar{P})}{\sqrt{\sum_{i=1}^N (O_i - \bar{O})^2 \sum_{i=1}^N (P_i - \bar{P})^2}} \quad (5.3)$$

Sig. level %	50	20	10	5	2	1	0.2	0.1
Fractile	0.75	0.90	0.95	0.975	0.99	0.995	0.999	0.9995
18 d.f.	0.688	1.330	1.737	2.101	2.552	2.878	3.610	3.922

Table 5.2: Extracts from the t-distribution table from Malmberg [1985]. Selected fractile values and significant levels for 18 degrees of freedom are printed.

The normalized mean square error gives a measure of the overall deviation between the observed and the predicted values [Brandt, 1998].

$$NMSE = \frac{1}{N \cdot \bar{O} \cdot \bar{P}} \sum_{i=1}^N (P_i - O_i)^2 \quad (5.4)$$

5.1.2 Two-tailed t-test

In order to conclude whether two model simulations are significantly different from one another the t-test for change in mean values has been performed Spiegel [1992]. If \bar{P}_1 denotes the mean of one data series and \bar{P}_2 denotes the mean of another data series the hypothesis H_0 has to be tested

$$H_0 : \bar{P}_1 = \bar{P}_2 \quad (5.5)$$

If the hypothesis can be rejected, one can conclude that the mean values of the two time series are not equal, which in this case means that there is a change in the mean values. To test the hypothesis H_0 the t-statistic (t) is calculated the following way;

$$t = \frac{\bar{P}_1 - \bar{P}_2}{\sigma \sqrt{\frac{1}{N_1} + \frac{1}{N_2}}} \quad \text{where } \sigma = \sqrt{\frac{N_1 s_1^2 + N_2 s_2^2}{N_1 + N_2 - 2}} \quad (5.6)$$

Here N_1 and N_2 denotes the number of degrees of freedom of the two data sets and s_1 and s_2 denotes the standard deviations given by ?

$$s = \sqrt{\frac{1}{N} \sum_{i=1}^N (x_i - \bar{x})^2} \quad \text{where } \bar{x} = \frac{1}{N} \sum_{i=1}^N x_i \quad (5.7)$$

Whether the hypothesis can be rejected or not, can now be looked up in a t-distribution table see table (5.2)

For example, if we have two data sets, each consisting of 10 samples, the number of degrees of freedom is $(N_1 + N_2 - 2) = (10 + 10 - 2) = 18$. The hypothesis H_0 can then be rejected within a significant level of e.g. 10% ($t_{0.95}$), if the t-value lies outside the range -1.737 to +1.737. Rejecting the hypothesis H_0 then means, that there is a significant difference between the mean of the two data series. This again means, that we can be 90% confident, that the two data sets are significantly different.

The number of degrees of freedom is defined as $(N_1 + N_2 - 2)$ because it is the number of independent observations (the length of the time series) minus the number of statistical parameters, which is being estimated from these observations [Brandt, 1994]. That means, when comparing the results of the ECHAM4-OPYC3 simulation with the results of the MM5 simulation for the control period 1990-1999, there are 10 years or so-called observations in each simulation and two statistical parameters (e.g. the mean value of each of the two observation sets), which lead to the definition; # degrees of freedom = $(N_1 + N_2 - 2)$, which is used above.

As the header of this subsection indicates, the t-test here is two-tailed. This simply means, that when the hypothesis H_0 is rejected, two alternative hypothesis's can be accepted. In the case of the test of mean value, the following two acceptance hypothesis's are a) the difference in mean value of the two data set are significantly positive or b) the difference in mean value of the two data set is significantly negative. The fact that there are two alternative hypothesis's to accept, makes the t-test two-tailed.

5.1.3 Ranking

Ranking is a good evaluation method of model performances, when different model simulations have been carried out. The method was e.g. used in the ETEX ATMES-II model exercise performance comparison (see e.g. Mosca et al. [1997]). In the validation process it is most convenient to compare the two simulations of the control period (1990-1999) with variable emissions, because these results then can be compared to real measurements. This comparison enables the evaluation of the ECHAM4-OPYC3 DEHM-REGINA setup vs real observations and relative to another model setup (MM5 DEHM-REGINA) which already is documented to perform well [Christensen, 1993], [Christensen, 1995], [Christensen, 1997], [Frohn et al., 2002a], [Frohn et al., 2002b], [Frohn et al., 2003], [Frohn, 2004], [Brandt et al., 2001b] and [Geels et al., 2004].

First the correlation coefficient, the fractional bias and the normalized mean square error have been calculated for the precipitation, as well as the wet depositions and concentrations of several chemical species.

In consistency with the ranking method used by Brandt [1998], for each model characteristics and for each statistical parameter, a local ranking has been performed. This means, that the best performing parameter of two simulations has been given the value 1 and the second best the value 2. In the case of two equal performing parameters, both have been given the value 1. Each statistical parameter of each characteristics (from now on called statistical index) has been given the same weight in this analysis.

After the local ranking of each statistical index, a global ranking has been calculated as the sum of the local rank. In this way, the result with the smallest global rank indicates the best performing model in terms of model results compared to measurements [Brandt, 1998].

5.2 Validation results for the control period 1990-1999

In this section the modelled and measured concentrations and wet depositions of several chemical species are plotted and analyzed. The choice of chemical species is determined by the available data from the EMEP measuring network (cf. section 3.2.6).

The EMEP measuring network provides diurnal mean or accumulated observational data of the following chemical species: NH_3 , NH_4 , sum of NH ($=NH_3 + NH_4$), HNO_3 , NO_3 , sum of NO_3 ($=HNO_3 + NO_3$), NO_2 , O_3 , SO_2 , SO_4 and finally the diurnal max. and hourly O_3 . Furthermore the precipitation as well as the wet deposition of NH_4 , NO_3 and SO_4 are available. Evaluation of the simulations carried out in this thesis is performed as an analysis of these particular species, since the observational data were present.

The analysis are carried out specie by specie since the model performance is different for the different chemical species. This is due to the fact that some species are subject to long-range transport while others are short-lived and deposit locally. This is also the reason why the meteorology becomes very important for some chemical species and less important for others, which is seen in the analysis results below.

The validation analysis is based on monthly mean values of simulated and measured data. The data have therefore been re-sampled from the daily values, since it does not make sense to validate a climate model result on a daily basis. On the other hand, it is expected that the climate model is able to simulate the seasonal variations, and therefore the analysis is based on monthly mean values. Furthermore the data have been averaged over space meaning that for every day a mean value has been made over all the measurement sites (both for measurements as well as for model results). The daily time series have afterward been averaged to monthly mean values.

5.2.1 Analysis of ammonia and ammonium

Figure 5.1 and 5.2 show the validation of the model results based on the MM5 and ECHAM4-OPYC3 meteorology, respectively. The figures include the results for ammonia and ammonium.

The calculated ammonia (NH_3) concentration (cf. figure 5.1 and figure 5.2) is on average much smaller than the measured. In this connection it is important to note, that there in most cases only are 4 or less measuring stations to compare with, which should be kept in mind, when the results are interpreted.

The deposition of NH_3 is dependent on the amount of acid present in the atmosphere, however it deposit relatively fast. When ammonia is emitted from a source the concentrations in the air near the source will be large (e.g. near a pig farm). If the measurement sites does not represent the background value of ammonia, it is expected to get far too low values in the calculated results. First of all we are comparing with the EMEP stations which not necessarily represents background level of NH_3 and secondly the resolution of the hemispheric DEHM-REGINA model is quite low for simulations of short lived species, which will tend to an underestimation of the concentrations. A higher model resolution will probably give a better result, partly because of the more accurate representation of the emission sources [Frohn, 2004]. The very low concentration values are as expected also seen in both the MM5 and the ECHAM4-OPYC3 simulation. In the case of the prediction of NH_3 levels and distribution the two model-setups are performing similarly.

The calculated concentrations level of NH_4 is very close to the measured values both in the case of the MM5 and the ECHAM4-OPYC3 simulation, but the correlation is very low in the ECHAM4-OPYC3 simulation. This is an indication of the weather from ECHAM4-OPYC3 possess the same statistical characteristics as the real weather, however lacks in timing of

the individual meteorological events. In contrast the MM5 weather is a closer simulation of the actual weather. In the results of both the ECHAM4-OPYC3 and the MM5 simulation a significant decrease in the NH_4 concentration over the 10 year period is seen. This is due to the decrease of acid in the air during the 1990's. Both ammonia and sulphur acid is part of the chemical reaction scheme when ammonium is produced. Therefore the decreasing emissions of sulphate during the 1990's results in a decrease in the NH_4 concentration.

Inspecting figure 5.1 and figure 5.2 reveals that the mean level for the sum of NH from both the MM5 and the ECHAM4-OPYC3 simulation is a little too low compared to the measurements. This difference must be a result of the far too low estimated mean values of NH_3 . For the results based on the MM5 meteorology the correlation coefficient is acceptable, whereas in the results based on ECHAM4-OPYC3 meteorology correlation is below 0.5.

The mean levels of the wet deposition of NH_4 is comparing acceptable well to the measured values. A clear seasonal variation is also seen in the results of both the MM5 and the ECHAM4-OPYC3 model setup. In the results of the ECHAM4-OPYC3 setup, it seems like the estimated wet deposition in the summer generally is too low. On the other hand the summer levels of the wet deposition in the results of the MM5 model setup is far too high. Since these two inconsistencies is pointing in opposite direction in the two simulations, the feature must originate from the weather of the two simulations (the meteorology is the only thing that differs in the two simulations). The wet deposition is of course very dependent of the amount, frequency, timing and type of precipitation and therefore it would be logical to conclude here, that the precipitation in ECHAM4-OPYC3 is significantly different than the precipitation in MM5, however both simulations fails to estimate the precipitation correctly in the summer.

In the lowest panel in figure 5.1 and 5.2 the precipitation is shown. The ECHAM4-OPYC3 simulation definitely fails to simulate the measured variation in precipitation, but it does have a seasonal variation and the mean levels fit very well. The failure in correlation is not surprisingly since the ECHAM4-OPYC3 weather is solely climatic and therefore it cannot be expected to simulate the timing of the real weather. Analyzing the results based on MM5 meteorology, the mean level is actually worse represented by the MM5 model than by ECHAM4-OPYC3. On the other hand the correlation of the results of the MM5 model setup compared to measurements is high, which was expected since MM5 is a day-to-day weather forecast model in contrast to ECHAM4-OPYC3, which is a climate model.

The precipitation level of the ECHAM4-OPYC3 model setup is very similar to the precipitation measurements of the EMEP stations both in the summer and the winter. This indicates, that it is precipitation timing and/or frequency and/or type, which differs from the observations with respect to the discussion about wet deposition above. When performing an analysis including a comparisons of results at a limited number of measurement stations, there is also a risk, that these stations do not represent the average observed weather and chemistry over Europe. Furthermore, the individual measurements only represent a point, whereas the predicted values from the two simulation are representing areas (grid cells). This will inherently introduce some uncertainties in the analysis carried out here.

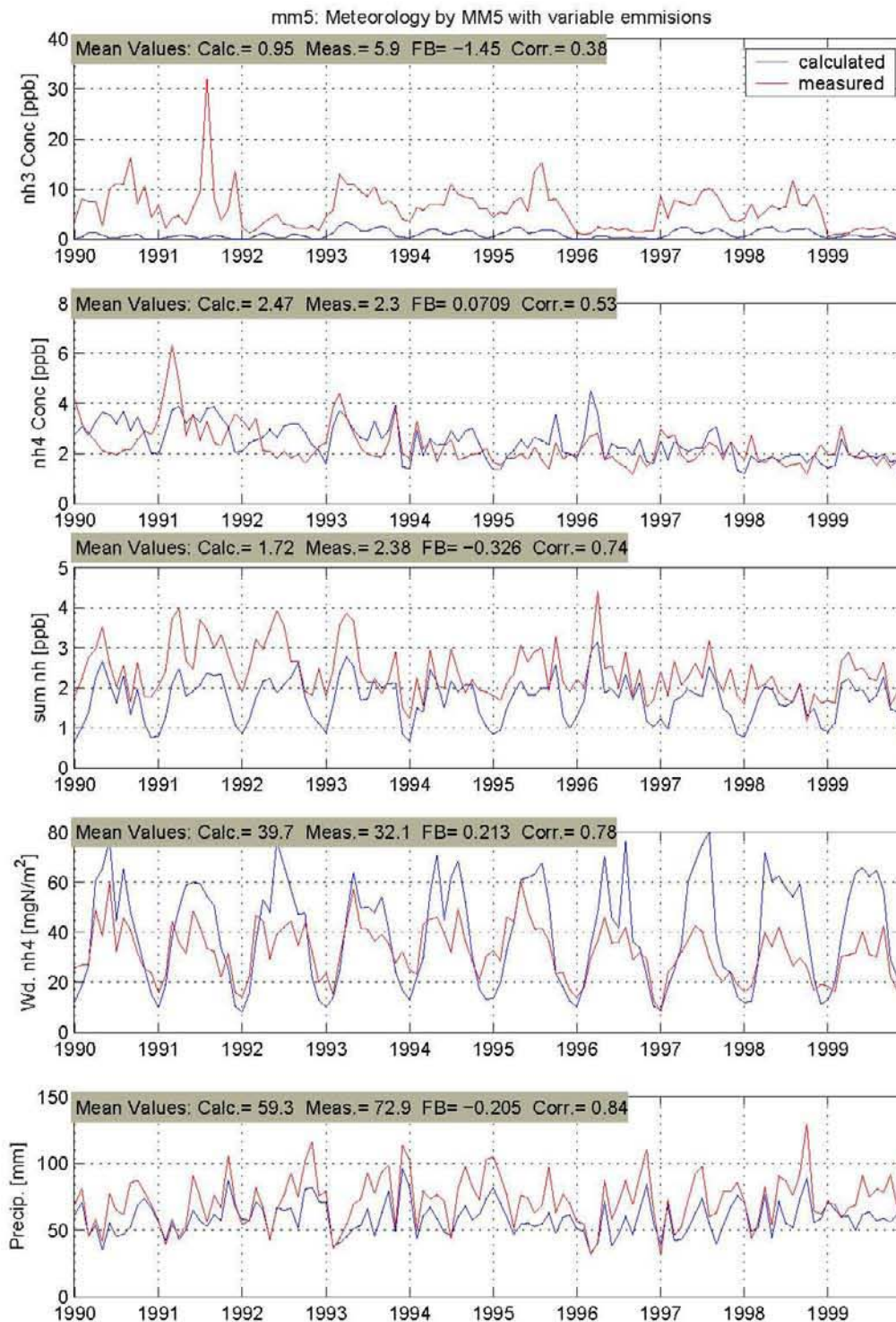


Figure 5.1: The calculated concentrations of NH_3 , NH_4 , sum of NH as well as the wet deposition of NH_4 and the precipitation is plotted against the observations from the EMEP measurement network (cf. section 3.2.6) for the period 1990-1999. The data are monthly averaged values averaged over all the available measuring sites. This means, that the data are averaged in space. The simulation is based on MM5 meteorology and the real 1990-1999 emissions. Also the mean values of the calculated and measured time series plus the fractional bias (FB) and the correlation coefficient (Corr.) between the two series are displayed in each panel.

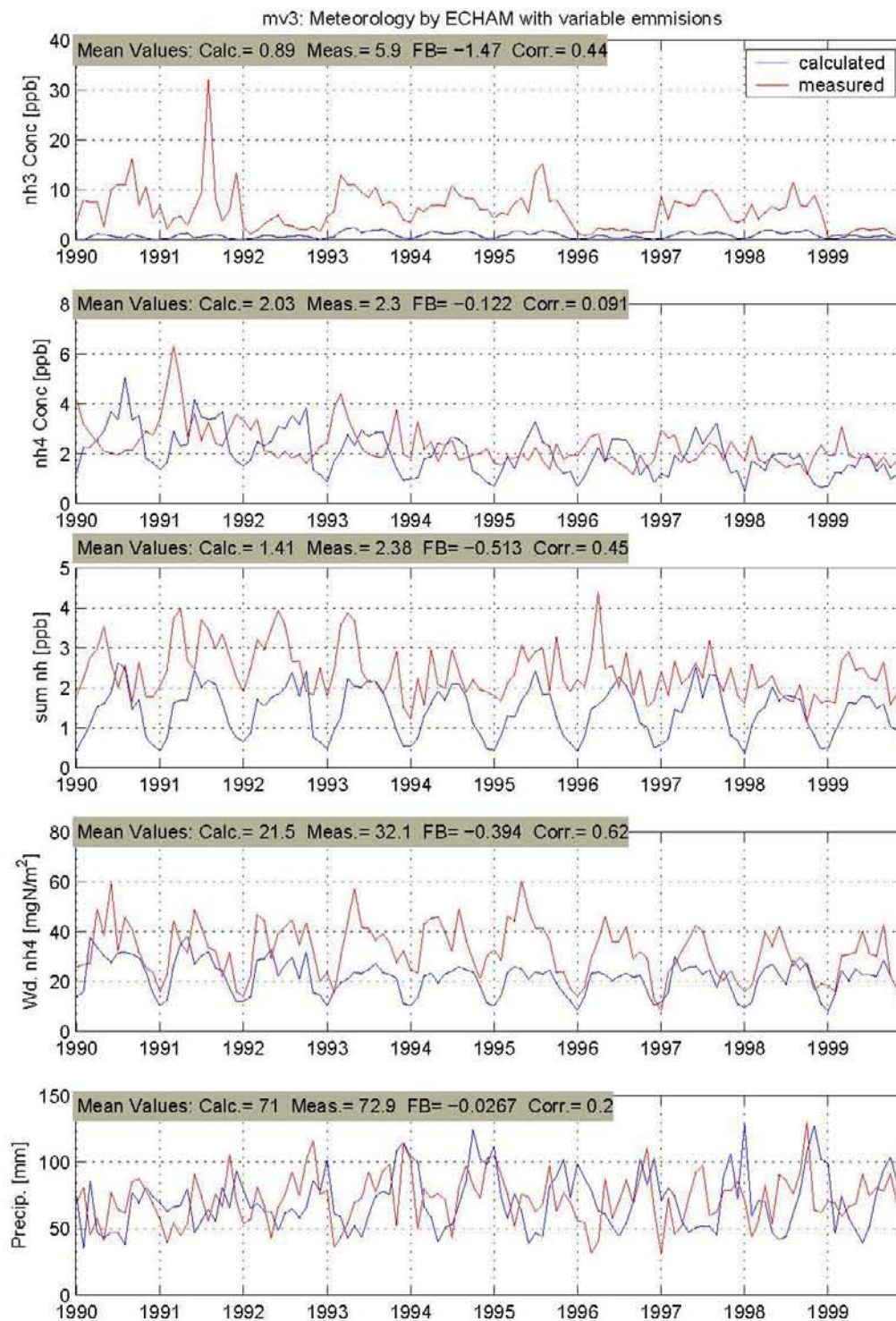


Figure 5.2: As in figure 5.1, but with the simulations based on ECHAM4-OPYC3 meteorology

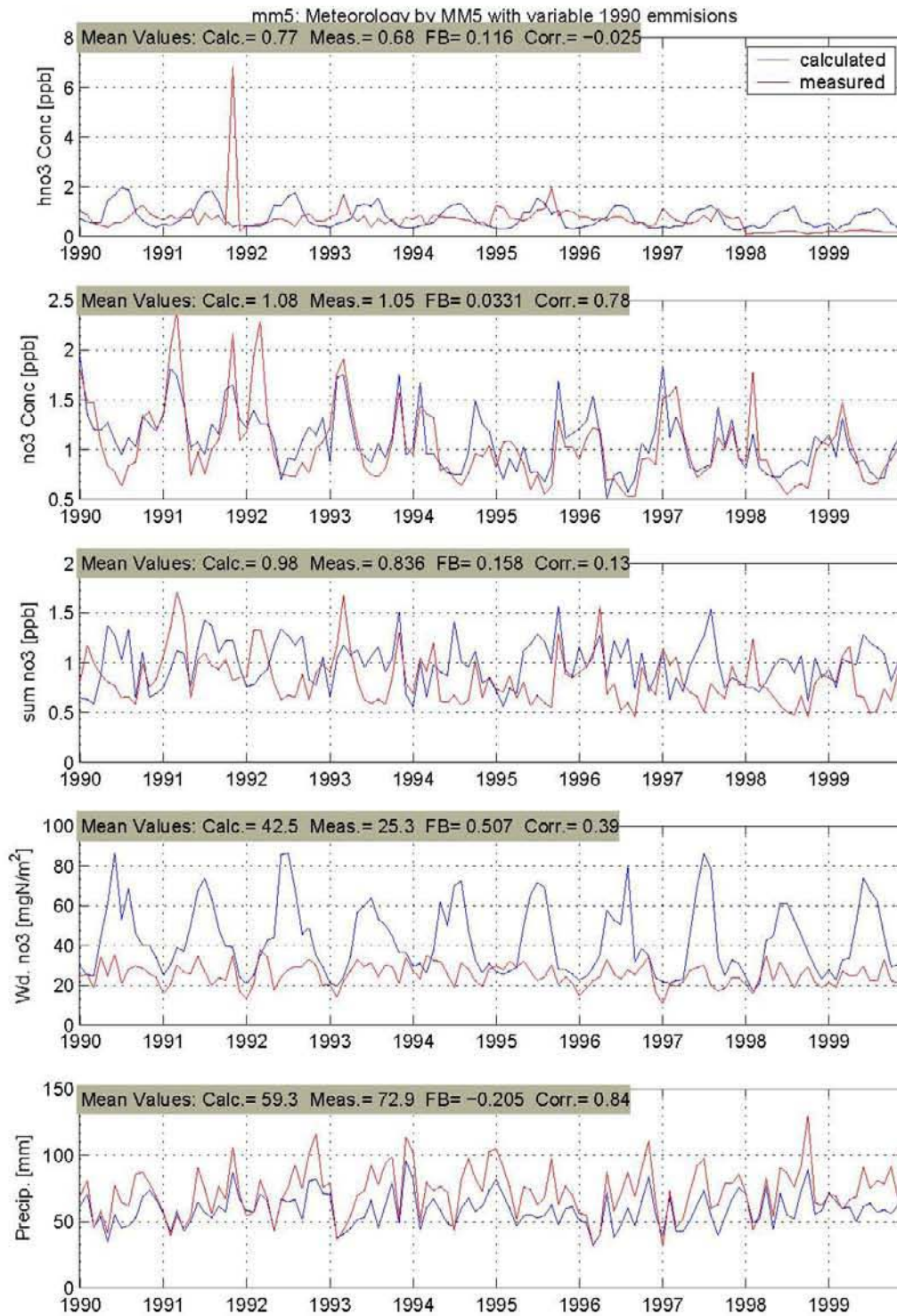


Figure 5.3: As in figure 5.1 with model calculations based on MM5 meteorology, but for concentrations of HNO_3 , NO_3 , SUM NO_3 ($HNO_3 + NO_3$), wet deposition of NO_3 and precipitation.

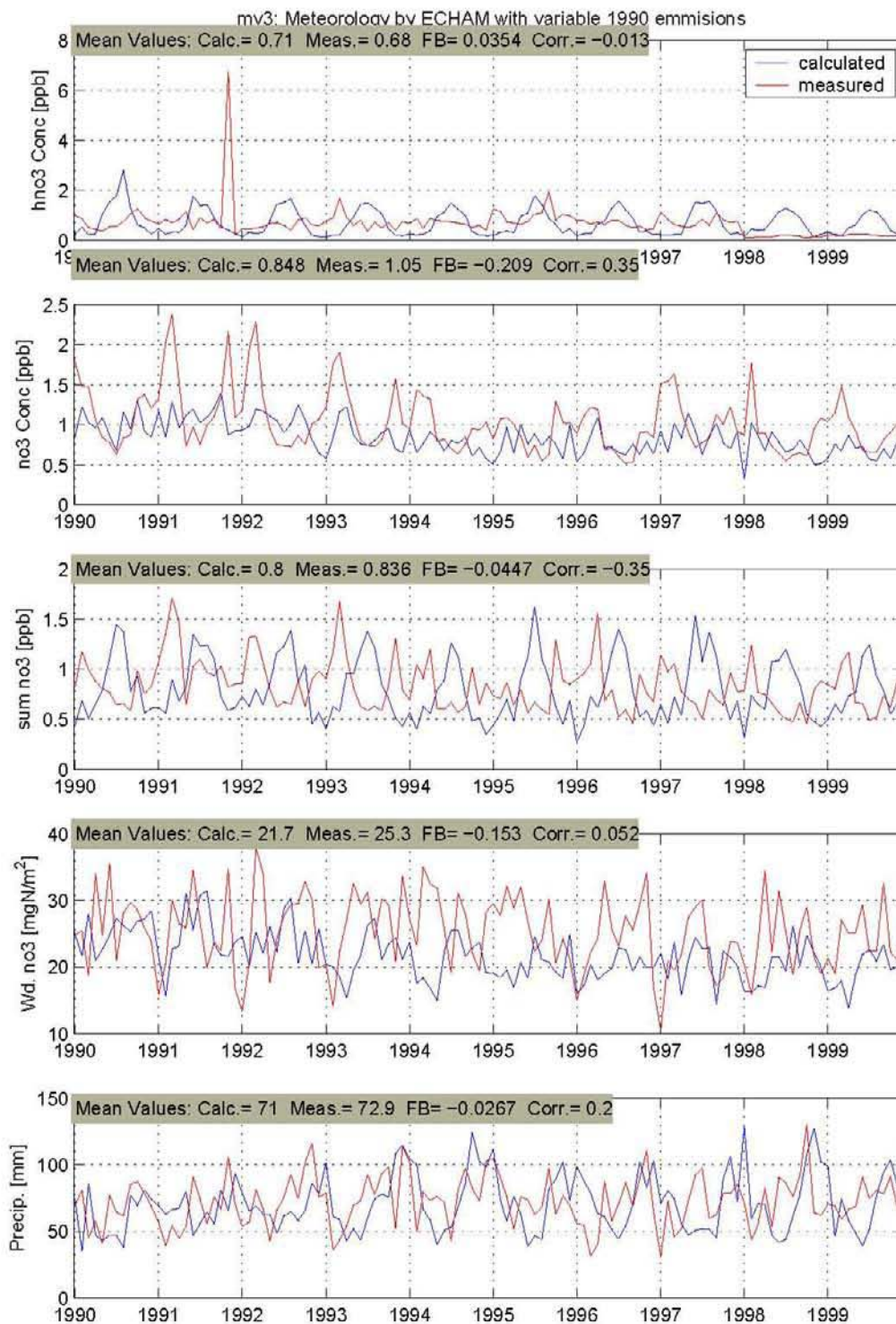


Figure 5.4: As in figure 5.3, but with the simulations based on ECHAM4-OPYC3 meteorology

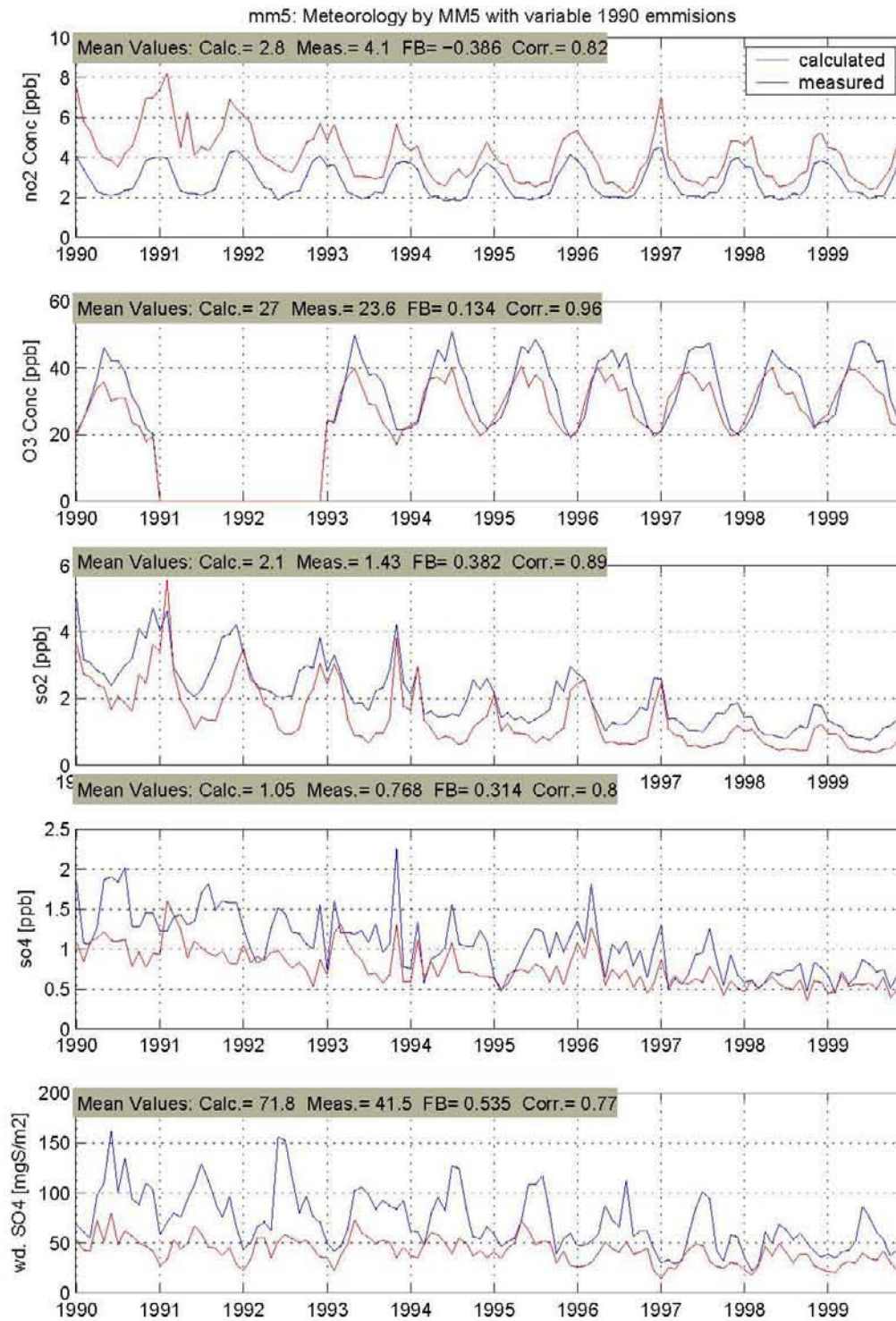


Figure 5.5: As in figure 5.1 with model calculations based on MM5 meteorology, but for concentrations of NO_2 , O_3 , SO_2 , SO_4 and wet deposition of SO_4 . Please note that measurement data of O_3 was missing for the years 1991 and 1992 in this study

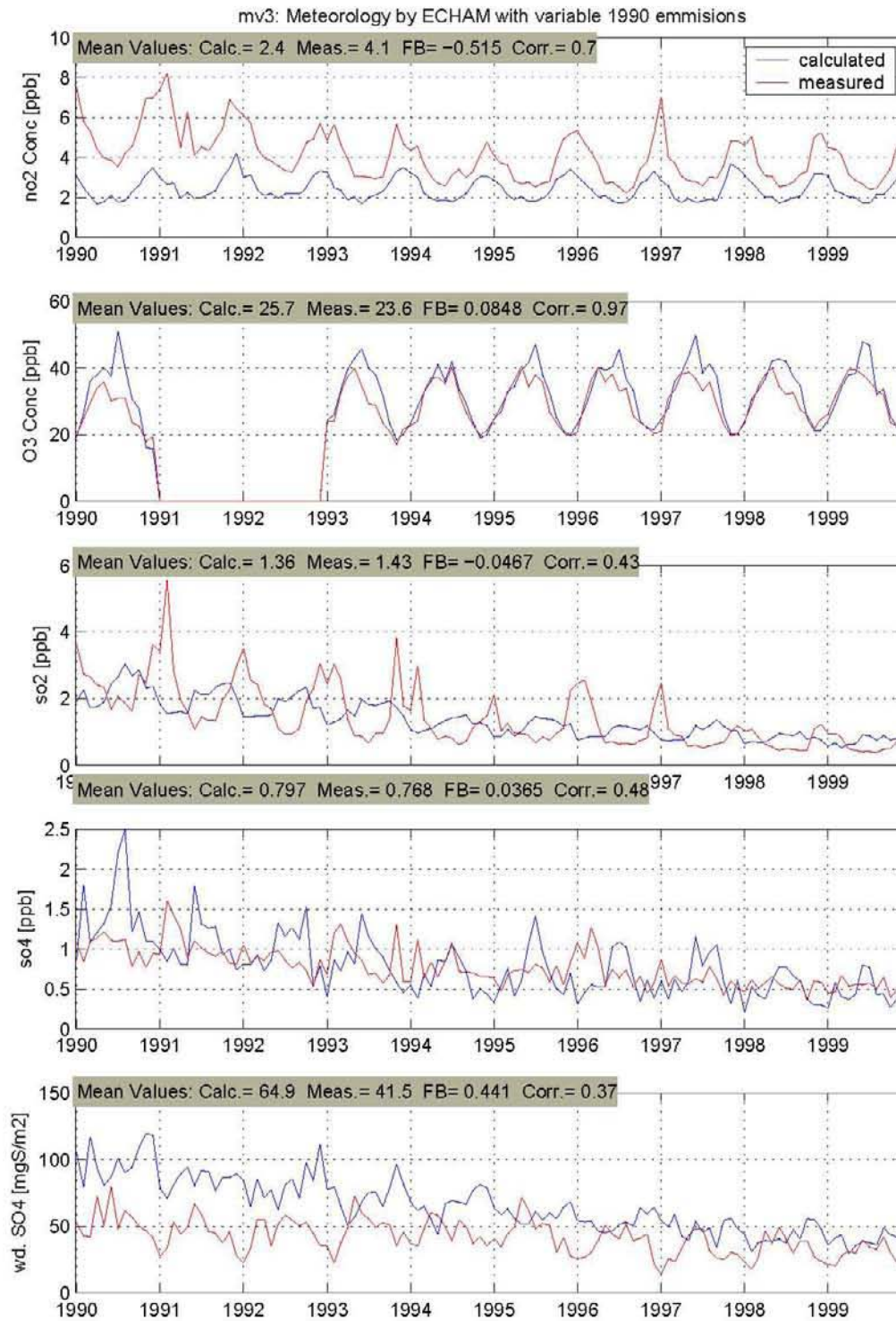


Figure 5.6: As in figure 5.5, but with the simulations based on ECHAM4-OPYC3 meteorology. Please note that measurement data of O_3 was missing for the years 1991 and 1992 in this study

5.2.2 Analysis of the nitric acid and nitrate

In the first panel of figure 5.3 and figure 5.4 the concentration of nitric acid HNO_3 is plotted. Generally both the results obtained from the MM5 and the ECHAM4-OPYC3 simulation reproduces the average level quite good. Actually, with respect to the fractional bias, the ECHAM4-OPYC3 setup is the best performing model compared to measurements. However, this might be a coincidence. First all there is an outlier in the observations (cf. in the end of year 1991) which inherently will shift the mean value of the observations and secondly the difference in mean value between the MM5 and ECHAM4-OPYC3 simulations is rather small. Both model results are very low correlated with the observations, which is not surprising since nitric acid is a very short-lived specie.

The second panel of figure 5.3 and figure 5.4 shows the concentration of nitrate. Again both simulations estimate the mean levels right. However, the climate model has a tendency of under-estimating, especially when high concentration events occur. In contrast to the results of ECHAM4-OPYC3 based simulation, the results of the MM5 based simulation correlates acceptably well with the observed data.

The sum nitric acid and nitrate is shown in panel three of the two figures (figure 5.3 and figure 5.4). Here none of the predicted model results performs well with respect to correlation. Earlier studies has indicated that the DEHM-REGINA model fails to simulate the seasonality of the sum NO_3 , probably due to lack of seasonality in the emission data [Frohn, 2004]. The low correlation coefficient confirms what was found in the first panels. The mean level is quite good for the ECHAM4-OPYC3 setup with a fractional bias on only -0.0447 compared two the MM5 setup which has a FB of 0.158.

In the two lowest panels the wet deposition of nitrate and the precipitation is shown. The wet deposition of any specie is of course very closely connected to the precipitation amount, frequency, timing and type as mentioned before. However in the plot here only the precipitation amount can be analyzed. The connection between the wet deposition and precipitation is visible in the results found here. The mean level of the precipitations is predicted very well by the ECHAM4-OPYC3 setup. In contrast the correlation is very low as could be expected from a climate model. These features are reflected in the wet deposition of nitrate, which posses the same statistical features as the precipitation (low correlation, well predicted mean level). Surprisingly the MM5 model setup have low performance with respect to mean value when predicting the precipitation level. This low performance is reflected in the wet deposition of nitrate where the mean wet deposition differs even more from the observed (FB=0.507). The correlation of the precipitation is quite high and this feature is rediscovered in the wet deposition.

5.2.3 Analysis of nitrogen dioxide, ozone, sulphur and sulphate

An analysis of the concentration of NO_2 is shown in the first panel of figure 5.5 and figure 5.6. For both the MM5 and the ECHAM4-OPYC3 setup, the picture is clear: The predicted data underestimates the observed value. This feature is probably due to the relative low resolution of the DEHM-REGINA model. There are large differences in measured NO_2 concentrations between urban and rural areas. The concentration of NO_2 is much higher in urban area, where the specie primary is emitted. With a resolution of 150 km x 150 km, the DEHM-REGINA model is not expected to resolve the urban areas very well. The model prediction will simply

smooth the high emissions close to urban area over a large area and therefore the resulting model prediction is underestimating the concentration of nitrogen dioxide. The results of Frohn [2004] support this finding. In Frohn [2004] an earlier version of the DEHM-REGINA model is simulated with two nests included and here it is found that the underestimation of the NO_2 in the model decreases with increasing resolution.

The correlation coefficient is high with respect to the prediction of the concentration of nitrogen dioxide for both model setups (MM5 and ECHAM4-OPYC3), however highest in the case of the MM5 setup.

In the second panel of figure 5.5 and figure 5.6, the concentration of ozone is predicted. Here it should be mentioned, that the missing data in 1991 and 1992 is due to an error in the observation set used for this analysis, however the missing data is not expected to change the results of this analysis.

In the case of the ECHAM4-OPYC3 model setup, the prediction of mean and variability in the ozone concentration is very good. Also the correlation is very high in the MM5 setup, however here the fractional bias is a little bit larger, than in the case of ECHAM4-OPYC3 setup. There is a tendency of the DEHM-REGINA model to overestimate the high concentration episodes during the spring. This feature is present in both model setups and therefore likely to be independent of the meteorology input.

The concentration of sulphur is shown in the center panel of figure 5.5 and figure 5.6. The ECHAM4-OPYC3 model setup succeed to predict the mean level very well, whereas the results of the MM5 based simulation shows a tendency to over-predict the mean concentration of sulphur. On the other hand only the MM5 model setup predicts the correlation successfully. In both figures the decreasing emission of sulphur during the 1990's can be observed.

Sulphate is displayed in the fourth panel of figure 5.5 and figure 5.6. The results here are very similar to what was found for sulphur. The results of the MM5 based simulation has a tendency of overestimating the mean level, however the data correlates very well with the observations. In contrast the ECHAM4-OPYC3 setup have the mean level right, however the predicted data do not correlate with the observations. Since sulphur and sulphate is very close connected through chemical conversion (sulphur \rightarrow sulphate), it is not surprising to re-discover the tendency of overprediction of the MM5 setup in the sulphate concentrations. Also the general decrease during the 1990's, which again originates in the reduced sulphur emission in the respective period, which are visible in sulphate.

Finally, the lowest panel of figure 5.5 and figure 5.6 displays the wet deposition of sulphate. Here both model setups overpredicts the mean level of wet deposition of sulphate. The MM5 model setup correlates acceptably well with the measurements in contrast to the climatic weather simulation (ECHAM4-OPYC3) which do not show any correlation with observed data. It could be expected that the tendency of both the model setups to over-predict the wet deposition of sulphate originates in the prediction of the precipitation, since the same tendency not generally is present in the concentration plots of sulphate. However inspecting the precipitation plots (lowest panel of figure 5.3 and figure 5.4, reveals that precipitation level is not over-predicted in the two simulations. It is rather the opposite! The precipitation plot shows only the amount of precipitation. The timing relative to concentration levels, the frequency of precipitation events and finally the type of precipitation, also have large influence on the size of wet depositions.

5.3 Ranking results

The purpose of this analysis is to document the performance of the model setup DEHM-REGINA ECHAM4-OPYC3. In this connection a ranking method similar to the method used in the ETEX experiment [Mosca et al., 1997] is used to validate the performance of the climate (ECHAM4-OPYC3) DEHM-REGINA setup vs the usual weather forecast (MM5) DEHM-REGINA setup. The method of ranking is described in section 5.1.3.

In table 5.3 the ranking results of the MM5 setup versus the ECHAM4-OPYC3 setup for the year 1990 is shown. The ranking has been performed on the correlation coefficient (Corr.), the fractional bias (FB) and the normalized mean square error (NMSE) of each of the chemical species (from the EMEP network). Each statistical index has been given the value one for best performance and the value two for second best performance and all these local ranks are summarized to a total rank for each statistical parameter of each simulation. Now the global rank is calculated as the sum of all total ranks for each simulation. The global rank is marked with red in the bottom of table. If the global ranks of the two model simulations are similar, it can be concluded that the two simulations have received a similar amount of one's and two's and therefore have similar performance with respect to the individual statistical parameters. In general, a lower global rank means a better performance. The MM5 model setup "wins" with 61 points, however it is marginal which determines the outcome since the ECHAM4-OPYC3 setup is nearly just as good with a global rank for year 1990 of 65.

This ranking analysis is now continued by doing a individual ranking for each year in the ten year validation period. In table 5.4, the total global results are shown. In the lowest line of the table, the total rank for a ten year period for every statistical parameter for both simulations is shown. ECHAM4-OPYC3 is the "winner" with respect to the ranking of the fractional bias and the normalized mean square error, however the MM5 model setup "wins" with respect to the correlation with only 40 points less than the ECHAM4-OPYC3 simulation.

Summing up all the results from all the years, for all the species and for all the statistics, it end up in a total global rank of 594 for the simulation based on MM5 meteorology and 598 for the simulation based on ECHAM4-OPYC3 meteorology. The message here is clear: The overall performance of the model setup with climatic weather as input to the DEHM-REGINA model is just as good as the known and well performing MM5 DEHM-REGINA model setup with respect to analysis of mean values over this ten-year period.

The fact that a climate model in a ten-year average predicts the weather just as correct as a weather forecast model with respect to annual mean values and seasonal variability if the data are used in a chemical transport model is a major finding with respect to the research field of climate change impact on air pollution. This finding constitutes the foundation for the further work within this thesis and within the research field in general. Furthermore the finding confirms the second hypothesis that states: "The Atmosphere-Ocean General Circulation Model ECHAM4-OPYC3 is able to provide a realistic and consistent picture of the meteorological key parameters applied in the air pollution model"

5.4 t-test results for the validation period 1990-1999

Since the climate model (ECHAM4-OPYC3) has a much lower resolution and in some cases simpler parameterizations, a systematic error in the air pollution results originating from the

Stat.	Option	Chemistry	Corr.			Fb			NMSE					
			MM5	Rank	MV3	Rank	MM5	Rank	MV3	Rank	MM5	Rank	MV3	Rank
1	NH4		0.72	1	0.70	2	0.192	2	0.101	1	0.28	2	0.27	1
	SUM NH		0.78	2	0.80	1	-0.352	1	-0.476	2	0.55	1	0.69	2
	WD. NH4		0.51	1	0.49	2	0.198	1	-0.232	2	0.54	1	0.63	2
	PREC		0.71	1	0.48	2	-0.164	2	-0.097	1	0.26	1	0.32	1
2	NO3		0.57	2	0.69	1	0.119	2	-0.114	1	0.34	2	0.33	1
	SUM NO		0.85	2	0.91	1	0.103	2	0.006	1	0.22	2	0.14	1
	WD. NO3		0.67	1	0.51	2	0.578	2	0.005	1	0.64	2	0.38	1
3	NO2		0.45	2	0.49	1	-0.607	1	-0.789	2	1.3	1	1.8	2
	O3		0.23	1	0.08	2	0.192	2	0.186	1	0.083	1	0.1	2
	SO2		0.52	1	0.5	2	0.294	2	-0.09	1	0.86	2	0.72	1
	SO4		0.63	1	0.54	2	0.403	2	0.353	1	0.57	2	0.52	1
	WD. SO4		0.54	1	0.37	2	0.636	1	0.647	2	0.93	1	1.2	2
4	O3 HOUR		0.2	1	0.02	2	0.197	2	0.166	1	0.088	1	0.095	2
	O3 DIUR.		0.51	1	0.45	2	0.006	1	0.017	2	0.016	1	0.03	2
Total	Rank			18		24		23		19		20		22
Global	Rank		MM5	61	MV3	65								

Table 5.3: The correlation coefficient (Corr.), the fractional bias (Fb) and normalized mean square error (NMSE) from 1990 plus ranking of these statistical parameters. The two simulations which are validated against each other are a DEHM-REGINA simulation with MM5 meteorology vs. a DEHM-REGINA simulation with ECHAM4-OPYC3 meteorology (MV3). The local ranking results are highlighted with gray and the global ranking with red.

Statistics	Corr.		FB		NMSE		Global	Rank
	Year/Run	MM5	ECHAM	MM5	ECHAM	MM5	ECHAM	MM5
1990	18	24	23	19	20	22	61	65
1991	17	16	16	17	16	17	49	50
1992	16	17	17	16	16	16	49	49
1993	18	23	23	19	21	21	62	63
1994	15	23	21	21	21	21	57	65
1995	20	21	22	20	23	19	65	60
1996	16	23	23	19	22	20	61	62
1997	20	22	24	18	23	19	67	59
1998	17	23	24	18	22	20	63	61
1999	18	23	23	19	19	22	60	64
Total	175	215	216	186	203	197	594	598

Table 5.4: The total and global ranks of the correlation coefficient (corr.), the fractional bias (FB) and the normalized mean square error (NMSE) are displayed for the MM5 based simulation and the ECHAM4-OPYC3 based simulation, respectively. The validation period is 1990-1999. The total rank is calculated for each statistical parameter and for each year and summed up to a total global rank in the lower right corner of the table.

meteorology could be introduced. The following analysis is carried out in order to test for any systematic biases of the results from the ECHAM4-OPYC3 based simulation relative to the results of the MM5 based simulation.

In this section the t-test is used to test for any significant changes in the annual mean values between the MM5 model setup and ECHAM4-OPYC3 model setup. The method of the t-test is described in general in section 5.1.2. Also the fractional bias between the two simulations (cf eq. 5.8) has been calculated in order to test for any systematic differences between the two model setups. In table 5.5 the results are shown.

$$FB = 2 \frac{MM5 - ECHAM4/OPYC3}{MM5 + ECHAM4/OPYC3} \quad (5.8)$$

From table 5.5 it can be seen that there are a systematic bias between the results based on the MM5 meteorology and the results based on ECHAM4-OPYC3 meteorology (see definition of FB in equation 5.8). The results of the MM5 based simulation generally predicts larger concentrations of the individual chemical species compared to the results of the ECHAM4-OPYC3 simulation. For most of the species (all except NH_3 , HNO_3 , O_3 and the wet deposition of SO_4) this bias is tested to be significant beyond a significance level of 10%. Whether the MM5 based simulation is overestimating the concentration of the individual chemical species or the ECHAM4-OPYC3 based simulation is underestimating relative to observations, can not be concluded from this analysis. However, from the total ranking of the fractional bias for every year (see table 5.4), it can be seen that the ECHAM4-OPYC3 model setup performs a little bit better (ECHAM4-OPYC3 186 points vs MM5 216 points) than the MM5 model setup with respect to the fractional bias. This indicates that the MM5 setup is over-predicting the concentrations. On the other hand the MM5 based simulation is much better in predicting the variability in the data (see Corr. and NMSE results of table 5.4).

The observed systematic bias between the two simulations must originate from the difference

Chemical specie	t-value	sig. level %	FB
NH_3	0.2588	>50	6.0
NH_4	1.982	10	19.3
SUM NH	5.7111	0.1	19.6
WD. NH_4	19.5549	<0.1	59.5
PREC	-5.2940	0.1	-17.8
HNO_3	1.2545	50	8.1
NO_3	3.4774	1	24.1
SUM NO	6.4189	0.1	20.2
WD. NO_3	18.54	<<0.1	64.7
NO_2	6.6202	0.1	13.6
O_3	0.2090	>50	4.9
SO_2	2.3982	5	42.6
SO_4	1.9056	10	27.8
WD. SO_4	0.8254	50	10.0
O_3	0.2090	>50	4.9
O_3 HOUR	0.2071	>50	4.9
O_3 DIUR. MAX.	0.0942	>50	22.2

Table 5.5: The DEHM-REGINA simulation with MM5 meteorology and real emissions is compared to the DEHM-REGINA simulation with ECHAM4-OPYC3 meteorology and real emissions with the t-test method. The t-value, the significant level in % and the fractional bias (FB) is displayed for the 16 selected types of chemical species (determined by the EMEP measuring network) and for the precipitation. Both the diurnal average, the hourly and the diurnal maximum concentration of ozone are included in this analysis, though only the diurnal average concentration has been discussed in the visual analysis in section 5.2.3

test	1990	vs	2040	1990	vs	2090	2040	vs	2090
Chem.	t-value	sig. level %	FB	t-value	sig. level %	FB	t-value	sig. level %	FB
NH_3	-0.0752	>50	-1.5	-0.1427	>50	-2.8	-0.0709	>50	-1.4
NH_4	0.9487	50	3.7	2.5771	2	9.1	2.0201	10	5.4
SUM NH	0.7522	50	3.5	1.7537	10	6.9	0.7745	50	3.4
WD. NH_4	-2.7840	2	-6.0	-5.1878	0.1	-14.3	-3.1180	1	-8.4
PREC	-0.0794	>50	-0.3	0.6912	50	2.2	0.8055	50	2.5
HNO_3	3.0434	1	10.1	7.0881	0.1	24.9	4.7032	0.1	14.9
NO_3	-0.5379	>50	-2.2	-2.0048	10	-7.6	-1.4130	20	-5.4
SUM NO	0.5421	>50	2.2	1.5985	20	5.6	0.9018	50	3.4
WD. NO_3	-2.5106	5	-4.2	-4.0056	0.1	-8.5	-1.9112	10	-4.3
NO_2	-0.2429	>50	-0.9	-1.0566	50	-4.0	-0.8535	50	-3.1
O_3	0.2759	>50	6.5	0.6543	>50	15.5	0.3807	>50	9.0
SO_2	1.0361	50	3.8	2.1420	5	7.9	1.4247	20	4.1
SO_4	1.1611	50	5.6	3.3354	1	14.0	2.7328	2	8.4
WD. SO_4	-3.2387	1	-5.4	-7.3648	0.1	-12.2	-3.1766	1	-6.9
O_3	0.2759	>50	6.5	0.6543	>50	15.5	0.3807	>50	9.0
O_3 H.	0.2687	>50	6.4	0.6492	>50	15.4	0.3827	>50	9.1
O_3 D.M.	0.2911	>50	6.9	0.6898	50	16.4	0.4011	>50	9.5

Table 5.6: Results from the DEHM-REGINA simulation with ECHAM4-OPYC3 meteorology and preserved 1990 emissions for the 1990's, 2040's and the 2090's, is compared using the t-test method. The t-value, the significance level in % and the fractional bias (FB) is displayed for the 16 selected chemical species and for the precipitation. The species marked with yellow are significant in all three tests. The species marked with green are significant in one or two out of three tests. Here the accepted significant level is chosen to be within 10%. The fractional bias is defined so a positive values denotes an increase and a negative value a decrease.

in meteorology between the two model setups, since everything else is similar in the two simulations.

5.5 t-test results for the periods 1990-1999, 2040-2049 and 2090-2099

Until now, the performance of the ECHAM4-OPYC3 model setup has been tested in the control period 1990-1999 for the specific EMEP measuring stations. In this section the future results are tested, but only for results at the same EMEP measuring sites of Europe. Now it is the three future scenario simulations of the 21'st century with preserved emissions, which are inspected (cf the simulations marked with red in table 5.1)

In table 5.6 results of the t-test is displayed. The t-test is used to test for any significant changes between the 1990's and 2040's, between the 1990's and 2090's and finally between the 2040's and 2090's. This test is performed to see, if the mean values of the concentrations or wet depositions of the individual chemical species are changing with a changed climate predicted by the ECHAM4-OPYC3 simulation. In table 5.6 the first three columns shows the calculated t-value, the significant level and the fractional bias when the annual mean values of

the species in 1990's is tested against the annual mean values of the same species in the 2040's. The next three columns shows the same result but for the periods 1990's against the 2090's and finally the three last columns shows the result of the period 2040's vs 2090's. A significant level of within 10% has been chosen as the threshold value for statistical significance. The cells marked with yellow are chemical species, which annual mean values are different within a significance of 10 % and which are changing significantly in all three periods. Similarly, cells marked with green are mean values that are changing significantly in one or two periods.

The first important conclusion which can be drawn from the results of table 5.6 is that the changes found in the first half of the century are continuing in the second half of the century. There are no significant changes which only happens in the beginning of the century. The chemical species which are changed, are either changed over the total period (increase/decrease between the 1990's and the 2090's) or only changed in the second half of the century. This makes it reasonable from now on only to analyze the 1990's against the 2090's and assume that the comparison of these two decades represents the changes during the whole century. Of course fluctuations in the evolution of the individual species and meteorological parameters are likely to have happen, however the results here indicates that the changes between the two decades represent the total change in the century well. From now on (in chapter 6) only the 1990's will be evaluated against the 2090's.

Both ammonium and the sum of NH are increasing significantly. On the contrary the wet deposition of ammonium is decreasing significantly. The same is the case for the sulphur-group. The concentration of sulphur and sulphate are increasing and the wet deposition of sulphate are decreasing.

A decrease in precipitation would logically decrease the wet deposition and thereby increase the concentrations of the corresponding species in the air. In the fifth row of the table 5.6 the evolution of the precipitation is shown. The averaged precipitation level over the total number of EMEP stations are not changing significantly between the two decades. This means there are no predicted changes in the precipitation level which can explain the observed evolution in ammonium and nitrate. But not only the precipitation amount which are shown here are important for the wet deposition process, also the timing of a precipitation events relative to the periods of high concentration, the frequency of the precipitation events and finally the type of precipitation (drizzle, snow, light to heavy rain etc) are crucial with respect to the amount of the wet deposition.

The concentration and wet deposition of nitrate is evolving differently. Here the concentration of nitrate are decreasing at the same time as the wet deposition of the nitrate is decreasing. However, the observed decrease in nitrate are only significant in the total period 1990's vs 2090's and the significance level is exactly 10% (just at the limit for significance by the definitions of this investigation).

5.6 Summary and discussion

Relative to observations the ECHAM4-OPYC3 model setup performs excellent with respect to the annual mean values of the different concentrations and wet depositions. However, the ECHAM4-OPYC3 setup fails to predict the variability in the data. The correlation coefficient relative to observations are very low for most of the species.

The ECHAM4-OPYC3 setup are also able to predict a general decrease in sulphur during the 1990's. This is not surprising since it originates from the reduced emissions and not the weather. However the model setup is also able to reflect the reduced emissions of sulphur in e.g. the ammonium concentration, which is reduced due to a decrease in acid in the air.

Generally the concentration of particles and the wet depositions are predicted very well with respect to their mean values. However the ECHAM4-OPYC3 setup have a tendency of underestimating the nitrate concentration when high concentration events occur. Also, for both model setups an underestimation of nitrogen dioxide is seen, probably due to the low resolution of the model.

Ozone is predicted very well with both respect to mean value and variability. This feature may result from a relatively low dependency of the weather relative to the dependency of the natural and anthropogenic emissions of ozone precursors and of the seasonal changes of global radiation and temperature.

The MM5 model setup is known to perform well (cf. Christensen [1997], Frohn [2004], Brandt et al. [2005], Geels et al. [2004], van Loon et al. [2004], and van Loon et al. [2006]) and the ranking carried out here shows that the performance of the ECHAM4-OPYC3 setup are very similarly. The ECHAM4-OPYC3 performs better with respect to mean values than the MM5 setup, however it is the other way around in the case of prediction of the variability of the data.

A bias between the two different setups has been identified, which inherently must originate from the meteorology which is the only thing that differs between the two simulations.

The analysis of the future scenarios results in the conclusion that it is reasonable just to include the 1990's and the 2090's in the further analysis.

Finally there is a tendency of increase in the secondary particles concentrations (NH_4, SO_4) and a tendency of decrease in the wet deposition of the same particles. The precipitation amount seems to remain unchanged in the investigated period. It is very important to remember that all these result are based on the EMEP measuring sites in Europe and there is a risk that these stations might not represent the actual pollution or precipitation distribution of Europe. However by assuming that these EMEP stations do represent the pollution distribution of Europe leads to the conclusion that the precipitation timing, frequency or type have changed between the two decades in order to explain the observed changes in particle concentration and the ancillary wet depositions.

Since the DEHM-REGINA model is a hemispherical model, it is possible to analyze the changes between the two decades (1990's and 2090's) in every grid cell for the entire hemisphere. This will give a more adequate picture of the projections found in this thesis. In the following chapter, this full data set are analyzed. This means that predicted data are analyzed in each grid cell instead of here only in specific grid cells spread randomly over Europe. Here it should be noted that the version of the DEHM-REGINA model used in the next section is a further developed version compared to the version used in this validation chapter. These simulations with the new improved version of the model were carried out since all the original simulated data were lost due to major power failure and disk crash at NERI.

6 Results and discussion

This chapter contains an evaluation of the results found in this thesis with respect to the change in meteorology and in air pollution levels and distributions in the future. First the ECHAM4-OPYC3 meteorology, which the DEHM-REGINA simulation is based on is summarized. After that eight selected chemical species are shown and analyzed with respect to their distribution in northern hemisphere in the decade 1990-1999 and in the future decade 2090-2099 and these results are discussed with respect to changes in physical and chemical processes in relation to a changed climate.

The chemical long-range transport model DEHM-REGINA, keeps track of the physical and chemical processes of 63 different species. To do a full analysis of all these chemical species is far beyond the scope of this thesis. Therefore a limited number of species has been analyzed and only eight of these chemical species will be displayed and discussed here. The chosen species are sulphur SO_2 , sulphate SO_4 , ozone O_3 , nitrogen dioxide NO_2 , particles PM_{10} , *seasalt*, hydroxyl radicals OH and isoprene C_5H_8 .

The results in this chapter are displayed similarly with one figure for each parameter. Each of these figures contains four subplots. In the first and second subplot (a) and (b), ten-years average values are shown. These ten-year average values are calculated from ten annual either accumulated or averaged values, depending on the characteristics of the actual parameter. For example the precipitation and the deposition is accumulated over each individual year before making a ten-year average, whereas e.g. temperature is first averaged over each year and afterwards averaged over the ten year period to give a ten-year mean value.

Subplot (a) shows an average of the parameter under study in the first decade (1990-1999) and subplot (b) shows the same parameter in the second decade (2090-2099). Subplot (c) shows the difference between the two decades. This difference is calculated both as an absolute difference (cf. equation 6.1) and as a percentage difference (cf. equation 6.2). However, for each of the parameters only one of these two differences has been selected for illustration since they basically shows the same and it varies which of the difference plot are most visual illustrative.

$$\text{Absolute difference} = 2090's - 1990's \quad (6.1)$$

$$\text{Percent} = \frac{2090's - 1990's}{1990's} * 100\% \quad (6.2)$$

In order to separate out insignificant low-level changes or to avoid noise where the 1990's mean values in equation 6.2 is close to zero, a white color is used to mark these uninteresting

areas. Mean values below 1% of the maximum mean value in the 1990's is colored white in both types of the difference plot (except for the case of SO_2 in figure 6.10 and isoprene in figure 6.20, where the threshold value is set to 1‰ of the maximum mean value of the 1990's).

Finally subplot (d) shows the statistical significance of the change of mean values between the two decades. This significance is derived from the students t-test discussed in section 5.1.2. The legend of the plot is constructed so that all colors besides white marks the areas of significant changes within different significance levels. Here the threshold value for significance is chosen to be within the 0.95 fractile corresponding to the 10% significance level.

6.1 Changes in meteorology calculated by the ECHAM4-OPYC3

In this subsection, the changes in mean values in the different meteorological parameters from the 1990's to the 2090's are investigated.

The mean values of the meteorological parameters are constructed from the ECHAM4-OPYC3 simulation modified to the higher resolution DEHM-REGINA grid. This modification is simply done by linear interpolation of the ECHAM4-OPYC3 data to the DEHM-REGINA grid projection (cf chapter 4). The mixing height and the global radiation are the only two parameters, which has been derived from other ECHAM4-OPYC3 parameters. The mixing height is based on simple energy balance considerations and the global radiation is calculated from the cloud cover from the ECHAM4-OPYC3 simulation (see subsections below).

The following 9 figures (6.1-6.9) shows precipitation amount, precipitation frequency, 2 meter temperature, mean sea level pressure, wind speed, specific humidity, mixing height, global radiation and finally sea ice derived from the ECHAM4-OPYC3 meteorology.

6.1.1 Precipitation amount

In figure 6.1 the precipitation from the ECHAM4-OPYC3 simulation is plotted. As explained above, subplot 6.1(a) shows the mean annual accumulated precipitation amount for the 10 year period (1990-1999). To compare with figure 6.1(b) illustrates the same mean annual accumulated precipitation levels but for the future decade 2090-2099 and figure 6.1(c) shows the differences between these two decades.

From figure 6.1(a)-6.1(c) it is clear that the precipitation amounts in the Arctic regions will increase in the future according to these simulations. At the same time southern Europe and the south-western United States will become more dry. This is important to remember when comparing with the validation results based on the EMEP stations (cf. section 5.6). In the analysis based on the EMEP station network, it was found that there were no significant changes in the EMEP area. However with the results presented here it becomes clear, that the northern increase and southern decrease in Europe in precipitation levels averages out, when solely comparing data extracted of the locations of the EMEP measuring network. This is an example of where the method used in section 5.6 fails to give a correct overall result, since the stations available for the analysis are situated randomly (with respect to the interest in this study) and the reason why the analysis carried out here is very important to do.

Subplot 6.1(d) shows that all the overall changes in subplot 6.1(a)-6.1(c) are significant by the definition of significance given above. The reddish colors represent the areas with significant increase and the green colors represent significant decreases. Also here the fact mentioned above, that the changes in the EMEP area averages out becomes clear. The area where the most EMEP stations are located is not significant with respect to changes in precipitation levels in the next century and the rest of the EMEP stations, which lies within the changing areas are divided between significant increasing and decreasing areas.

It is noteworthy that the increase in the Arctic region is very significant. Over large areas the significance level is within 0.1%, which is extremely significant. The same thing is valid for southern Europe, Caribbean, Mexico, California and a large maritime area close to the Hawaiian islands. However, here the significance values are negative, which means that the precipitation amount is decreasing in these areas during the next century.

Precipitation frequency

Figure 6.2 illustrates the results for the precipitation frequency. The precipitation frequency is defined as an on-off process. Each time a chosen precipitation threshold is exceeded the similar 6-hour interval is given the value 1 or else the interval is given the value 0. Now the average of these ones and zeros is taken in the respective periods and this average is plotted. This means, that values close to one represent a high frequency of precipitation in a given grid cell and similarly values close to zero represents areas with a low frequency of precipitation. In the frequency plot of the precipitation a 1 mm threshold value is used to define the precipitation frequency. This means that only precipitation values above 1 mm in a given six-hour interval is taken into account, when it is decided, if there has been a significant amount of precipitation in a specific grid cell. This threshold value is chosen as the best estimate of when there is enough precipitation to wash-out a significant amount of particles or gas from the air. The estimate is based on the results in table 6.1 and personal conversation with J. Brandt, NERI, and J.H. Christensen, NERI, (2006).

Table 6.1 shows examples of typical scavenging rates of SO_2 , SO_4 and HNO_3 due to precipitation. The first column contains the number of mm rain in a given six-hour interval. The second column illustrates the below-cloud scavenging in percent and finally the third column shows the in-cloud scavenging in percent. This means, that if it rains for example 3 mm within a six-hour interval, then approximately 36% of SO_4 particles will be washed-out of the unsaturated air below the cloud base and approximately 59 % of the SO_4 particles will be washed-out of the saturated air within the cloud. The same wash-out fractions are shown for HNO_3 and SO_2 . The percentage values in the table are calculated from the parameterizations of the in- and below-cloud scavenging in the DEHM-REGINA model [Christensen, 1997], [Frohn et al., 2002a] and [Frohn, 2004].

In the percentage difference plot (subplot 6.2(c)) some white areas appear. This is areas with very low precipitation frequencies below 1% of the maximum 1990's value (cf. definition above).

In the precipitation frequency plot the same tendency as in the precipitation amount plot is evident. The Arctic region is characterized by an increase and the southern mid-latitudes and the subtropics (except Asia) is characterized by a decrease. All together this means, that the ECHAM4-OPYC3 simulation projects less precipitation and less frequent in the

	mm pr 6 hour	below cloud %	in cloud %
SO_2	1	9.9	63.0
	3	26.8	95.0
	5	40.5	99.3
	7	51.7	99.9
	9	60.8	100.0
SO_4	1	13.9	25.9
	3	36.2	59.3
	5	52.8	77.7
	7	65.0	87.8
	9	74.1	93.3
HNO_3	1	39.3	75.3
	3	77.7	98.5
	5	91.8	99.9
	7	97.0	100.0
	9	98.9	100.0

Table 6.1: In the table typical values of the wash-out of SO_2 , SO_4 and HNO_3 from the air due to precipitation are shown. The second column shows the number of mm rain in a six hour interval. The third column shows the below-cloud scavenging in percent and finally the fourth column shows the in-cloud scavenging in percent. This means, that if it rains for example 3 mm within a six hour interval, then approximately 36% of SO_4 particles will be washed-out of the unsaturated air below the cloud base and approximately 59% of the SO_4 particles will be washed-out of the saturated air within the cloud. The same wash-out fractions are shown for HNO_3 and SO_2 . The percentage values in the table are calculated from the parametrization of the in- and below-cloud scavenging in the DEHM-REGINA model [Christensen, 1997] [Frohn, 2004].

mid-latitudes and subtropics and more precipitation in the Arctics. Denmark is situated in an area between decreasing and increasing values and from subplot 6.2(d), it can be seen that there are no significant changes predicted in this area. The fact that ECHAM4-OPYC3 projects increasing precipitation over a very large areas like the whole Arctic region, together with the very large changes, confirms that the changes are very likely to occur in the future. This feature is also in good agreement with other model results [Stendel et al., 2002].

6.1.2 2 meter temperature

In figure 6.3 the 2 meter temperature (T2) is shown. In the temperature analysis carried out in this thesis both the 3D temperature from the fifth layer (height approximately 230 above MSLP Frohn [2004]) of the DEHM-REGINA model and the 2 m temperature was analyzed. However, since the results were very similar, only the 2 m temperature is shown here.

Concerning the difference plot (fig. 6.3(c)), it is important to note, that the color-scale is changed, so all colors are positive. In other words the temperature is increasing everywhere. Also the significance plot 6.3(d) emphasizes this fact by showing extremely positive significance everywhere. This general temperature increase with local hot spots over Southern Europe and the Arctics is similar to other model results [Stendel et al., 2002]. In relation to the climate in Denmark in the next century, it is interesting to note, that the warming is rather small in the path of the wandering lows over the North Atlantic.

6.1.3 Mean sea level pressure

Figure 6.4 includes the mean sea level pressure (MSLP). A rather large decrease in MSLP over the Arctic region is detected (note the legend of the plot). Around 30-50 degrees north the mean sea level pressure seems to increase between the two decades. Inspecting the significance plot (subplot 6.4(d)) reveals that the pressure decrease in the Arctic region is very significant. The white area in the significance plot is areas with insignificant or no changes and it is interesting to see, that there especially over sea and over central Europe, is a tendency of the noise to exceed the signal or there is no signal at all. This could imply that there are alternation between high and low pressure in these regions. This is of course true in the storm tracks where the mean sea level pressure continually changes with the passing of the lows and therefore the signal-to-noise ratio becomes relatively small.

In connection to the discussion here it is interesting to note that the NAO (North Atlantic Oscillation) index in both the 1990's and the 2090's decade is positive for the ECHAM4-OPYC3 simulation used here. The results are displayed in figure 15a in Stendel et al. [2002]. The fact that the NAO index is similar in the two decades separates out the long-term natural effect of the pressure patterns in the northern hemisphere as an explanation of possible changes in the pollution levels when analyzing the final data set from the DEHM-REGINA model.

6.1.4 Wind speed

In figure 6.5 the windspeed is shown. By comparing subplot 6.5(a) and subplot 6.5(b) visually, it is very difficult to detect any significant changes in the wind speed between the two decades. However subplot 6.5(c) reveals some apparently small changes (note the color scale of the plot).

However relative to the absolute wind speeds in the two decades, the differences comprises up to approximately 10% of the total wind speed. The wind speed are generally increasing over Arctic, Scandinavia and the Baltic. A decrease in wind speed is projected over parts of the Atlantic ocean, however this could indicate a northwards shift of the storm tracks. Also these changes in wind speed are significant when testing the results according to equation 5.6.

6.1.5 Specific humidity

Figure 6.6 shows the specific humidity. As in the previous figures, subplot 6.6(c) illustrates the difference between the 1990's and the 2090's. The color scale for this difference plot is changed so all colors represent an increase. The specific humidity increases everywhere, however the increase is largest over the southern maritime regions. This is easy to explain since it was shown in figure 6.3(c) that the temperature increases everywhere in the domain of interest. When air temperature increases, the ability of the air to contain water becomes larger. Over the maritime areas more water will evaporate than over terrestrial areas and therefore a homogenous temperature increase can lead to an differentiated humidity increase, with largest enhancement over sea (see e.g. over the Mediterranean sea in figure 6.6).

From subplot 6.6(d) it is clear that just like the temperature increase, the increase in the specific humidity is very significant everywhere in the northern hemisphere (except over a small area in the Rocky Mountains).

6.1.6 Mixing height

The mixing height here is not a direct parameter extract of the ECHAM4-OPYC3 data. The mixing height is calculated from a simple energy balance equation for the internal boundary-layer [Berkowicz and Olsen, 1990], [Gryning and Batchvarova, 1990], [Christensen, 1997] and [Brandt, 1998].

Physically the mixing height depends on two main processes in the air, mechanic and thermal turbulence, respectively. The mechanical turbulence is a result of the vertical wind profile i.e. dependent on the surface characteristics, the stratification in the boundary layer and the wind speed. The thermal turbulence on the other hand depends on the temperature profile in the atmosphere and the temperature gradient between the surface of the earth and above lying air. The larger the vertical temperature gradient is, the more convection and thereby the higher mixing height. The vertical temperature profile can change due to at least three main processes: The first process is the global radiation, which heat up the air and earth surface differently. This differentiated heating results in both horizontal and vertical temperature gradients and the latter leads to a sensible heat flux and to thermal turbulence. Obviously, there is also a latitudinal, a diurnal, a seasonal and a annual dependency of the ability of the global radiations to heat up the atmosphere and the surface.

The second process, which participate in changing the thermal turbulence, is atmospheric and oceanic transport of heat. The wandering lows is an atmospheric main agent, when considering transport of heat across the latitudes. On longer time scales the oceanic transport of heat also becomes important. For example the surface currents of the thermohaline circulation contributes to a very large part of the cross-latitude transport of heat in the ocean and through thermal process also in the air.

Finally the third process, which can alter the vertical temperature gradient and thereby the amount of thermal turbulence, is the latent heat flux. The ability of water to condense and evaporate can move and release large amounts of heat in the atmosphere. The latent heat flux can play a major role in the vertical temperature profile of the air and earth surface.

In figure 6.7 the mixing height is displayed. By inspection of the absolute difference (cf. equation 6.1) between the two decades in figure 6.7(c), it becomes clear that the mixing height generally increases over central and southern Europe. This increase coincides with the enhanced temperature increase (cf. figure 6.3(c)). The same phenomena is seen over the western United States, however here it is less pronounced. Over sea the mixing height is either unchanged or decreasing.

Furthermore, the mixing height can be advected with an air mass. This complicates the detective work when searching for explanations to a certain change. This means, that one should be very careful, when concluding on such a complicated parameter as the mixing height. In order to get a more nuanced picture of which processes dominate, further investigation of the surface heat flux and the friction velocity are needed.

However comparing the predicted changes in mixing height with wind speed figure 6.7 reveals that the mixing height is also closely connected to the wind speed. With a rough view it can be seen that in many places (besides of central and southern Europe) the increases in mixing height is projected to occur over the same areas as the wind speed is increased. This could lead to the conclusion that the mechanical contribution to changes in mixing height are dominating in these places. The coincidence of increasing temperature and increasing mixing height is a typical example of the thermal effect on mixing height. Also along the east coast of United States and across the Atlantic towards Scandinavia a decrease in the mixing height can be observed (figure 6.7, subplot (c)). A warming of the the cold air in north could explain this observed feature, since this will reduce the temperature gradient from the sea surface and up in the atmosphere.

6.1.7 Global radiation

In equation 6.3 and 6.4 the derivation of the global radiation from the ECHAM4-OPYC3 cloud cover is given.

$$\text{Global radiation} = \max(0, 1353 * \cos(\text{sunangle}) * c1 * \text{clouds}) \quad (6.3)$$

where the constant $c1=0.75$ (corresponding to the transparency of the atmosphere), the sunangle is the varying angle of the sun relative to a specific point of the earth and finally the clouds is derived as

$$\text{Clouds} = 1 - c2 * \text{clc2d} \quad (6.4)$$

where the constant $c2=0.9$ and clc2d is the 2-dimensional cloud cover from ECHAM4-OPYC3 given as a fraction between zero and one.

The two constant $c1$ and $c2$ in equation 6.3 and 6.4 is empirical found by J. Brandt (NERI) by inspection of measurement data from two locations in Denmark (Ålborg and Risø). This final parametrization of the global radiation has been tested against measurements and it

is found to give vary good results compared to observations from Denmark [Brandt et al., 2001a],[Brandt et al., 2001b] and [Brandt et al., 2000]. However, it has not been shown to be valid for other parts of the earth, but that is not considered to be vital in this study.

In figure 6.8 the global radiation is shown. The global radiation is, of course, very latitude dependent and shows a very clear latitude-dependent structure in all the four polar-sterographic plots of figure 6.8. The areas marked with yellow and the red colors in subplot 6.8(c) are all areas with increasing global radiation between the two decades. Because of the construction of the global radiation in this analysis an increased global radiation value should be a result of less 2D cloud cover. Only in the Arctics and in the southern edge of the domain (especially over Asia), the global radiation is decreasing which here is equivalent to an increase in 2D cloud cover. Inspecting the significance of the results reveals that an increase in global radiation at temperate and subtropical latitudes is highly significant. Also the decrease in global radiation detected over South Asia is a highly significant between the two decades. However the detected decrease over the Arctic area is insignificant.

6.1.8 Sea ice

Figure 6.9 shows the sea ice extend and the significant changes between the two periods. Again it is important to note the color-bar in the difference plot, since the sea ice is decreasing everywhere (both green, yellow and orange colors). The sea ice is in this analysis defined as a fraction between one and zero in each grid cell. This means that this sea ice plot does not express anything about the sea ice thickness. From the results here it can only be concluded if there are any sea ice at all and how large the given fraction is in a specific grid cell on average. The existence of sea ice is interesting with respect to the reflective properties of the surface and to the atmosphere-ocean interaction. Surprisingly, the largest decreases in sea ice cover is found within the Arctic basin (cf east of Svalbard and north of the Bering Strait) and not as one could expect at the ice edge.

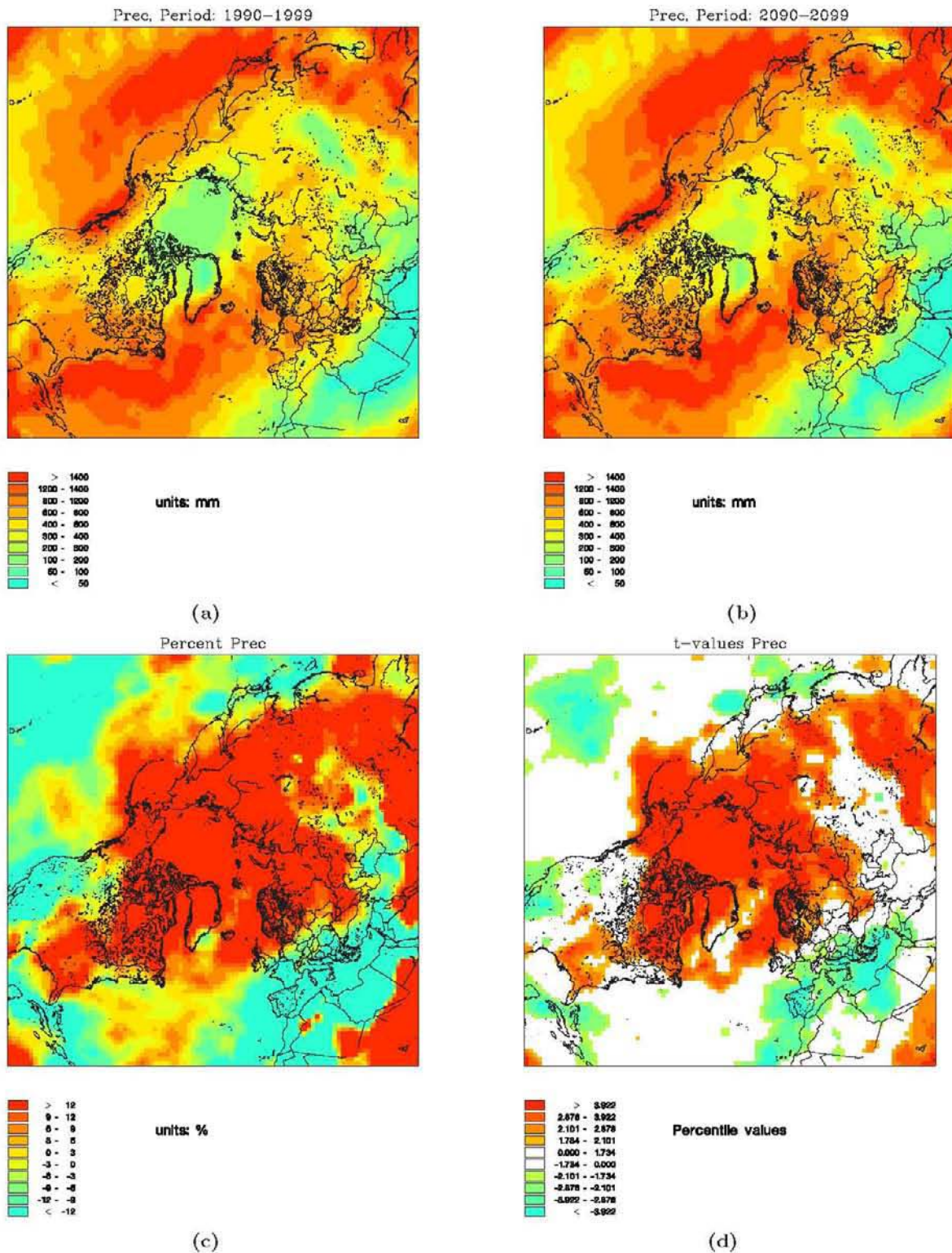


Figure 6.1: The annual accumulated precipitation amount. In subplot (a) accumulated annual averaged precipitation amount is shown for the decade 1990-1999. Subplot (b) illustrates the same accumulated precipitation but for the decade 2090-2099. In subplot (c) the difference between the two decades are shown and finally subplot (d) illustrates the significance level of the results found in subplot (c) according to the t-statistics. Generally the precipitation amount is increasing in the polar and mid-latitudes and the precipitation amount decreases over the central and southern part of Europe, south western part of United States, over Japan and over the Isles of Hawaii

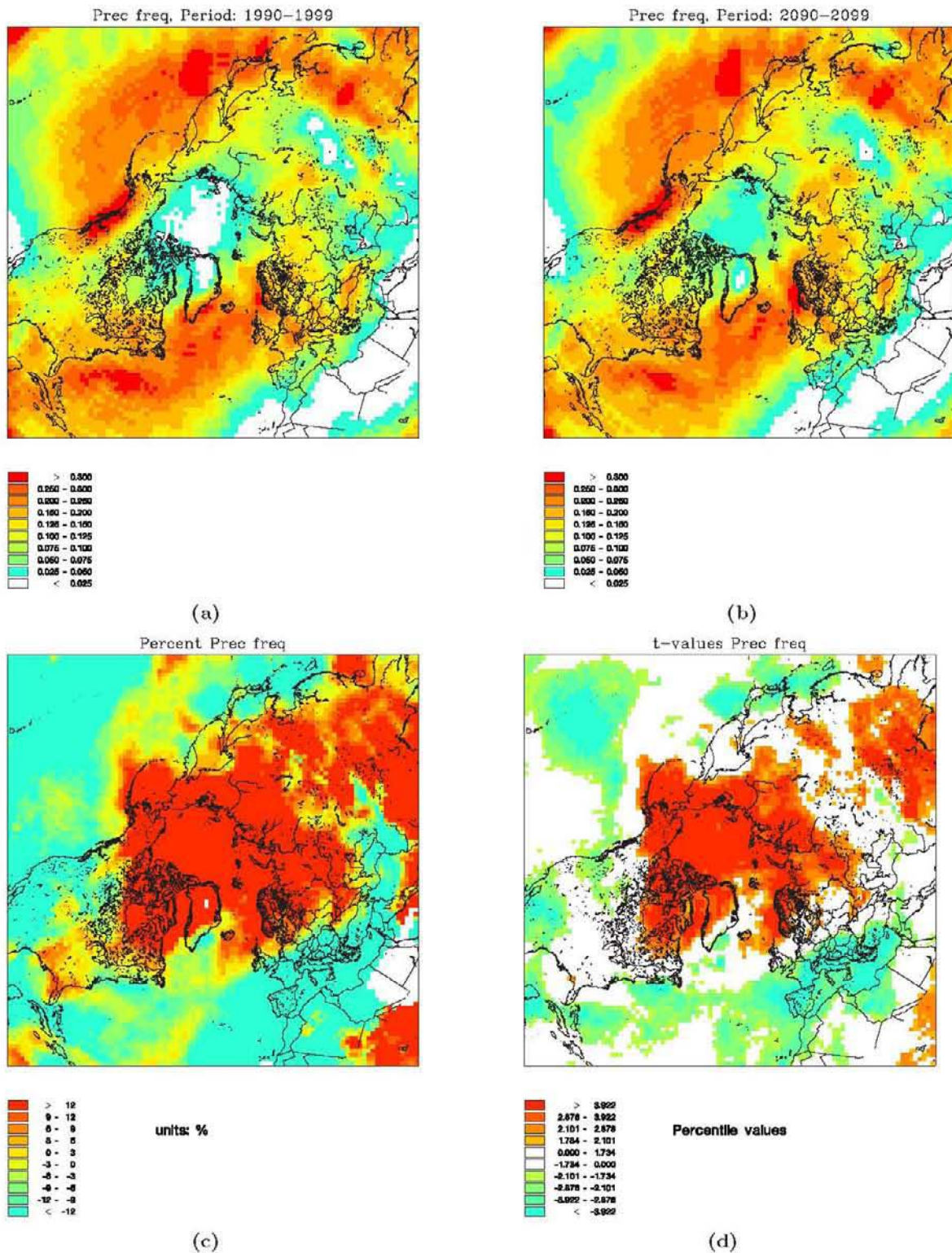


Figure 6.2: Precipitation frequency, as in figure 6.1.

The precipitation frequency is defined as a fraction between 0 and 1, the threshold value for precipitation in a given six-hour interval is 1 mm. From the difference plot (c) it can be seen that the frequency of precipitation episodes generally are projected to increase over the polar and subpolar regions. On the contrary a decrease in frequency is predicted to occur further to the south (central and south Europe, over most of the United States and central Asia)

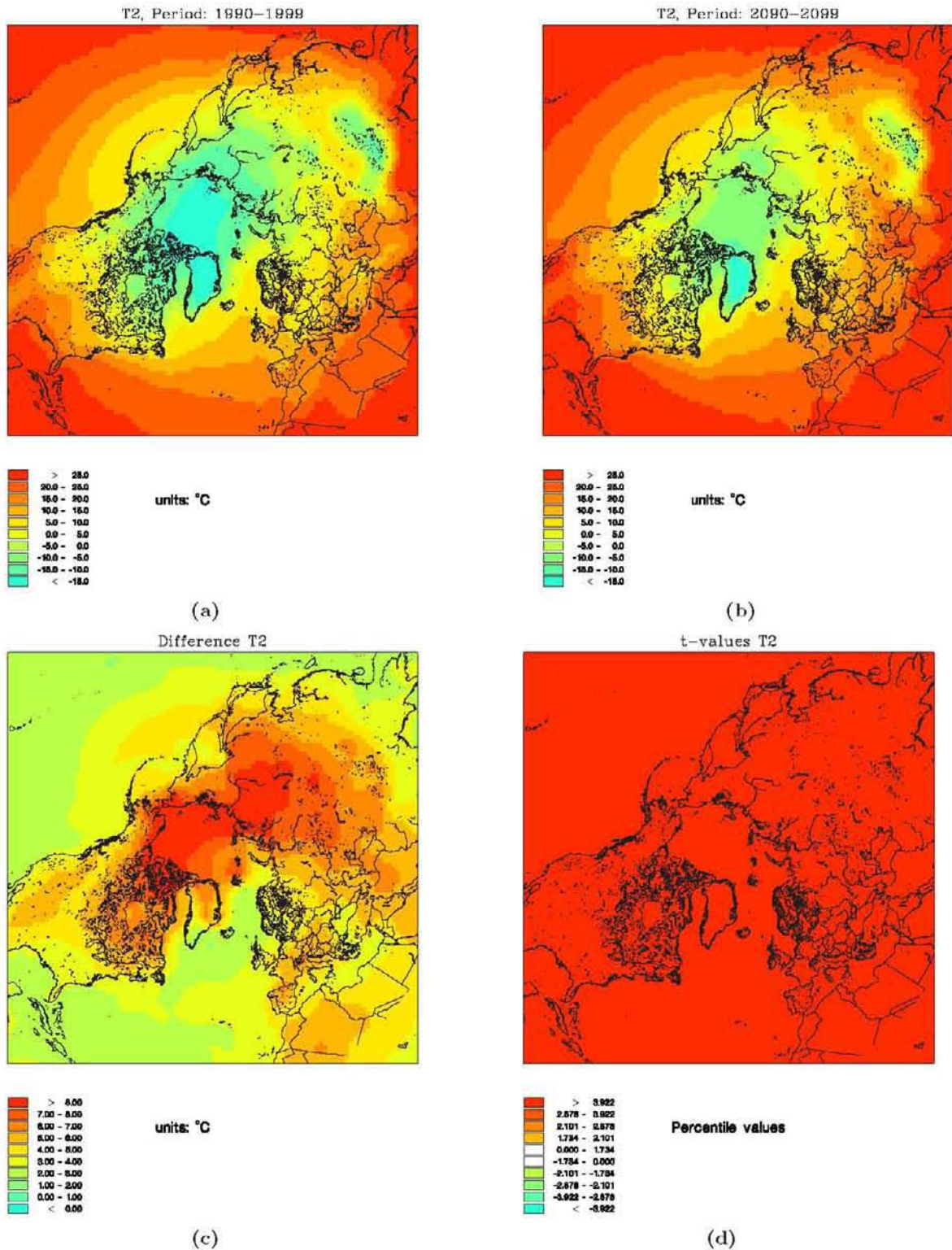


Figure 6.3: 2 meter temperature, as in figure 6.1.

The 2 meter temperature is predicted to increase everywhere in the domain (note color scale of the difference plot (c)) and from the plot of significance level (d) it is shown that this projected increase is highly significant everywhere in the domain

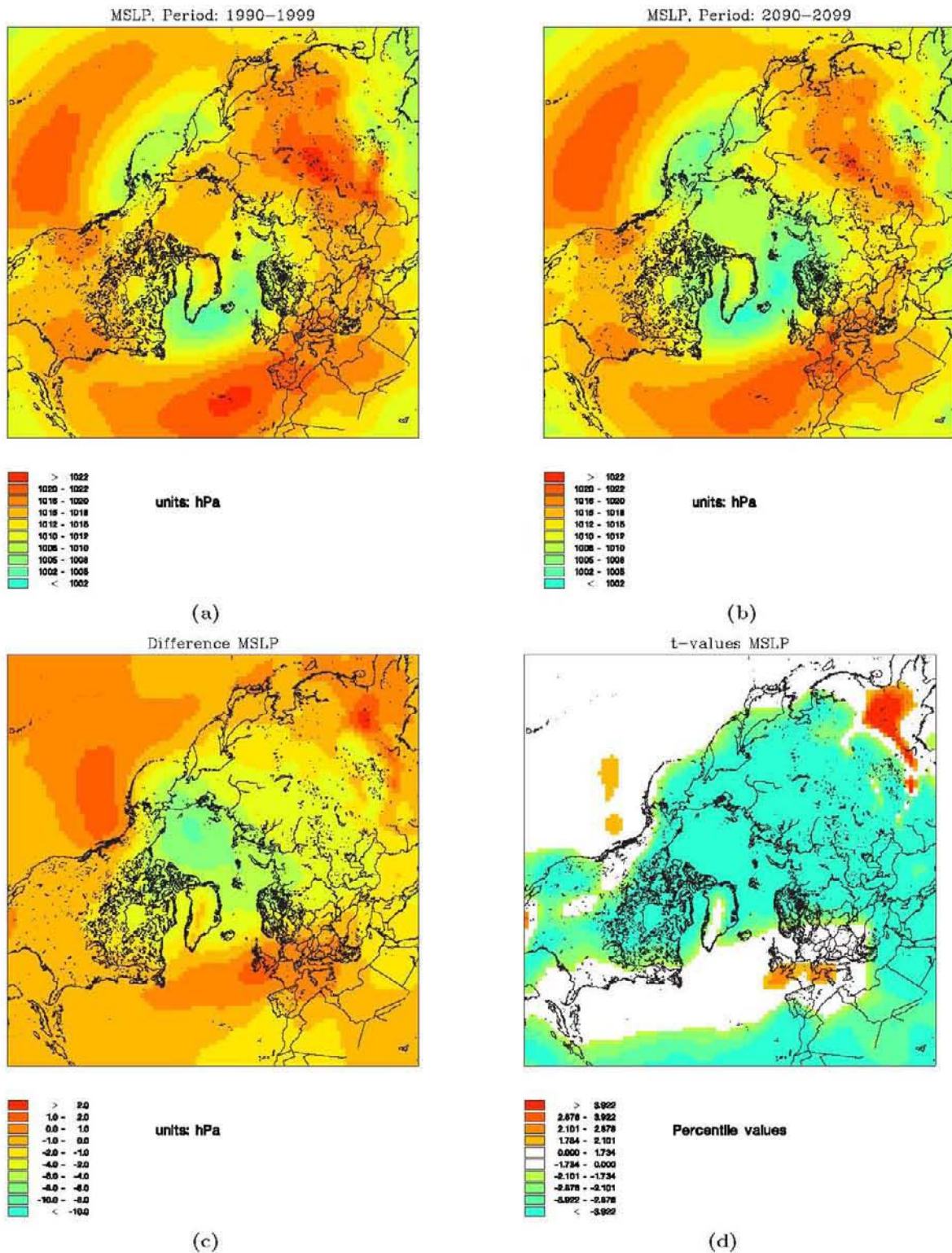


Figure 6.4: Mean sea level pressure (MSLP), as in figure 6.1.

The MSLP is predicted to decrease over the Arctic and subpolar regions of America and Asia. On the contrary pressure increases are predicted over Central Europe, southeastern Asia and over the Bering sea. The significant plot reveals that the predicted decrease in MSLP is highly significant in a very large area cf. subplot (d)

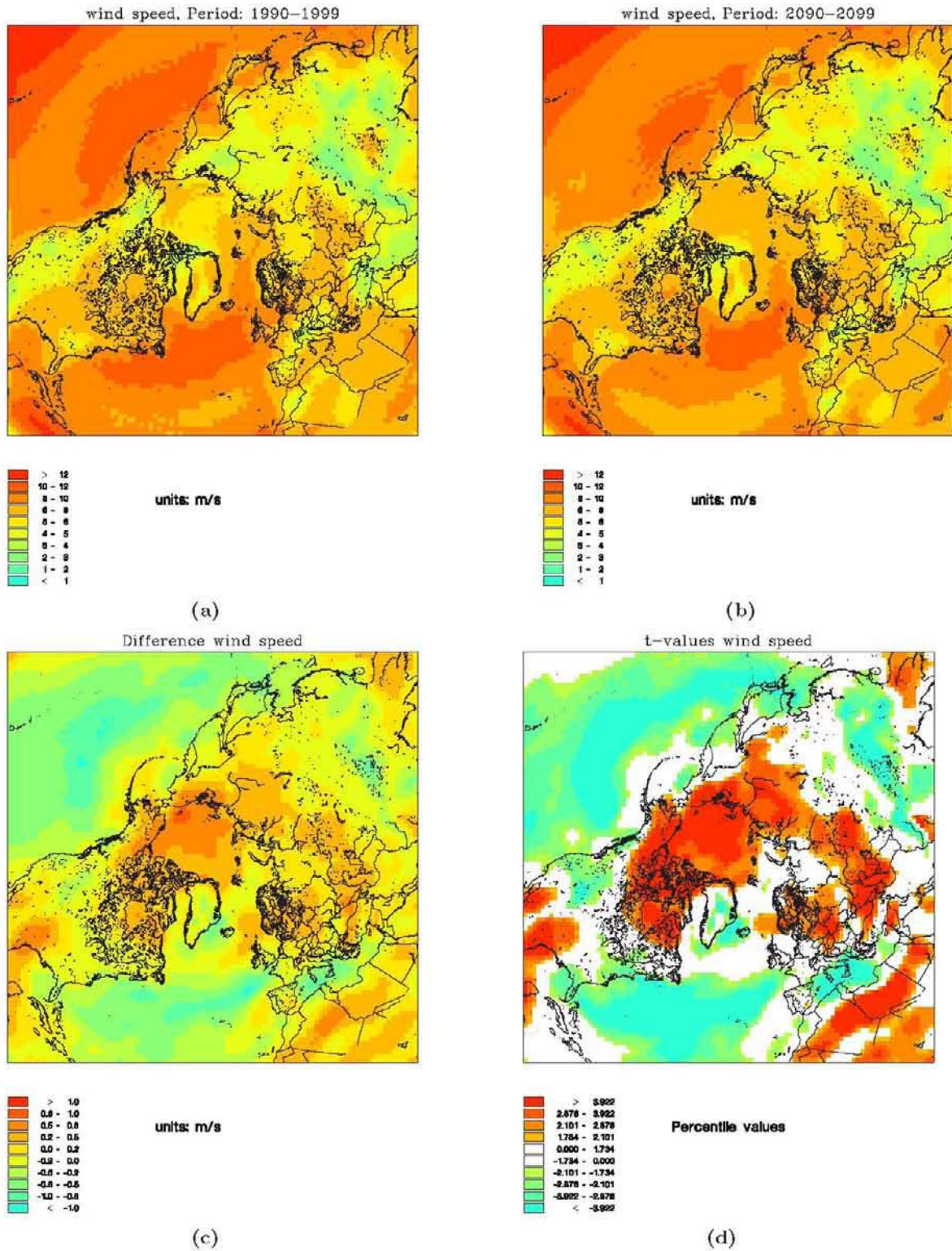


Figure 6.5: Wind speed, as in figure 6.1.

The largest decrease in the wind speed is found over sea in the storm tracks. Over the Arctic, Scandinavia and subpolar parts of Asia, the wind speed is projected to increase. From subplot (d) it can be seen that the observed changes are highly significant. The largest changes in the wind speed is approximately 10% of the absolute wind speed

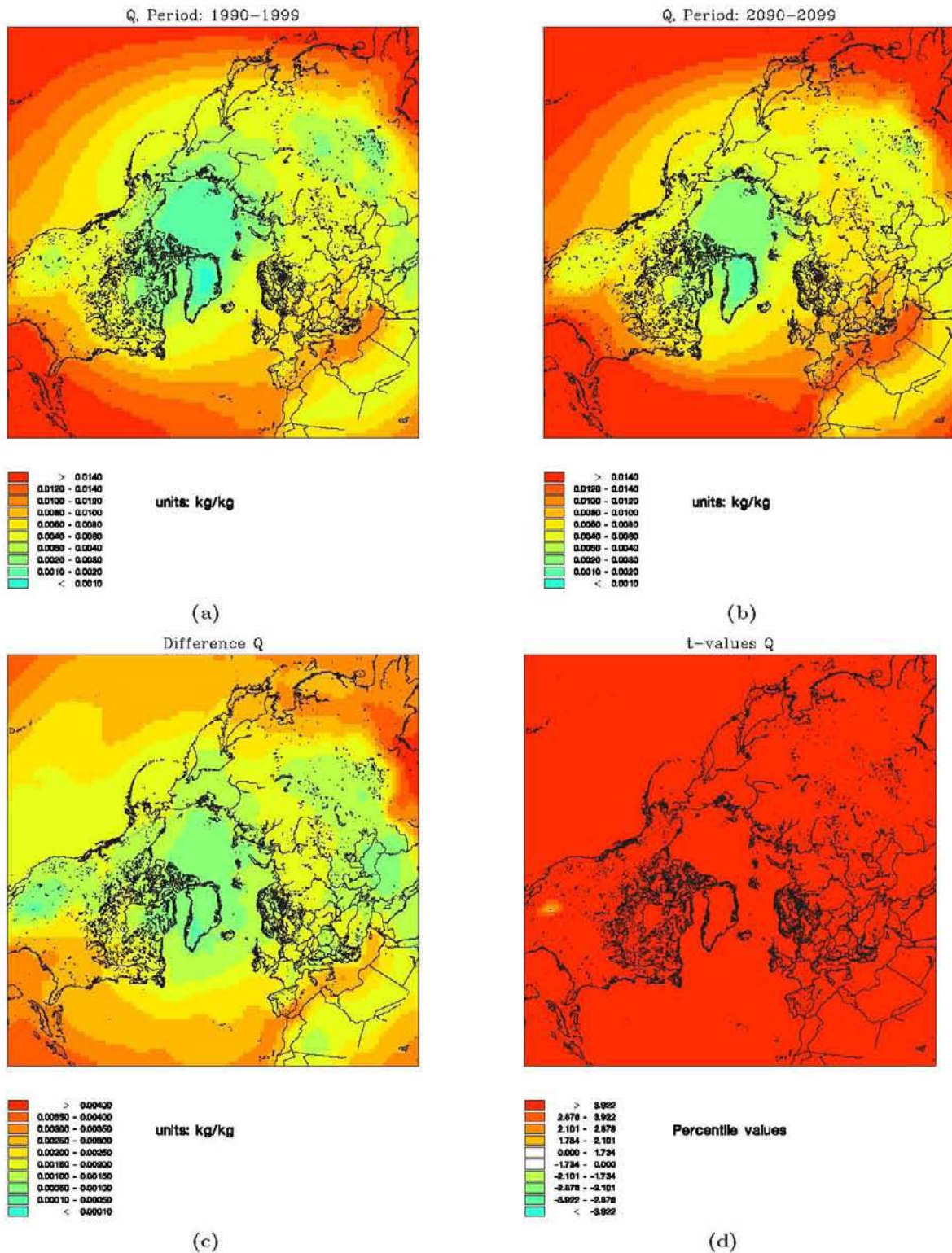


Figure 6.6: Specific humidity Q , as in figure 6.1.

The specific humidity is predicted to increase everywhere in the model domain (note the color-scale of the difference plot (c)). However the increase gets larger towards south. The results are highly significant according to the t-statistics (subplot (d)) with the exception of an very small area over the Rocky mountains where the significance is a little bit lower.

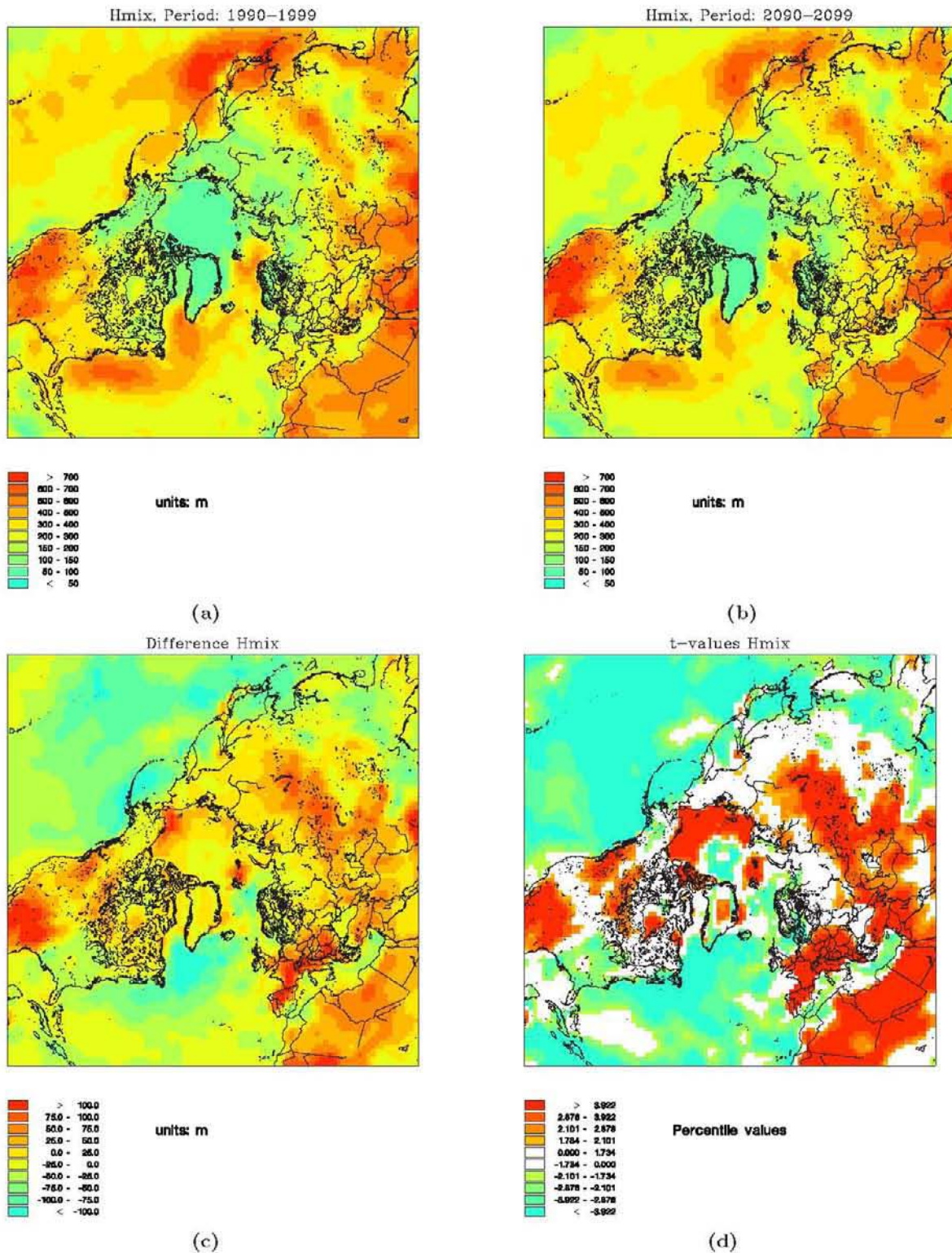


Figure 6.7: Mixing height, as in figure 6.1.

The mixing height is derived from other ECHAM4-OPYC3 meteorological parameters. The calculation is based on a simple energy-balance method, described in Christensen [1997]. The respective increases and decreases in the mixing height vary, however comparing the differences in mixing height (subplot c) to the differences in wind speed (cf figure 6.5), similar patterns are found in the two parameters.

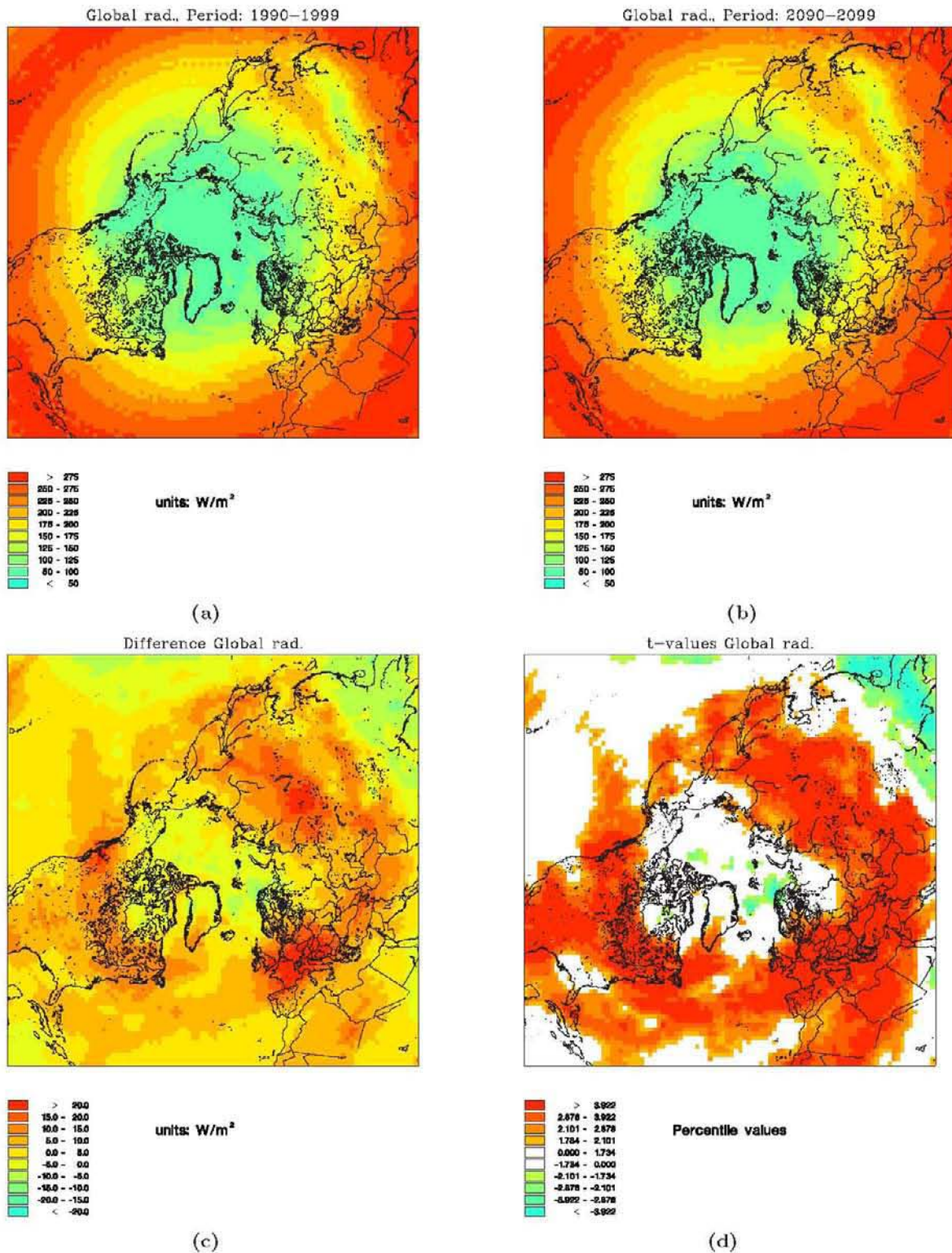


Figure 6.8: Global radiation, as in figure 6.1.

The global radiation is calculated from the cloud cover, which again has been derived from the specific humidity of the ECHAM4-OPYC3 simulation. For further details see the text in this chapter. Both the absolute values of the two decades and the changes between these two decades shows a highly latitude dependency. The largest increases in global radiation is projected to occur in a latitudinal belt covering the mid-latitudes and subtropics. The results in these regions is calculated to be highly significant according to the calculated t-statistics (subplot (d))

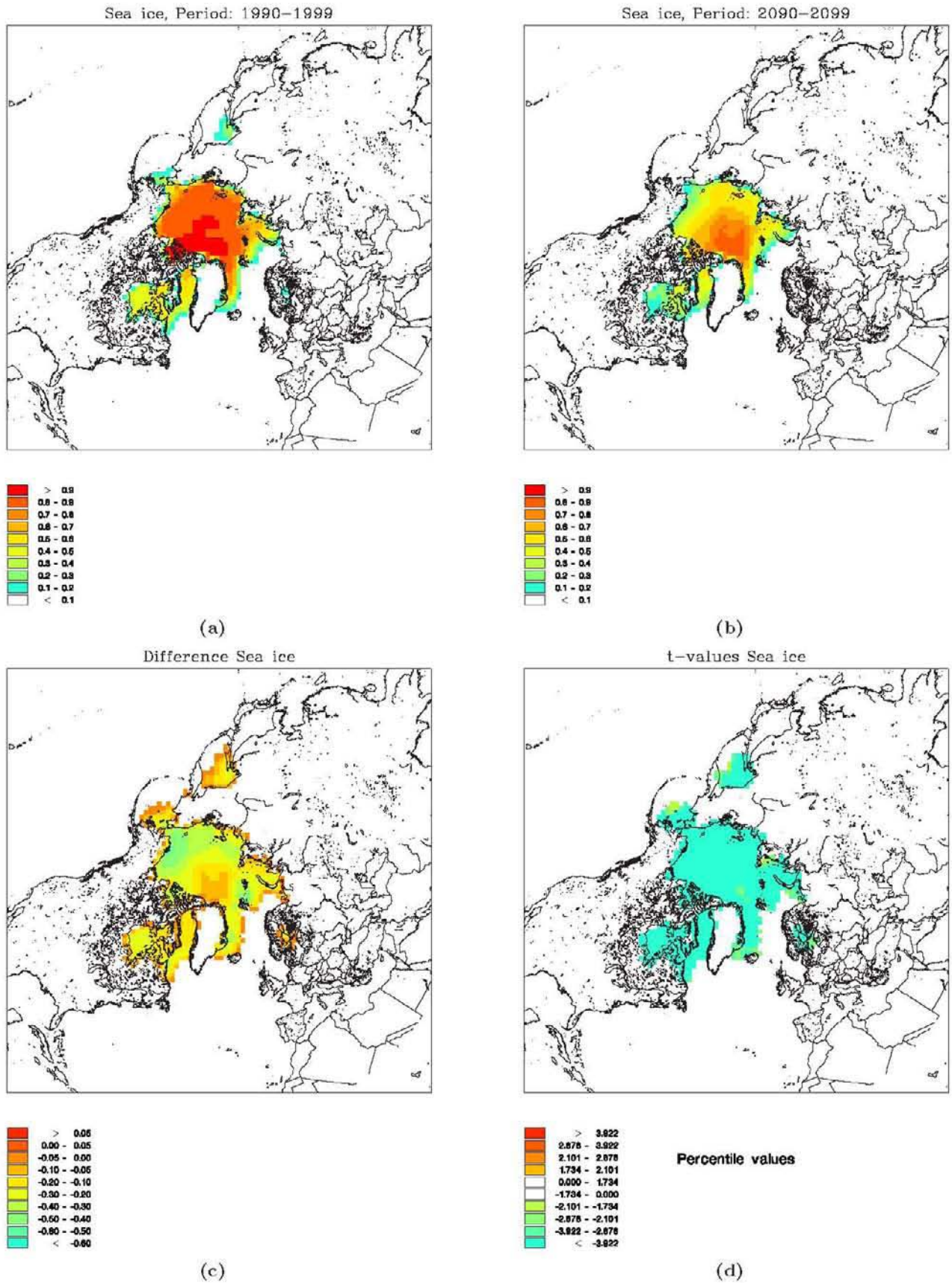


Figure 6.9: Sea ice, as in figure 6.1.

The sea ice is defined as a fraction between one and zero in a specific grid cell. The largest decreases in sea ice cover is found within the Arctic basin (cf e.g. East of Svalbard and North of the Bering Strait)

6.2 Changes in air pollution levels calculated by DEHM-REGINA

The DEHM-REGINA model is a chemical long-range transport model, which keeps track of the concentrations and depositions of 63 different chemical species. By the simulations carried out in this thesis, it would therefore be possible to analyze all 63 chemical species with respect to their future evolution of the concentrations and wet and dry depositions. Again these three properties of every chemical specie could be analyzed with respect to a large number of meteorological parameters and the analysis could be carried out over the total northern hemisphere comparing three decades. To do a full analysis is as mentioned earlier far beyond the scope of this thesis. Therefore the most interesting chemical species has been selected and analyzed with respect to the main meteorological parameters described in section 6.1 above.

The chemical species analyzed and described in this thesis are, sulphur SO_2 , sulphate SO_4 , ozone O_3 , nitrogen dioxide NO_2 , PM_{10} (particular matter with diameters below $10\ \mu\text{m}$), sea salt, hydroxyl radical OH and isoprene C_5H_8 . Also ammonium NH_4 , ammonia NH_3 , nitrate NO_3 , nitrogen oxides NO_x , TSP (total suspended particles) and $PM_{2.5}$ (particular matter with diameter below $2.5\ \mu\text{m}$) has been treated in this analysis. However the results of NH_4 looked very similar to the results of sulphate SO_4 . Furthermore NO_2 is more expressive than NO_x in the context here (see discussion below, section (6.2.4)). Finally both $PM_{2.5}$ and TSP can be visually derived from the two selected particle species PM_{10} and sea salt. Therefore in order to restrain the work in this thesis, the results of NH_4 , NH_3 , NO_x , NO_3 , TSP and $PM_{2.5}$ have not been included.

6.2.1 Sulphur

In figure 6.10 the concentrations of sulphur are shown. Sulphur is a relatively short-lived species (a few days to a few weeks) and for this reason the concentrations of sulphur are largest close to the sources. Sulphur emissions are mainly due to burning of fossil fuels (coal, diesel etc.). These features are very clear in subplot 6.10(a) and 6.10(b) which represents the mean concentrations of the 1990's and the 2090's. Here the largest concentrations of sulphur is found close to the industrial areas which often coincides with the densest populated areas. For example central Europe, Asia and eastern United States are all areas of very high concentrations of sulphur. In Russia there are several hot spots of areas with high concentration of sulphur, which not necessarily coincides with the large cities. The Arctic situated city, Norilsk, is an example of this. Norilsk is a city in the Arctic part of Russia, which existence is solely based on the industrial extraction of nickel, copper, palladium, platinum etc. The city houses 300.000 people, who works with this metal production. The emission of sulphur in Norilsk is approximately 2000 kton/year [AMAP, 2006] in contrast to Denmark, which in total emits approximately 24 kton/year in 2004 [www.dmu.dk, 2006]. It is not surprising, that the sulphur signal of Norilsk is very clear in the hemispherical concentration plots (subplot (a) and (b) in figure 6.10).

Over the Pacific and the Atlantic ocean some lines of high sulphur concentrations appears. These lines are the international routes of ships (diesel emitters). Since sulphur is relatively short-lived, these very local maritime emissions, becomes evident in the concentration plots (subplot 6.10(a) and 6.10(b))

With respect to the difference plot (subplot 6.10(c)), first of all it is important to note that the color-scale has been changed in order to identify all interesting features. Also the threshold value of 1% in the difference plot has been changed to 1‰. Inspecting the figure (subplot 6.10(c)) reveals that the sulphur concentration are predicted to decrease significantly everywhere in Siberia in the next century. The industrial city of Norilsk vary from it surroundings by having less changes in sulphur concentration than the rest of Siberia. This result will be discussed later

The largest increase in the sulphur concentration is found over the populated areas (western United States, central and south Europe and eastern Asia). Here it should be kept in mind that the emissions are kept constant in this experiment, so the changes found here must be due to changes in the meteorological parameters. The sulphur concentration from ship traffic seems to intensify a little both in the Atlantic and the Pacific Ocean in the future. Inspecting the significance subplot 6.10(d) reveals that the observed enhancement is significant in both oceans. However the changes in the Pacific are quite small and only visible because the threshold of 1% has been changed to 1‰ in this plot. Besides the ship routes, the areas of increasing sulphur concentrations over eastern United States, central and southern Europe and eastern Asia are also significant.

6.2.2 Sulphate

In figure 6.11 the future evolution of sulphate SO_4 is shown. SO_4 is a secondary aerosol which is created from sulphur SO_2 . The reactions takes places relatively soon after the emissions of SO_2 to the atmosphere, which is the reason why SO_2 is short-lived (days to few weeks). Sulphate on the other hand is dominated by long-range transport and therefore it is a very weather dependent parameter. For this reason it would be reasonable to search for changes in one or more meteorological parameters in order to explain changes in the sulphate concentrations.

Subplot 6.11(a) and 6.11(b) shows that the concentration of sulphate is small over the Pacific ocean and over the whole Arctic region. This indicates that even though SO_4 can be long-range transported, the regions of high concentration is situated relatively close to the main emission sources of SO_2 .

It is interesting to note, that the sulphate concentration over Norilsk is predicted to increase significantly in the future decade due to climate change (cf. 6.11(c) and 6.11(d)). Also over eastern United States and over a large area around and over southern Europe is the SO_4 concentration expected to increase. The observed fact that the SO_4 is predicted to increase can either be an expression of decreasing lifetime of SO_2 and therefore a higher production of SO_4 or an enhanced transport of SO_4 into the areas, since the emissions are kept constant in this experiment. A decrease in SO_2 is closely connected to an increase in ozone through the chemical process described in equation 6.5.



By a quick inspection of figure 6.14 (which will be described later) it can be seen that an increase in ozone over the area of Norilsk is predicted, which makes the explanation above plausible. Furthermore an increase of the specific humidity (H_2O) is seen everywhere which will enhance the reactions described in 6.5. The increase in SO_4 concentration is seen as a very local phenomena close to the source area of Norilsk. The surroundings of Norilsk is dominated by a significant decrease in SO_4 concentration. This phenomena will be discussed later in this chapter.

Concerning the evolution in and near Denmark it is worth to note, that Denmark lies within a belt of insignificance. North of this belt significant decreases in the SO_4 concentration levels are expected to occur and south of this belt significant increases are expected to take place according to these results. Over the Arctic and the Pacific Ocean the concentrations of SO_4 are small in both the past and the future decade.

In figure 6.12(a) the wet deposition of SO_4 is shown. The wet deposition of SO_2 is included in the wet deposition of SO_4 , since SO_2 almost immediately transform into SO_4 when getting in contact with water. Therefore from now on the wet deposition of both SO_2 and SO_4 will be mentioned solely as the wet deposition of SO_4 .

The wet deposition of SO_4 is logically located at the same spots as the areas of high concentrations of SO_4 . In some areas of the northern hemisphere the wet deposition is increasing and in other areas the wet deposition is decreasing in this model simulation. However from the significance plot 6.12(d) it is clear that none of these changes are significant. This insignificance is probably connected to the large variability in precipitation, which inherently must introduce small signal-to-noise ratio!

Figure 6.13 shows the dry deposition of SO_4 . This figure reveals that the dry deposition of SO_4 is very low everywhere compared to the wet deposition. The changes between the two decades are insignificantly, besides over the ice cap of Greenland and over Bering sea where a significant decrease are found. However this significance coincides with areas of small change.

6.2.3 Ozone

The concentration of ozone O_3 is displayed in figure 6.14. The areas of high ozone concentrations are partly situated over the populated areas (cf figure 6.14(a) and 6.14(b)). However also a latitude dependent structure is evident in all four subplots of figure 6.14. In the difference plot (subplot 6.14(c)) this structure is very clear. The ozone concentration levels increases in the future and the increase gets stronger with increasing latitude. North of approximately $30^\circ N$ the increase is very significant, everywhere south of $30^\circ N$ difference in ozone concentration changes and in the equatorial areas the ozone concentrations levels tends to decrease significantly between the two decades. However also a blurred land-ocean contrast in the ozone increase is evident. The ozone concentration generally increases less over the ocean. This increase is in contrast to the findings of Johnson et al. [2001] who estimates a net loss of ozone by a photochemical split of ozone into $O(^1D)$ which results in a net loss of ozone due to $O(^1D)+H_2O \rightarrow 2OH$.

6.2.4 Nitrogen dioxide

In figure 6.15 the levels of nitrogen dioxide are shown. The emissions of NO and NO_2 originates mainly from traffic and power plants, which is also evident in the two concentration plots (cf 6.15(a) and 6.15(b)). Generally the nitrogen dioxide levels are decreasing where the ozone levels are increasing and vice versa (see for example over Europe in figure 6.15 and 6.14). Also the Himalayan mountains is a good example of this inverse nature. Here a significant increase in NO_2 concentrations is detected in contrast to a decrease in the ozone concentration and both these changes are significant! NO_2 and O_3 is linked through a chemical process (see equation 6.6). However more investigation are needed to determine if new equilibria will occur during changed climate conditions between the involved chemical species of O_3 , NO_2 and NO .



Only the Caribbean differs from this inverse structure. Here both O_3 and NO_2 are increasing significantly! In this case an explanation must be found elsewhere.

NO_x is the sum of NO and NO_2 . From equation 6.6 it can be seen that under variance of O_3 , this sum stays constant in the reaction scheme. This explains why the prediction of NO_x is less interesting to study when one wishes to see the interaction between NO , NO_2 and O_3 . However the general level of NO_x is very closely related to ozone, since NO_x together with VOC's are important precursors in ozone production.

6.2.5 Particles with diameter below 10 μ -meter

PM_{10} includes all particular matter with a diameter below 10 μm . In the DEHM-REGINA model used here, PM_{10} consists of secondary non-organic aerosols (for example SO_4 , NH_4 , NO_3), primary aerosols (seasalt), primary emitted particles (from the primary emission sources; industry, traffic, agriculture etc.) and finally unspecified particles such as for example mineral dust. The primary emitted particles only contribute to the changes seen in this experiment through changes in transport due to changes in meteorology, since the emissions are kept constant throughout all years simulated. The secondary organic aerosols are by definition also a part of the PM_{10} , however these are not yet included in the DEHM-REGINA model. For example presently terpenes (a subgroup of VOC), which are naturally emitted from biogenic sources and are believed to generate secondary organic aerosols, is not presently included in the model.

The concentration, the difference and the significance of the change in PM_{10} particle levels are shown in figure 6.16. From subplot 6.16(c) it can be seen that, there is a general increase in concentration of PM_{10} particles over the eastern part of the Atlantic ocean, the central Europe, the Mediterranean sea and north Africa. This increase is highly significant. In contrast the PM_{10} concentrations seems to decrease in the future over the northern and central Asia, - over large parts of the Arctics and finally over the Pacific ocean. Around and in the surroundings of Japan, over the populated parts of United States and over the

Aleutian islands an increase in PM_{10} particles is predicted by this simulation. All these increases (except the Aleutian) could be explained by an enhanced concentration of secondary inorganic aerosols (SO_4 see figure 6.11, NH_4 (not shown) and NO_3 (not shown)). Regarding the increase seen over the Aleutian the explanation must be found elsewhere (see discussion below).

6.2.6 Sea salt

In figure 6.17 the predicted evolution of the concentration of sea salt is shown. Subplot 6.17(a) and 6.17(b) shows the obvious fact that sea salt primarily is found in the air masses over sea and in the coastal regions. The exchange of sea salt from the ocean to the air is driven by the wind in the model. In subplot 6.17(a) and 6.17(b) the storm tracks stands out very clearly. Subplot 6.17(c) and 6.17(d) reveals that the significant increasing concentration of sea salt in the future decade will be over North and Central Europe, the Baltic, the Aleutian islands and over western Russia, whereas the significantly decreasing concentrations are expected to be found over the Mediterranean sea, the central Atlantic Ocean and the Pacific ocean.

6.2.7 Hydroxyl radicals layer 1 and layer 5

In figure 6.18 and figure 6.19 the prediction of the concentration of hydroxyl radicals in the surface and the fifth layer (height approximately 230 m above MSLP [Frohn, 2004]) of the DEHM-REGINA simulation are shown respectively. The general lifetime for the hydroxyl radical is less than one second [McGuffie and Henderson-Sellers, 2001]. Due to this very low existence time of OH , it is very difficult to evaluate the predicted concentrations with respect to measurements or prognostic statements. Furthermore a long-range transport model with a coarse resolution is not expected to simulate the real OH concentrations. However in the DEHM-REGINA model the lifetime of a great number of chemical species is dependent on the amount of hydroxyl radicals present. For this reason the changes in the concentration of OH can give some important information in the analysis of many other chemical species and their transformations. Also in the DEHM-REGINA model the existence of OH radicals are instantaneously, since the model do not posses any memory of this specie, but is only estimated via a production term and a loss term.

From subplot 6.18(c) it is clear, that the hydroxyl concentration in the surface layer is predicted to increase over the maritime areas in contrast to the terrestrial areas where the hydroxyl radical concentration are predicted to decrease during the next century. In subplot 6.18(d) it can be seen, that almost all these changes are either positively or negatively significant.

Comparing the surface layer hydroxyl concentration (figure 6.18) with the concentration from approximately 230 meters altitude (figure 6.19) reveals some differences. Most importantly is this land-ocean contrast seen at the surface, which higher up in the atmosphere gets more blurred. The general decrease in the hydroxyl radical concentration over land is less pronounced in subplot 6.19(c) compared to subplot 6.18(c). These features will be discussed later in this chapter.

6.2.8 Isoprene

Figure 6.20 shows the prediction of the Volatile Organic Compound (VOC) isoprene. Isoprene is included in the DEHM-REGINA model and is through participation in chemical reactions with OH acting as a sink for hydroxyl radicals (cf. pp. 48 Frohn [2004]) which explains the low OH concentration over land in figure 6.18. In subplot 6.20(c) the 1% threshold value (explained in the introduction to this section) is changed to 1‰ in order to visualize even very small changes in the isoprene concentration. From subplot 6.20(a) and 6.20(b) it is very clear, that isoprene primarily exists over land. Isoprene is a Volatile Organic Compound (VOC), which is emitted from trees and other plants. Isoprene in these simulations are only emitted over the terrestrial areas, which is in good agreement with the results found here. From the absolute difference (subplot 6.20(c)) it is clear that the biogenic emission of isoprene is expected to increase everywhere, where there are emitters (plants) available and this increase are highly significant (cf. subplot 6.20(d)) This feature is not surprising, since it is already observed, that the temperature will increase by this model prediction. The emission of isoprene is a function of temperature, because the size of emission is highly dependent on the growth of trees and other plants. In DEHM-REGINA, the submodel BEIS (Biogenic Emissions Inventory System) is included to account for the biogenic isoprene emissions [Guenther et al., 1995]. Isoprene is an important precursor for ozone, see the discussion in the next section (6.3).

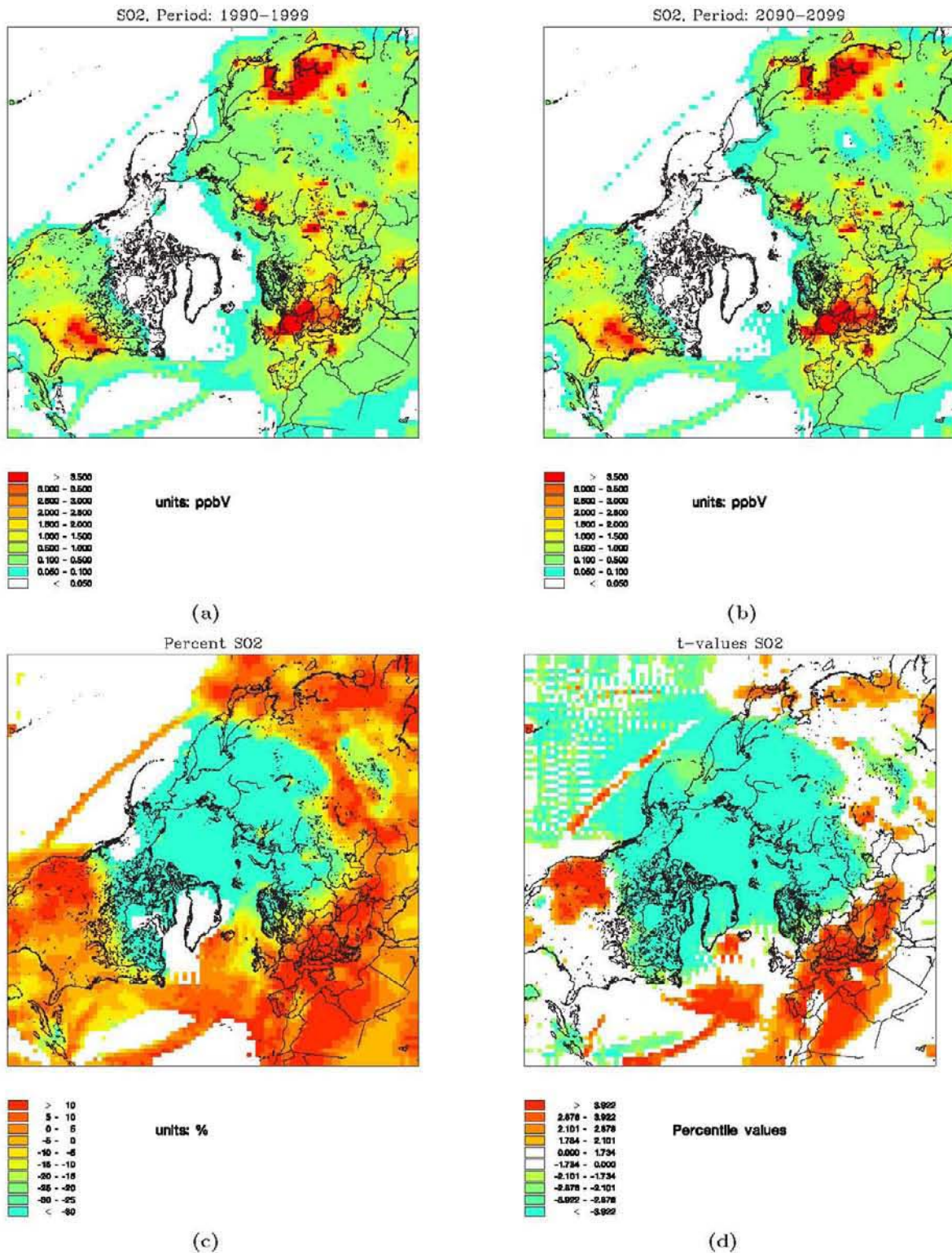


Figure 6.10: SO_2 concentration, as in figure 6.1.

The highest concentration of sulphur is found close to the emission sources, because of the relatively short life-time of sulphur. From the percentage difference plot (subplot (c)) it can be observed that the sulphur concentration is predicted to increase in the future decade over the terrestrial mid-latitudes, subtropics and tropics. Over the ocean it is only in the tracks of international ship routes an increase in sulphur concentration is observed. In the Arctic a decrease in sulphur concentration is predicted. This decrease is highly significant according to subplot (d). Also the changes in the international routes of the ships and over Europe shows high significance.

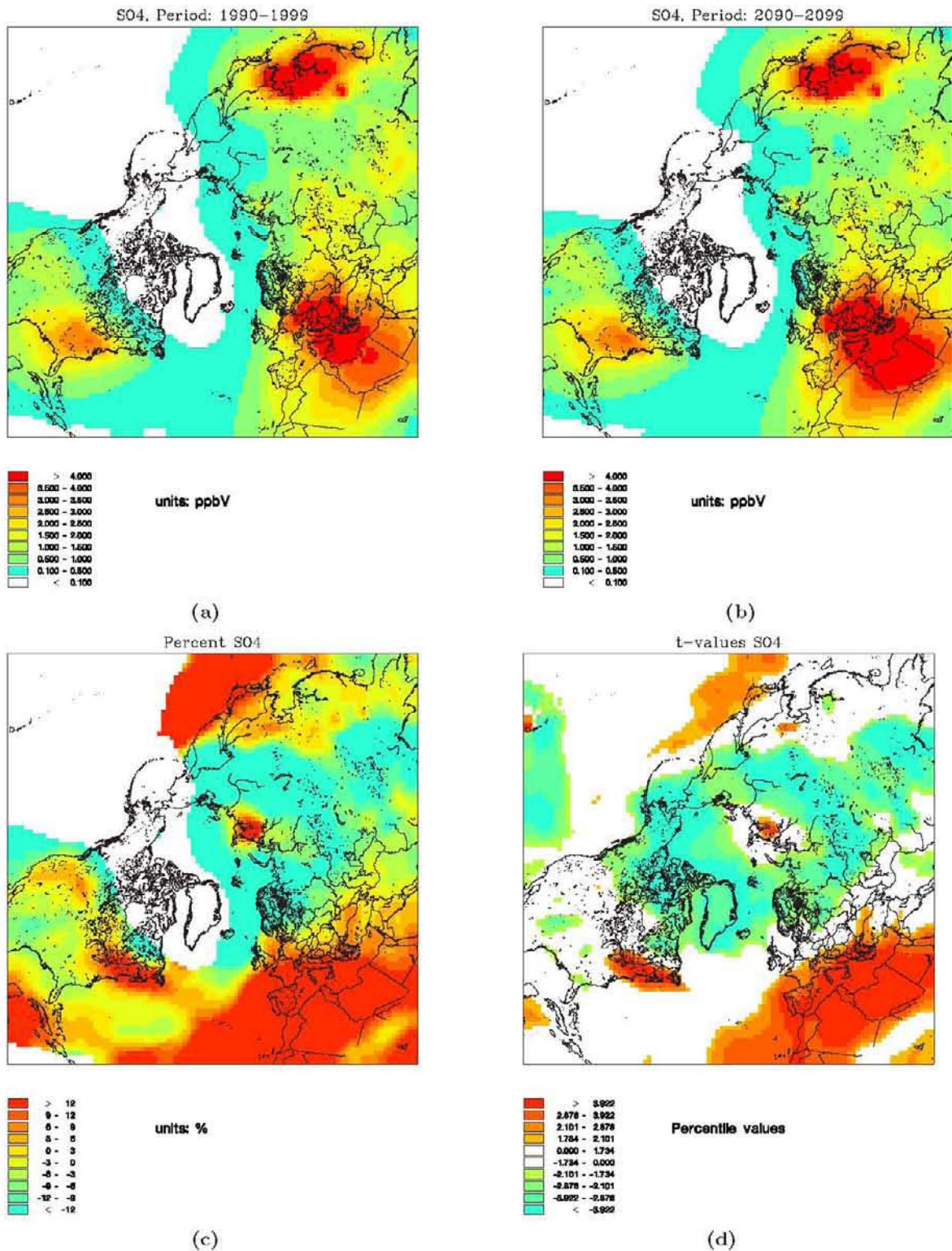


Figure 6.11: SO_4 concentration, as in figure 6.1.

Sulphate is predicted to increase over Europe and Northern Africa, the isles of Caribbean, Japan, Northeast America and finally over the industrial city of Norilsk. Generally a decrease is projected over the eastern part of the Arctic (with the exception of Norilsk). This decrease and the increase over Europe, Japan, northeast America and Norilsk is according to the calculated t-statistics highly significant (cf. subplot (d))

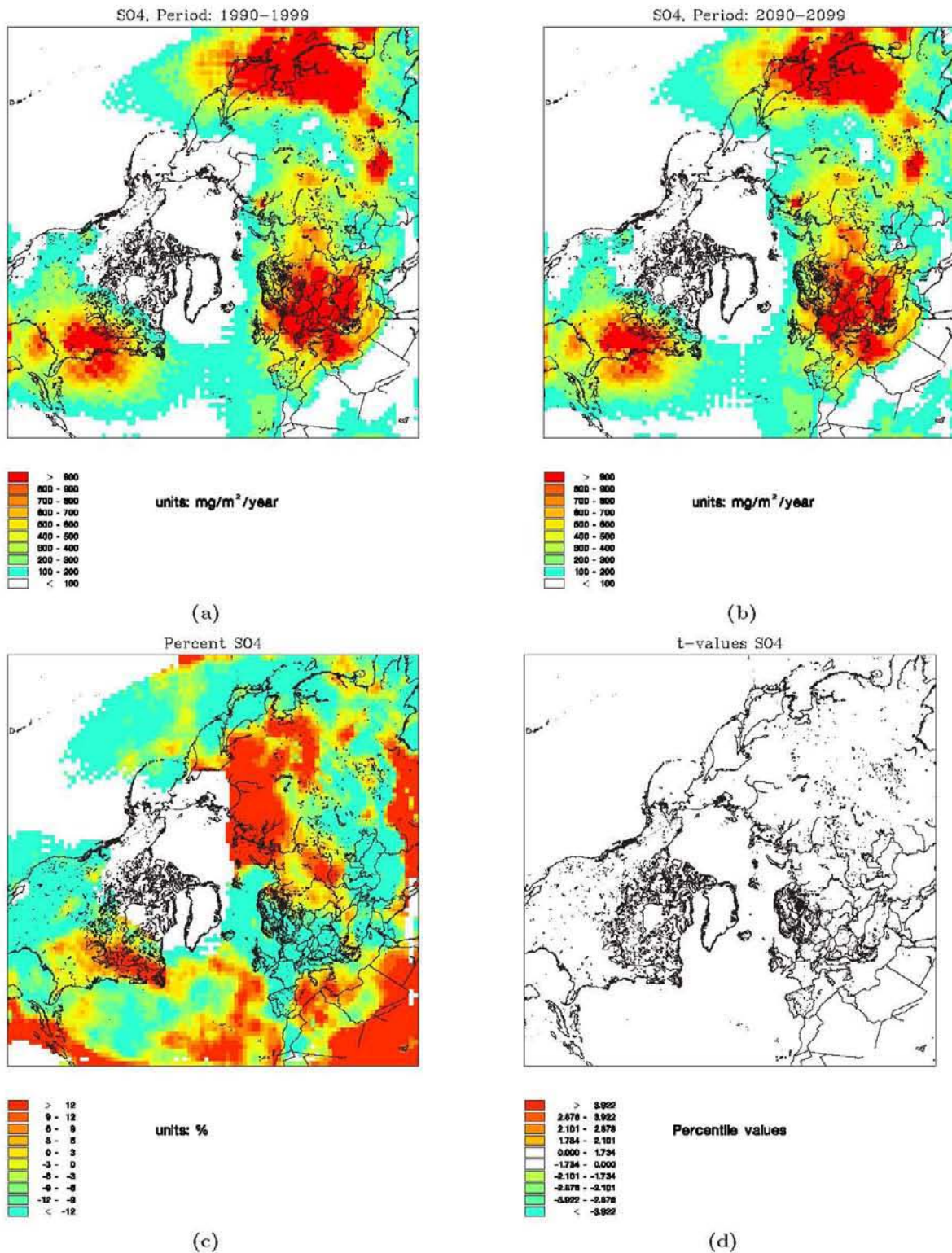


Figure 6.12: SO_4 wet deposition, as in figure 6.1.

The changes in wet deposition of sulphate vary quite a lot and is of course very dependent on the precipitation amount and frequency. This dependency can also be observed by comparison with figure 6.1 and figure 6.2. However none of these changes in the wet deposition of sulphate are significant according to subplot (d). This feature originates from the high dependency of precipitation, which is a highly fluctuating parameter. These fluctuations introduce a small signal-to-noise ratio, making the results insignificant.

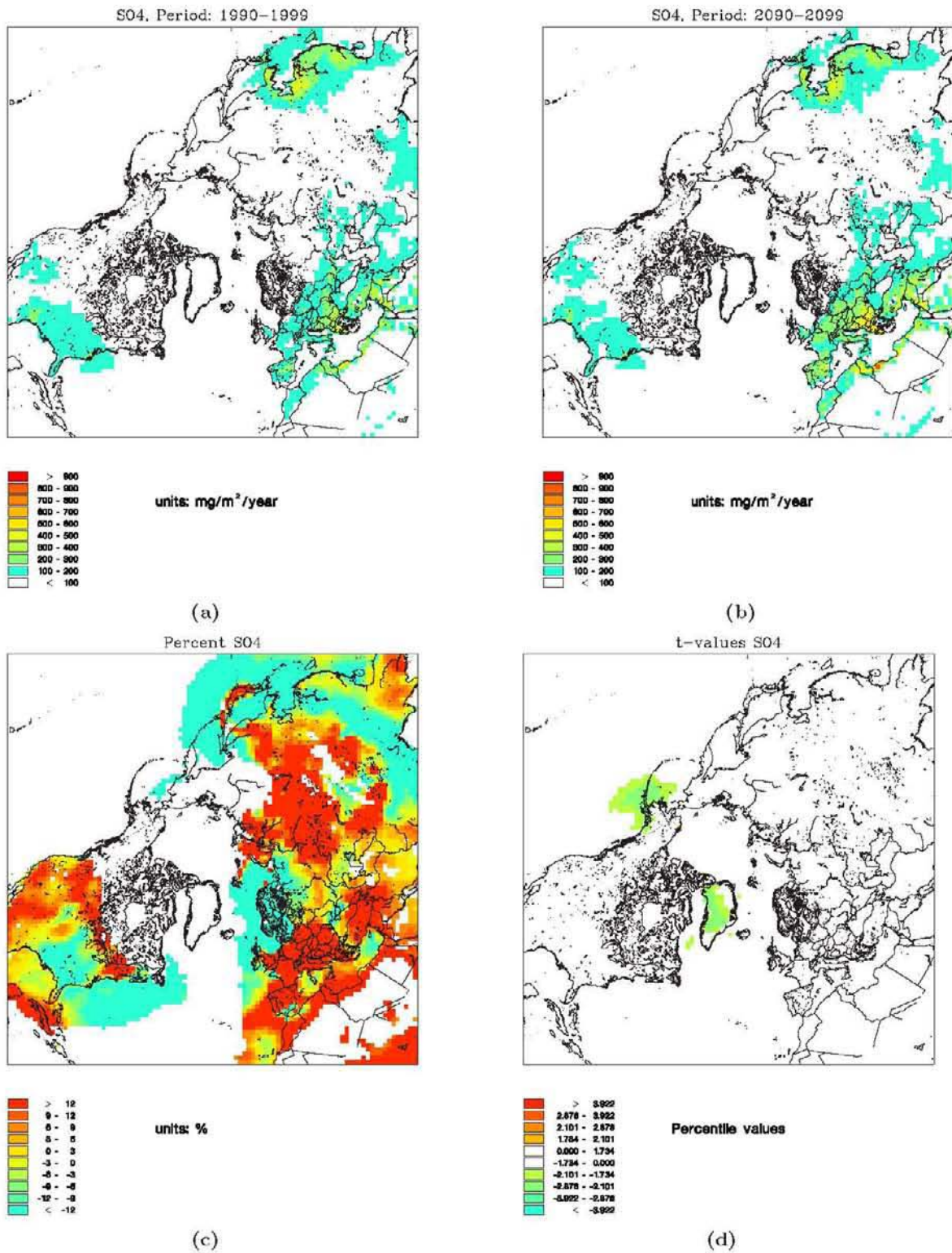


Figure 6.13: SO_4 dry deposition, as in figure 6.1.

The dry deposition of sulphate tends to vary a lot, however none of the changes are significant according to the calculated t-test. Only over the Ice cap of Greenland and over the Aleutian islands, some significance appear however these areas are areas of very small changes

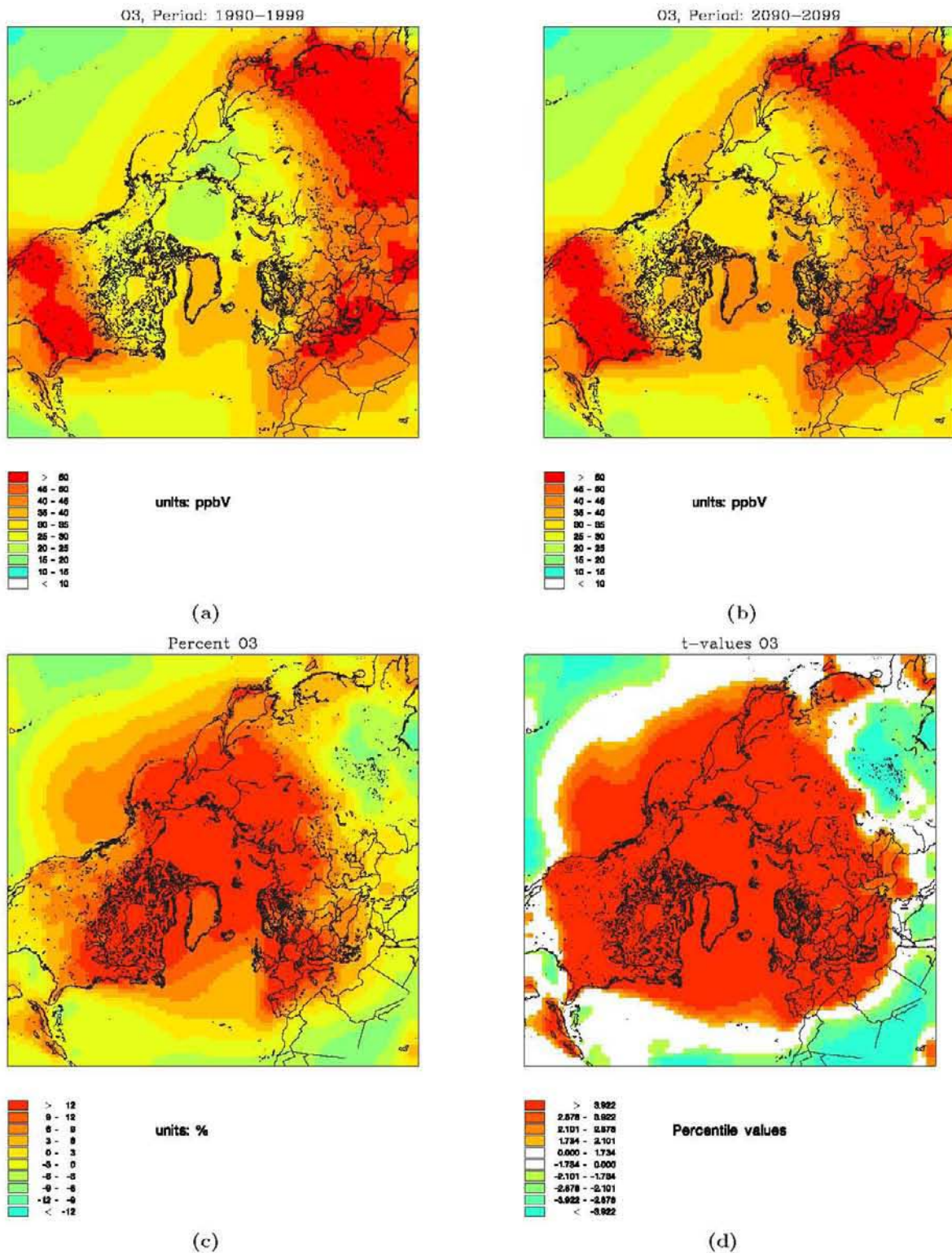


Figure 6.14: Ozone, as in figure 6.1.

The changes in ozone appear to depend highly on latitude and the land-sea contrast. The largest increases are found over the Arctic, North America, Central and North Asia and Europe

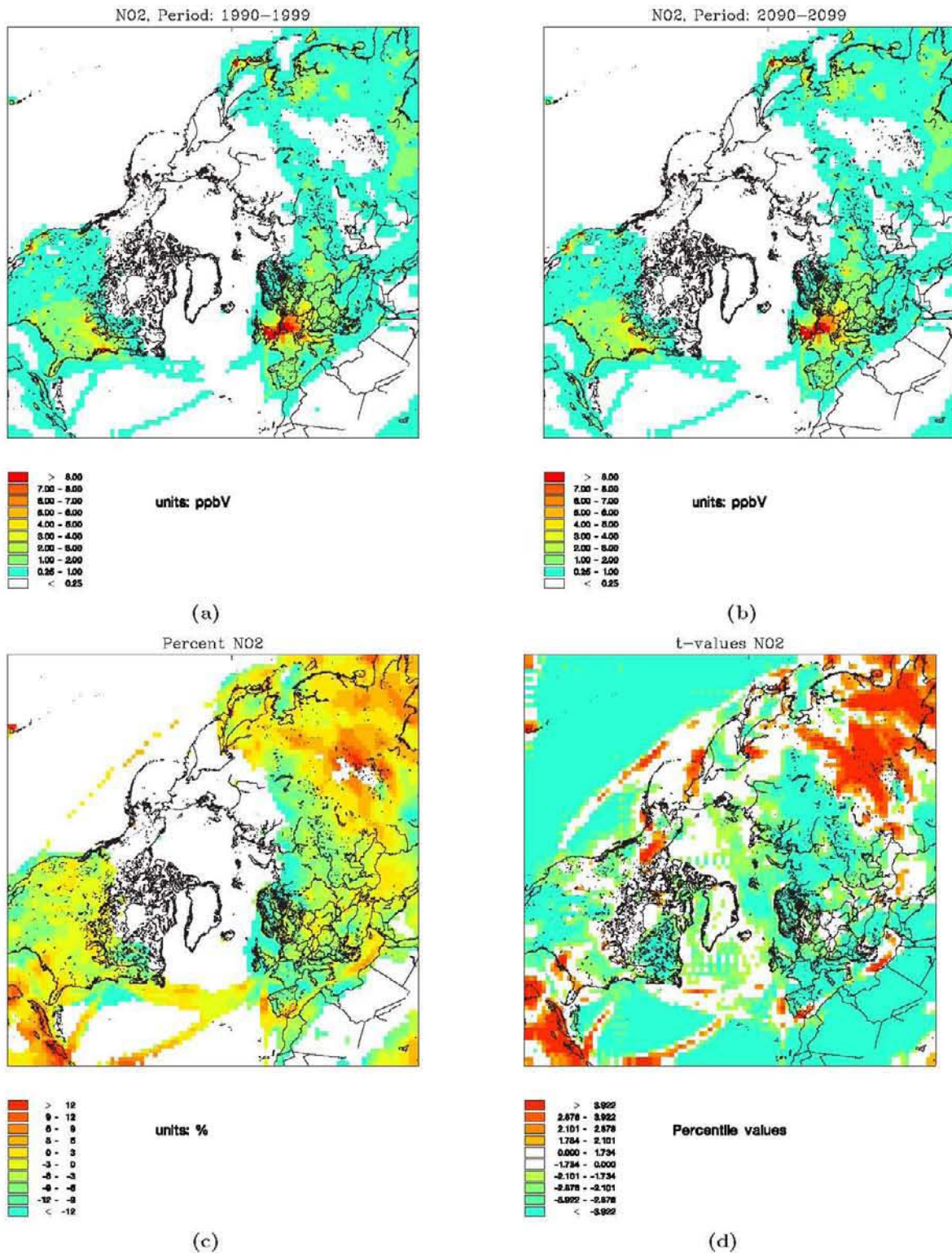


Figure 6.15: NO_2 , as in figure 6.1.

The concentration of nitrogen dioxide is highest close to the sources. This means over the dense populated areas and close to the international ship routes. Over Europe a significant decrease in nitrogen dioxide is projected in the future. On the contrary a significant increase is predicted over the Caribbean islands and over Central and Southeast Asia (cf. subplot (c) and (d)).

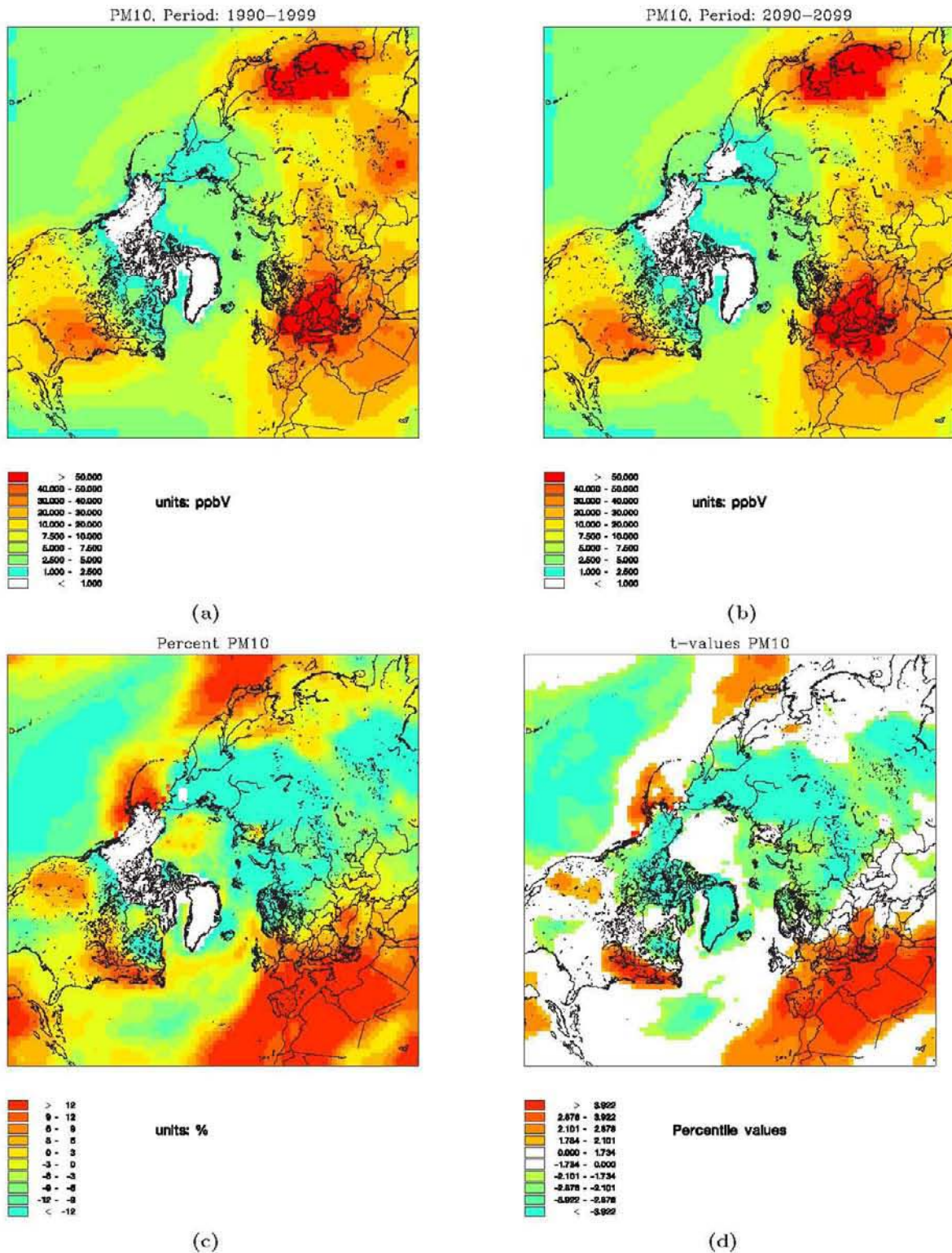


Figure 6.16: PM_{10} , as in figure 6.1.

PM_{10} represents particular matter with diameter below $10 \mu\text{m}$. Significant increases in the concentration of PM_{10} particles are found over the eastern Atlantic, Europe, Japan, the Aleutian islands and over Northeast America. These concentration increases are closely connected to the industrial areas or the maritime areas (sea salt).

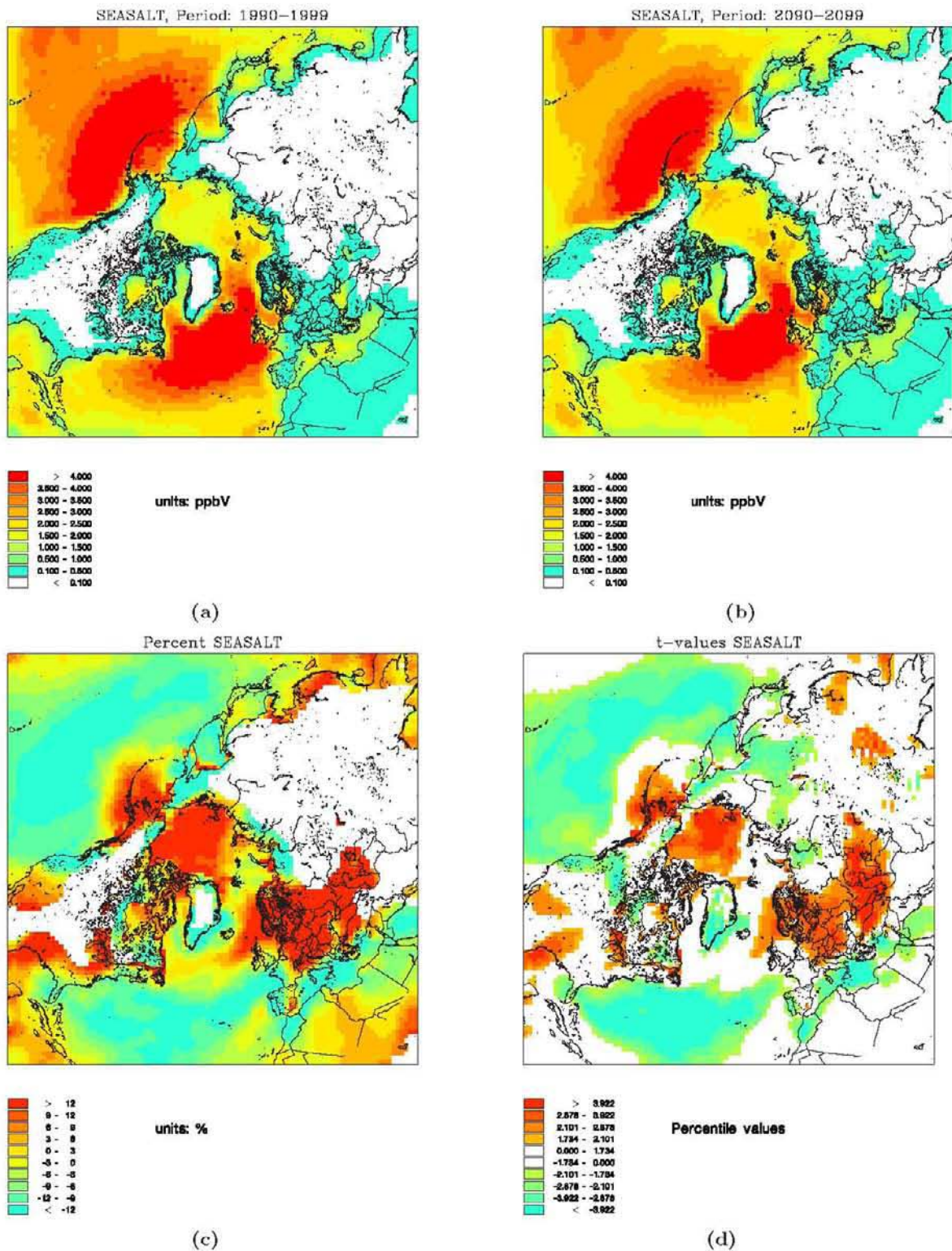


Figure 6.17: Sea salt, as in figure 6.1.

By comparing the changes in sea salt with the changes in wind speed reveals large similarity. This results from the parametrization of sea salt in the DEHM-REGINA model, for further details see the text in this chapter.

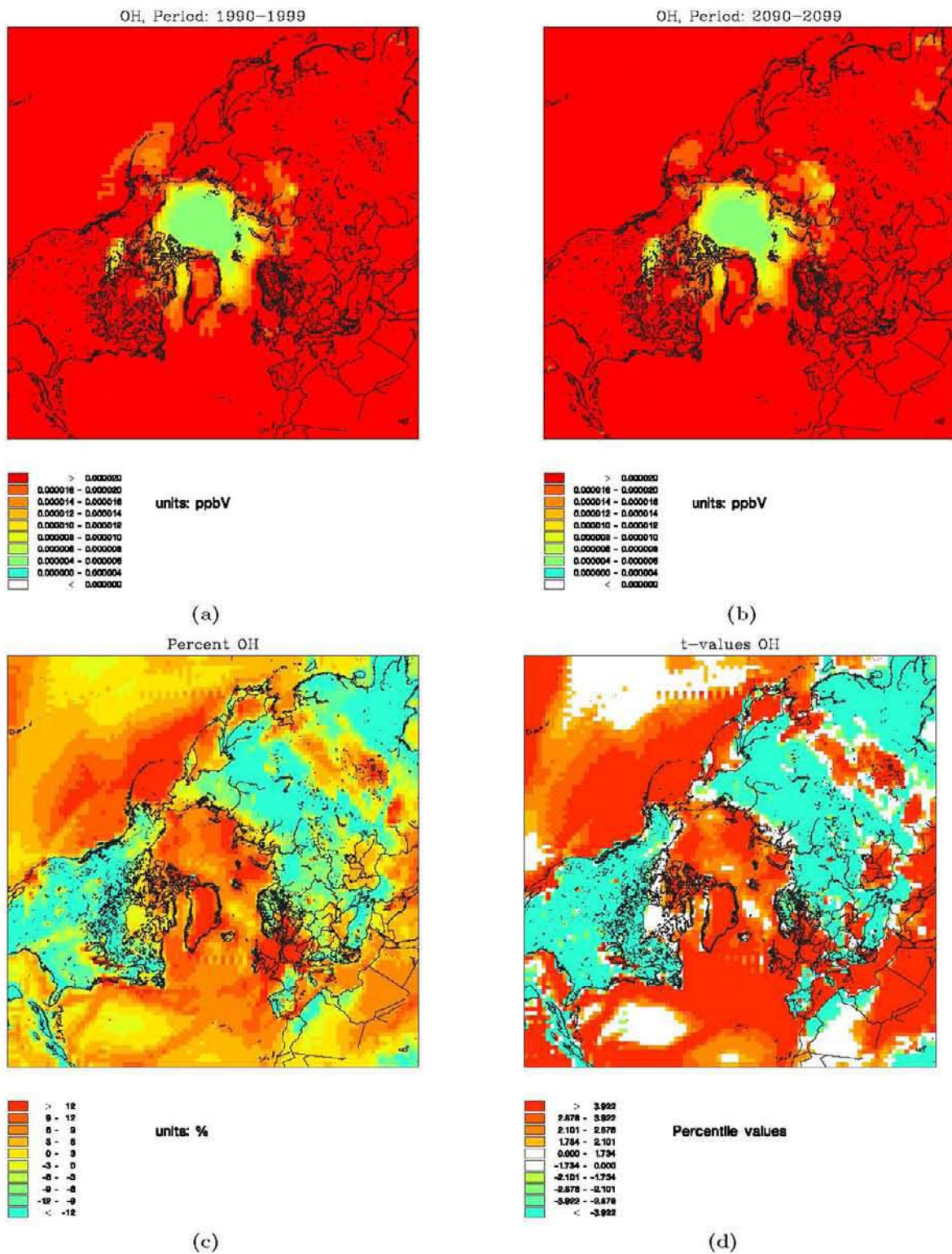


Figure 6.18: OH layer 1, as in figure 6.1.

From subplot (c) and (d) a clear land-sea contrast is evident in the data with generally decreasing values over land and increasing values over sea

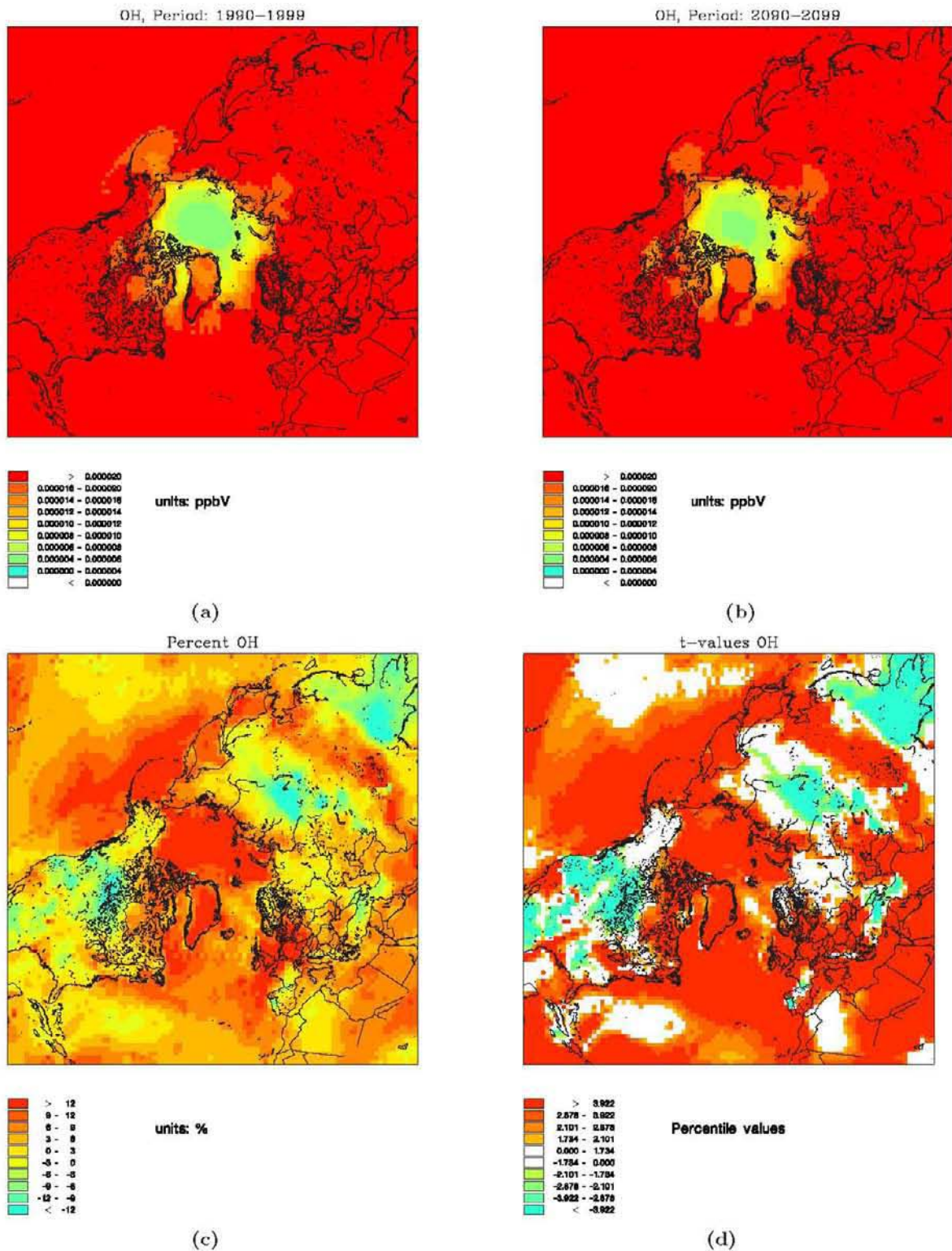


Figure 6.19: OH layer 5, as in figure 6.1.

Layer 5 is situated approximately 230 meter above the surface and inspecting subplot (c) and (d) with respect to the result from layer one, it is clear that this land-sea contrast tends to be blurred in layer 5.

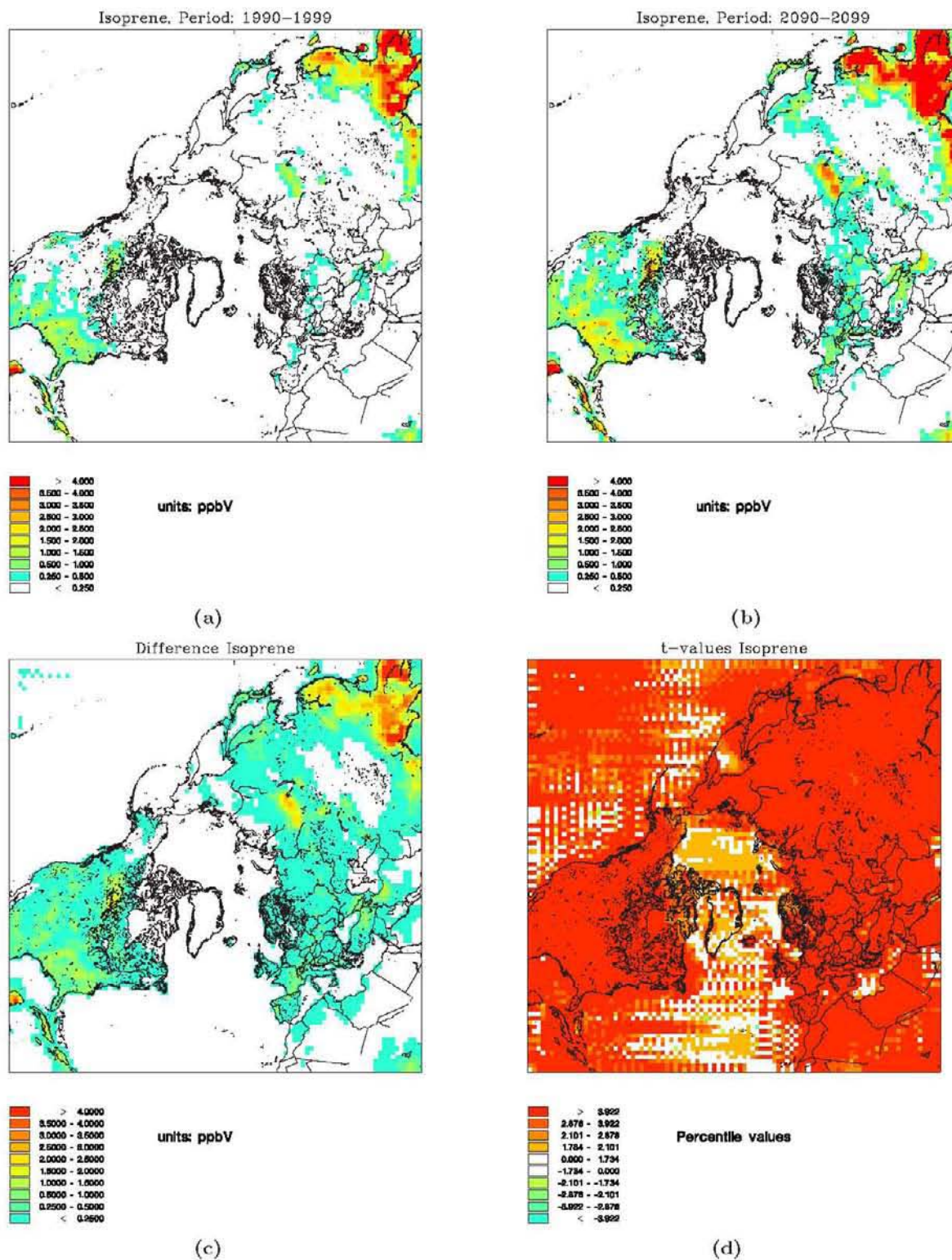


Figure 6.20: Isoprene, as in figure 6.1.

Emission of isoprene is the only variable VOC emission in these simulations, since it originates from natural emitters which can be altered due to climate change. Isoprene emissions are connected to trees, bushes etc. and is therefore found over land. The results here show that the isoprene concentration is predicted to increase significantly over land (note color-scale of the difference plot)

6.3 Summary and discussion

In the first subsection 6.3.1 the main findings of the analysis of the individual meteorological parameters and the chemical species will be summarized. After that the main significant changes in meteorology and chemistry are compared and discussed and some preliminary conclusions of this analysis are drawn.

6.3.1 Summary

Both the precipitation amount and the precipitation frequency is increasing significantly over the Arctics and subpolar regions and this feature is similar to other model results [Stendel et al., 2002]. In contrast it is generally becoming more dry in South Europe and Southwest United States and this change is also very significant. This means that North and South Europe in the future decade are becoming more wet and dry, respectively in the future. It was also found that the precipitation amount and frequency patterns are very similar. This indicates that is a change in the precipitation frequency that gives the change in the precipitation amount.

A hemispherical temperature increase is found. This increase is largest over e.g. the Arctic and South Europe, which is consistent with the results from other models [Stendel et al., 2002]. The specific humidity shows a temperature/latitudinal dependency by showing an enhanced increase towards south. Especially over sea in the southern part of the domain, the humidity is found to increase the most.

The wind speed is generally predicted to increase over the Arctic, Scandinavia and the Baltic. Also an indication of a northward shift of the storm tracks are found. An enhanced wind field is found over the Arctic and central Scandinavia and at the same time the wind speed are projected to decrease over the southern part of the North Atlantic.

The evolution of the mixing height is mixed. A general decrease in mixing height is found over the Arctic and subpolar region with the exception of the Bering Sea, where the mixing height are predicted to increase.

Finally there is the global radiation which not surprisingly was very latitude dependent. The global radiation was generally projected to increase significantly in the midlatitudes and the subtropics.

In the analysis of the predicted distribution of the chemical species a general decrease in sulphur concentration is predicted in Siberia. However the industrial city of Norilsk differs from this result and here an increase in the sulphur concentration is predicted. The international routes of the ships and the densely populated areas stands out clear in the results found here, showing a general increase in concentration. Also the sulphate concentration of over Norilsk is predicted to increase in contrast to the surroundings. The significance from the wet deposition of sulphate stands in shade of the signal-to-noise ratio of the precipitation process.

Also the distribution of particles of sea salt and particles with a diameter below 10 μm have been analyzed. The conclusion here is that the distribution of PM_{10} particles can generally be explained by the presence of secondary inorganic particles. Over the Aleutian islands the explanations to the predicted increase in PM_{10} particles originates from an increase in the concentration of sea salt particles. The distribution of sea salt particles follows the wind

patterns very closely. An enhanced wind field increases the sea salt content of the air. This is also why the storm tracks stand out very clearly in the plot of the sea salt concentration.

Ozone are predicted to increase significantly everywhere north of approximately 30°N. Nitrogen dioxide are mainly found over land and over the international routes of the ships, since it originates mainly from traffic. The nitrogen dioxide posses an inversely distribution relative to ozone. The concentrations of nitrogen dioxide are generally increasing, where the concentration of ozone are decreasing and vice versa (see e.g. over the Himalayan mountains).

Also the concentration of hydroxyl radicals are connected to the ozone concentration and here a sharp gradient between sea and land occurs. This gradient tends to blur higher up in the atmosphere.

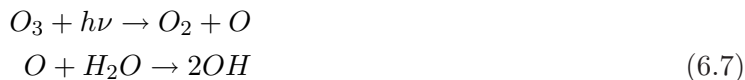
Finally there are the concentration of isoprene which exhibit a very clear difference between land and sea. The isoprene concentration is found to increase significantly over land where the emitters of isoprene are present.

6.3.2 Discussion

One of the most pronounced changes in meteorology predicted by the ECHAM4-OPYC3 simulation is the global temperature increase. The temperature is predicted to increase everywhere in the northern hemisphere, however the temperature increase enhances towards the north pole.

By the DEHM-REGINA simulation carried out in this analysis it was found that also the ozone concentration is increasing everywhere north of approximately 30°N. The ozone production is very dependent on the presence of the precursors NO_x and VOC 's. In the experiments analyzed here, the anthropogenic emissions are kept constant. However VOC 's also have biogenic emitters, which can alter their emissions due to changes in meteorology in this experiment. The only natural VOC emitter included in the DEHM-REGINA model is isoprene (cf. figure 6.20) and it was found that isoprene increases everywhere over land due to the temperature increase and this can explain the increase in ozone

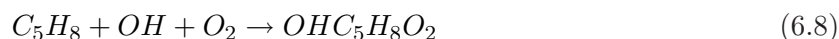
In figure 6.6 it was found, that the specific humidity was increasing in the whole hemisphere. Increasing temperature results in an increasing humidity and thereby an increasing number of H_2O molecules in the atmosphere. When ozone already are present, more H_2O molecules will lead to more hydroxyl radicals (OH) through the process shown in the reaction scheme (6.7) below



With the DEHM-REGINA simulation it was predicted that the temperature, specific humidity and ozone concentration (only north of approximately 30°N) will increase from the 1990's and to the 2090's. By the reaction scheme (cf. 6.7 these observed increases must lead to an increase in the number of hydroxyl radicals. In figure 6.18 and 6.19 the concentration of these hydroxyl radicals are shown. The predicted increase by the reasoning above are confirmed from the concentrations plots of the two layers (cf figure 6.18 and figure 6.19). However in the difference plot of figure 6.18 and figure 6.19 it became evident that the OH concentrations

in the surface layer are increasing over sea and decreasing over land. In connection to the discussion above, it is easy to jump to the conclusion that the future temperature increase leads to an enhanced humidity increase over the maritime areas, which again results in more hydroxyl radicals due to more water molecules. However inspecting the plot of the predicted specific humidity reveals that the increase in humidity is much more latitudinal dependent and there are no similarities between the specific humidity figure and the OH concentration predictions.

This finding of a very sharp discontinuity between the terrestrial and the maritime concentration of hydroxyl radicals leads to the possible connection of the isoprene concentration (cf. figure 6.20). As mentioned earlier isoprene emissions are only present over land and the concentration of isoprene is confined to the source areas, because of a very short chemical lifetime. The reaction 6.8 below reveals that isoprene consumes hydroxyl radicals. In the DEHM-REGINA model this is the only chemical reaction included, where OH radicals are removed from the atmosphere by isoprene. Besides isoprene a great number of other chemical species reacts with the hydroxyl radical and remove it from the atmosphere, however the observed concentration of isoprene over land (cf. figure 6.20) seems to be the dominating OH -sink in this experiment near the land surface.



By the observed general increase in the ozone, it can be concluded that the DEHM-REGINA simulation used here, predicts an increase of a great number of chemical reactions over sea and at higher altitudes due to the resulting increase in hydroxyl radicals (cf. eq. 6.7). Since hydroxyl radicals are a very important agent in a great number of chemical reactions, an increase in the number of hydroxyl radicals must necessarily lead to an increase in the number of chemical reactions taken place and this will have a great influence on the lifetimes of many chemical species. As an example the lifetime of nitrogen dioxide will be reduced and lead to an increased level in nitrate NO_3 and nitric acid (HNO_3). Also the sulphate production through the conversion of sulphur will increase and so on with many other chemical reactions.

The study here leads to a new interesting hypothesis; the sulphur to sulphate reaction rate will increase in the future due to increased OH concentrations. Again further sensitivity studies are needed in order to determine the sizes of the individual processes affecting this transformation rates and to quantify the reduced lifetimes. In the DEHM-REGINA model a great number of chemical reactions are going on. These many processes can confuse the picture if one solely wishes to study the transport and conversion of two species like sulphur and sulphate.

The DEHM-REGINA model is also made in a much simpler version, where only the sulphur chemistry is included. Since the concentration of OH radical are not included in this simple model version another parametrization of the chemical lifetime of sulphur is needed. In this case here the lifetime of sulphur is parameterized solely as a function of the sun angle [Christensen, 1997]. The lack of OH chemistry in this sulphur version of the DEHM model makes it a good tool for analyzing changes in atmospheric transport pathways of sulphur and sulphate.

Alternatively if one wishes to study the transport alone a tracer study could be carried out. In the definition of a tracer lies the fact that it is a chemically specie, which do not react

chemically with other species. This feature makes tracer models very suitable for transport pathways studies.

Another interesting result of the analysis carried out here is the fact that the concentration of SO_4 increases over the Arctic metal industry city, Norilsk, even though the surroundings of Norilsk is characterized by a general decrease. The general observed decrease in sulphate concentration over Siberia can be explained by an increase in wet deposition due to an increase in precipitation over the area. In figure 6.10(c) and 6.10(d) it is clear that the concentration level of SO_2 is significantly decreasing and SO_4 is significantly increasing over the city of Norilsk. This means that the increase in SO_4 concentration do not originate from an increase in the concentration SO_2 . However since it is observed, that there will be more free OH^- radicals in the future, it could be concluded, that more of the present SO_2 will transform into SO_4 and thereby increasing the SO_4 concentration and decreasing the SO_2 concentration in the future.

Inspecting (c) in figure 6.12 some changes in the wet deposition of SO_4 is shown, however subplot 6.12(d) reveals that none of these changes are significant. This results from the characteristics of precipitation. Precipitation is a highly fluctuating on/off process, which in this statistical connection introduces a low signal-to-noise ratio. This suggest, that all the changes in wet deposition of SO_4 are rather a result of a great amount of noise connected to the intermittent precipitation process, than an expression of insignificant changes in the wet deposition of SO_4 !

From both figure 6.10 and 6.11 it is seen that Denmark lies just at the border between positive and negative changes in concentration levels of SO_2 and SO_4 . In northern Europe the concentrations of SO_2 and SO_4 are decreasing and in southern Europe the same concentrations are increasing. The wet deposition is of course highly dependent on the precipitation rate and the feature described above is the same as what was found in the analysis of the precipitation frequency.

Over the Aleutian islands the concentration of sea salt is increasing. This increase originates from a increase in wind speed in this area. In the DEHM-REGINA model the parametrization of sea salt only dependents on the wind speed, so even though the wind speed (figure 6.5) shows a relatively small changes this must be the explanation to the observed changes in sea salt concentration. In the parametrization of sea salt, the sea salt concentration is proportional to the third root of the wind speed which inherently will amplify even very small changes in wind speed when calculating the sea salt concentration. The observed increase in sea salt over the Aleutian islands can explain the observed increase in PM_{10} , which could not be explained by an increase in secondary inorganic aerosols.

Another contribution to the increased sea salt content of the atmosphere over the area of the Aleutian could be found in the changes in mixing height. From figure 6.7 it can be seen that the mixing height is decreasing in the area, which means that the dispersed sea spray particles have less air to mix in and therefore the concentration is very likely to increase.

Also sea ice (6.9) is an interesting parameter concerning this local increase in sea salt content of the air. It is found that the sea ice cover is retreating in the area due to the temperature increase. Melting of sea ice can have a little effect on the sea salt content of the above lying air masses, since the sea salt can increase in the air due to more open waters, when the sea ice melts. In nature melting of sea ice leads to release of fresh water making the ocean less saline, which obviously also will affect the amount of sea spray particles in the above lying

air, however this effect is not included in the parametrization in the DEHM-REGINA model and therefore can not contribute to the conclusions drawn here.

In summary it can be concluded, that the increasing sea salt content of the air is due to changes in wind, however through indirect effects also mixing height and more open waters can contribute to the observed increase in sea salt content. To estimate the size of the individual effects of each parameters, is impossible by this experiment. To investigate this subject further, it would probably be more convenient to run a climate model like ECHAM4-OPYC3 including a sea spray particle module in order to include the salinity of ocean model in the parameterizations.

The natural emitted VOC, isoprene is a strong ozone precursor. In figure 6.20 it was found that the isoprene concentration were increasing everywhere over the terrestrial areas. Trees and bushes are typical isoprene emitters and therefore the emission of isoprene only takes place over land. The projected observed level of isoprene will alter the ozone production in a positive direction and thereby enhancing the ozone level.

Langner et al. [2005] used the regional chemistry/transport/deposition model MATCH to simulate the distribution of surface ozone in the future. The Rossby Centre regional Atmospheric climate model (RCA) version 1 provided the projected meteorology in these simulations. Langner et al. [2005] found a general increase in the surface ozone concentration over southern and Central Europe. They calculated the domain-total emission of isoprene to increase with 59% due to the predicted temperature increase in the case where the ECHAM4-OPYC3 model was used as boundary condition for the RCA regional climate model (the increase was 47% in the case where the HAdCM2 model was used as boundary conditions [Johns et al., 1997]). This is generally consistent with the results found in this thesis. However, Langner et al. [2005] also found a decrease in surface ozone in northern Europe. In contrast, it was found in this study that there was a smaller increase in surface ozone over southern and central part of Scandinavia.

Langner et al. [2005] states that the predicted changes found in surface ozone concentrations are substantial and if the climate scenario (IPCC, IS92a) are representative for the future climate, the increase in surface ozone due to the predicted warming would be significant compared to the expected reductions resulting from the emission reduction protocols currently in force.

Tuovinen et al. [2002] have made a sensitivity analysis of which factors will effect the surface ozone concentration in Europe. They found that the increased biogenic VOC emissions significantly will counteract the effects of reduced anthropogenic emissions.

As stated in section 3.1 the model also includes annual mean flux corrections for heat and fresh water which unfortunately introduces a warm bias of approximately 0.3 Kelvin in the resulting output data. In relations to the temperature dependency of the natural VOC's in the DEHM-REGINA model, this bias introduce an overprediction of the isoprenes and thereby also an overprediction of the surface ozone concentration. However compared to a predicted general temperature increase of 2-3 Kelvin (locally up to 11 Kelvin) the bias of 0.3 Kelvin is relatively small and therefore not expected to change the results found here significantly.

In parallel with this master thesis work Murazaki and Hess [2006] have carried out similar experiments for the same time periods with the global chemical transport model MOZART-2. As input meteorology they used results from the National Center for Atmospheric Research (NCAR) coupled Climate System Model (CSM) 1.0 forced with the IPCC A1 scenario [Na-

kicenovic et al., 2000]. Substantially different from the simulations carried for this thesis, Murazaki and Hess [2006] kept both the anthropogenic and biogenic emissions constant [Personal e-mail correspondence with P. Hess, 2006]. On the contrary only the anthropogenic emissions were kept constant in the simulations carried out here. The biogenic emitters in the DEHM-REGINA model consist solely of isoprene. The concentration of isoprene is highly dependent on temperature in the parametrization of isoprene in the DEHM-REGINA model. Murazaki and Hess [2006] concludes: "Overall, the change in background ozone can be viewed as a competition between increased ozone production over high-emission regions combined with a shorter ozone lifetime in travel across remote regions. The net effect is a decrease in background level of ozone over the United States". Here Murazaki and Hess [2006] have divided the surface ozone into two contributions; the local produced ozone and the background ozone. In the high emission areas the local increase in ozone is expected to exceed the decrease in background ozone resulting in a net increase. On the contrary a net decrease in ozone are predicted away from these high-emission zones. In this work the ozone concentration is predicted to increase all over the United States. This difference relative to results of Murazaki and Hess [2006] is due to their lack of the temperature dependent biogenic emissions. These emitters are as earlier mentioned ozone precursors and by the results of this thesis they contributes with a relatively large increase in ozone concentration over land (where the emitters are present).

Johnson et al. [2001] found that the impact of climate change decreases the net production of ozone with approximately 120 Tg/yr in the troposphere. However Johnson did not include the climate change effect on the natural VOC emitters. This means that the effect from isoprene on the ozone production found in this work is not included in the results of Johnson et al. [2001]. In the DEHM-REGINA model the process which Johnson et al. [2001] addresses the loss of ozone production to $(O(^1D)+H_2O \rightarrow 2OH)$ is included. This means that the results found here includes both effects and the result is clear: The net ozone production is predicted to increase in the future due to climate change..

7 Summary, conclusions and future perspectives

A three dimensional chemical long-range transport model has been used to simulate the air pollution in the three decades 1990's, 2040's and 2090's. The input meteorology has been provided by the atmosphere-ocean general circulation model ECHAM4-OPYC3 which has been forced with the IPCC A2 emission scenario. This model setup has been validated against simulations based on MM5 meteorology and against observations from the EMEP measuring network in Europe. The predicted results for the future decades has been evaluated with respect to meteorology and the levels and distributions of some important chemical species have been analyzed.

One of the main goals of this thesis was to test if it was possible at all to run a chemical long-range transport model on climate data and thereby receive reliable results of the future air pollution distribution and levels due to climate change. If this objective could be fulfilled and documented, the next step was to analyze some chemical species with respect to changes in concentration level and distribution in the future century due to climate change.

7.1 Summary and conclusions

The period 1990-1999 were used as a control and validation period. The long-range chemical transport model DEHM-REGINA were used with climatic meteorology from the atmosphere-ocean general circulation model ECHAM4-OPYC3 to do four simulations. Three of these simulations with preserved emissions were carried out in order to identify the impacts of climate change on air pollution levels and distribution in the next century and one simulation with variable emissions from the period 1990-1999 were used in the evaluation of the model setup. Furthermore a simulation with MM5 meteorology as input to the DEHM-REGINA model (known performance) and variable 1990-1999 emissions has been used in the validation.

In the following it was assumed that: "The atmosphere-ocean general circulation model ECHAM4-OPYC3 is able to provide a realistic and consistent picture of the meteorological key parameters applied in the air pollution model"

Several statistical evaluations methods has been performed. The climate model (ECHAM4-OPYC3) fails of course to predict the exact timing of the various meteorological parameters and this feature is reflected in the output of the DEHM-REGINA model. The precipitation in a climate model is statistical and therefore it cannot be expected of the ECHAM4-OPYC3 model to time e.g. the precipitation events correctly and this influences the resulting wet

depositions and concentrations in the air. However, averaging over a long period this feature becomes insignificant.

The data from the test period has been evaluated with the ranking method. Here the DEHM-REGINA model setup with ECHAM4-OPYC3 meteorology has been tested against a simulation based on MM5 meteorology and against observations. The DEHM-REGINA model setup predicts the mean level of most of the selected chemical species right and in many cases the simulation based climatic weather suites the mean levels even better than the simulation based on weather forecast data (MM5 setup). In conclusion, the overall performance of the model results based on ECHAM4-OPYC3 meteorology has similar performance as the MM5 setup and both model setups simulates the observational data acceptable well with respect to annual mean values and seasonal variation. The performance of the MM5 - DEHM-REGINA is known to be good from earlier studies. Therefore it can be concluded that: Running a chemical long-range transport model on data from a "free run" climate model like the ECHAM4-OPYC3 is scientifically sound!

From analysis of the data of three future decades (1990's 2040's and 2090's) it was found that the tendency for the selected chemical species is the same between all three decades, when evaluation solely takes place in the sites where the EMEP stations are present. It was concluded that it is reasonable to discard the 2040's decade in the further analysis.

The total hemisphere has been analyzed with respect to meteorology and concentration, wet and dry deposition of some selected species. By comparison of the meteorological results from ECHAM4-OPYC3 it was found that the temperature increase was the dominating impact factor in these studies. The temperature increase resulted in an increase in the biogenic emissions of isoprene. Isoprene is a strong ozone precursor and the ozone production are observed to increase significantly. Secondly this increase in ozone together with an increase in specific humidity was found to increase the chemical reaction rate of a great number of chemical reactions. The humidity and ozone increase resulted in a increase in the number hydroxyl radicals, which are the activating agent in many chemical processes. For example an indication of an enhanced sulphur to sulphate conversion was found and decreased lifetimes of SO_2 , NH_3 and NO_2 was observed.

This study is only the beginning of a accelerating research field with respect to the impacts of climate change on air pollution. From the work of this thesis the main conclusions are that it is scientifically sound to run chemical transport model on climate data and that the temperature increase predicted by a great number of climate models seems to have dominating effect on the future air pollution levels and distributions. Therefore the objectives of this work has been fulfilled. However, most importantly the work of this thesis have created a wide range of new hypothesis which will be very interesting to study and to test in the future.

7.2 Future perspectives

This study is based on climate data from the ECHAM4-OPYC3 atmosphere-ocean general circulation model. The simulation used has been forced with the IPCC A2 scenario. IPCC has proposed a wide range of scenarios, since nobody can be sure what the future will bring. It could be interesting to make a whole range of simulations with the DEHM-REGINA chemical transport model based on meteorology, which were forced with the different IPCC emission scenarios. A study like this will create an understanding of the resulting variety of air pollution

distributions and levels as a result of the impact of climate change due to the different scenarios.

In order to understand and quantify the effects on the different air pollutants from a single meteorological parameter, a large amount of sensitivity studies are needed. For example, it can be hypothesized that climate change will have a large influence on the typical atmospheric transport patterns. In this thesis it was found that the signal from a projected temperature increase is so strong that the signal from e.g. a change in transport patterns has been difficult to distinguish from other important processes in the model results. Therefore, it is necessary in the future to carry out a great number of sensitivity studies where all parameters are kept constant except the parameter under examination. In this way it will be possible to test the effect of the meteorological parameters separately and hereby get an idea of the sign and size of the various effects.

In this thesis the contribution from the biogenic VOC emitters due to temperature increase are documented to be very significant. Today the parametrization of the natural VOC emitters are relatively simple and is only including isoprene. Terpenes is another VOCs, which is known to be released from biogenic sources as a function of temperature. The temperature dependent natural VOC emissions is composed of many contributions. Isoprene is known to produce ozone in contrast to terpenes, which are acting as a loss term for ozone. Also NO_x is a significant ozone precursor, which are emitted naturally from soil and from lightning. Therefore NO_x is very likely to change due to climate change and should be included in an improvement of the natural emissions in the model.

Finally the experiments carried out in this thesis has been time-sliced in order to save computing time. In a future study it might be feasible to do the simulations in one continuous run in order to identify any possible fluctuations within the century. Another initiative could be to integrate data from a regional climate model like e.g. HIRHAM [Hesselbjerg Christensen et al., 1996] and thereby only simulate one of the smaller domains of DEHM-REGINA by running it in nested mode. This regional experiment would result in having relatively high resolution data over a limited area like e.g. Europe.

There is no doubt that the ultimate challenge here will be a two-way coupling of the chemical transport model and the climate model. This would enable the air pollution impacts to feedback on the climate, thereby creating a much more realistic simulation of the total climate-air pollutant system. Furthermore it would be interesting to run the system with future emission reduction scenarios in order to quantify the impacts from climate change vs. the impacts from the emission reductions.

A huge number of suggestions for future work exist and there is now doubt that this branch of combined climate change and air pollution research will grow. This research will inherently contribute with decisive knowledge to the policy makers in the future.

8 Acknowledgement

This project has been a successful project towards more multi-institute research between the National Environmental research Institute (NERI) and the Danish Meteorological Institute (DMI). The modelling work has been performed at the National Environmental Research Institute with supervising of Jørgen Brandt and Jesper H. Christensen (NERI). The climate data has been provided by the Danish Meteorological Institute with help from Eigil Kaas, Martin Stendel (DMI) and Ole B. Christensen (DMI).

Many people has been involved in the project and contributed with their knowledge and practical advice. First I like to pay a very special thank to my external supervisor Jørgen Brandt (NERI) for supporting, teaching and advising me through this master thesis work. A special thank for being patient despite the long extension of my work due to my family loss and gain. Also I like to thank my bonus-supervisor Jesper H. Christensen (NERI) for supporting me with his knowledge through all the computer crises and for being the "chemistry detective".

I would like to thank my formal supervisor at the university Aksel Walløe Hansen for guiding me through this work and supporting me with his knowledge within the field of climate modelling. A special thanks is payed to Martin Stendel (DMI) and Ole Bøssing Christensen (DMI) for helping me out with the ECHAM4-OPYC3 data. Also Eigil Kaas is thanked for his help during this project. Lise M. Frohn, Camilla Geels, Carsten Ambelas Skøjth and Kaj M. Hansen are acknowledged for providing me with their experience and with knowledge. A special thank to Lise M. Frohn for supporting me and helping with the transport of data during my maternity leave.

Bibliography

- AMAP (2006). Amap assessment 2006: Acidifying pollutants, arctic haze, and acidification in the arctic. Scientific report, AMAP. in press.
- Andersson, C., Langner, J., and Bergström, R. (2006). Inter-annual variation and trends in air pollution over europe due to climate variability during 1958-2001 simulated with a regional ctm coupled to the era40 reanalysis. *Tellus B*, in press.
- Bach, H., Andersen, M., Illerup, J., Møller, F., Birr-Pedersen, K., Brandt, J., Ellermann, T., Frohn, L. M., Hansen, K. M., Jensen, F. P., and Seested, J. (2006). Vurdering af de samfundsøkonomiske konsekvenser af kommissionens temastrategi om luftforurening. Dmu rapport, DMU.
- Bartnicki, J. (1989). A simple filtering procedure for removing negative values from numerical solutions of the advection equation. *Environmental Software*, 4(4):187–201.
- Berkowicz, R. and Olsen, H. R. (1990). Modelling the internal boundary layer at a coastal site. In *Ninth Symposium on turbulence and diffusion*, National Environmental Research Institute, Denmark. NERI.
- Boville, B. and Gent, P. (1988). The NCAR Climate System Model, version 1. *Journal of Climate*, 11(6).
- Brandt, J. (1994). En analyse af klimamålinger. Master’s thesis, University of Copenhagen, Risø National Laboratory.
- Brandt, J. (1998). *Modelling Transport, Dispersion and Deposition of Passive Tracers from Accidental Releases*. PhD thesis, University of Copenhagen, National Environmental Research Institute and Risø National Laboratory.
- Brandt, J., Christensen, J. H., Frohn, L. M., and Berkowicz, R. (2001a). Operational air pollution forecasts from regional scale to urban street scale. part 1: System description. *Physics and Chemistry of the Earth Part B*, 26(10):781–786. Elsevier Science Ltd.
- Brandt, J., Christensen, J. H., Frohn, L. M., and Berkowicz, R. (2001b). Operational air pollution forecasts from regional scale to urban street scale. part 2: Performance evaluation. *Physics and Chemistry of the Earth Part B*, 26(10):825–830. Elsevier Science Ltd.
- Brandt, J., Christensen, J. H., Frohn, L. M., Berkowicz, R., and Palmgren, F. (2000). The dmu-atmi thor air pollution forecast system: System description. Tech. Rep. 321, NERI, available at www.dmu.dk.

- Brandt, J., Christensen, J. H., Frohn, L. M., Berkowicz, R., Skjøth, C., Geels, C., Hansen, K., Frydendall, J., Hedegaard, G., Hertel, O., Jensen, S., Hvidberg, M., Ketzel, M., Olesen, H., Løfstrøm, P., and Zlatev, Z. (2005). THOR -an operational and integrated model system for air pollution forecasting and management from global to local scale. In *Proceedings from the First ACCENT Symposium*, page pp. 6, Urbino, Italy.
- Brasseur, G. P. and Madronich, S. (1992). *Climate System Modelling*, chapter 15: Chemistry-transport models. Cambridge University Press.
- Charney, J. G., Fjordtøft, R., and von Neumann, J. (1950). Numerical integration of the barotropic vorticity equation. *Tellus*, 2:237–254.
- Christensen, J. H. (1993). Testing advection schemes in a three-dimensional air pollution model. *Mathematical and Computational Modelling*, 18(2):75–88.
- Christensen, J. H. (1995). *Transport of Air Pollution in the Troposphere to the Arctic*. PhD thesis, Department of Environment and Research, NERI.
- Christensen, J. H. (1997). The Danish Eulerian Hemispheric Model - A three-dimensional air pollution model used for the Arctic. *Atmospheric Environment*, 31(24):4169–4191.
- Christensen, J. H., Brandt, J., Frohn, L. M., and Skov, H. (2004). Modelling of mercury in the arctic with the danish eulerian hemispheric model. *Atmospheric Chemistry and Physics*, 4:2251–2257.
- Cubasch, U., Heger, G., Hellbach, A., Höck, H., Mikolajewicz, U., Santer, B., and Voss, R. (1995). A climate change simulation starting from 1935. *Climate Dynamics*, 11(2):71–84.
- Ebel, A., Memmesheimer, M., Jakobs, H., Kessler, C., Piekorz, G., and Weber, M. (2001). Simulation of photochemical smog episodes in europe using nesting techniques and different model evaluation approaches. *Air Pollution Modeling and its Application*, pages 145–153.
- Forester, C. (1977). Higher order monotonic convective difference schemes. *Journal of Computational Physics*, 23:1–22.
- Fouquart, Y. and Bonnel, B. (1980). Computations of solar heating of the earth’s atmosphere: A new parametrization. *Beitr. Phys. Atmos.*, 53:35–62.
- Frohn, L. M. (2004). *A study of long-term high-resolution air pollution modelling*. PhD thesis, University of Copenhagen and National Environmental Research Institute.
- Frohn, L. M., Christensen, J. H., and Brandt, J. (2002a). Development and testing of numerical methods for two-way nested air pollution modelling. *Physics and Chemistry of the Earth*, 27:1487–1494.
- Frohn, L. M., Christensen, J. H., and Brandt, J. (2002b). Development of a High-Resolution Nested Air Pollution Model. The Numerical Approach. *Journal of Computational Physics*, 179(1).
- Frohn, L. M., Christensen, J. H., Brandt, J., Geels, C., and Hansen, K. (2003). Validation of a 3-D hemispheric nested air pollution model. *Atmospheric Chemistry and Physics*, 3:3543–3588.

- Geels, C. (2003). *Simulating the Current CO₂ Content of the atmosphere: Including Surface Fluxes and Transport Across the Northern Hemisphere*. PhD thesis, University of Copenhagen, NBI.
- Geels, C., Brandt, J., Christensen, J. H., Frohn, L. M., Hansen, K. M., and Skjøth, C. A. (2004). Long-term calculations with a comprehensive nested hemispheric air pollution transport model. In *Proceedings from the First ACCENT Symposium*, pages 185–196, Borovetz, Bulgaria. NATO ARW workshop, Springer.
- Graedel, T., Bates, T., Bouwman, A., Cunnold, D., Dignon, J., Fung, I., Jacob, D., Lamb, B., Logan, J., Marland, G., Middleton, P., Pacyna, J., Placet, M., and Veldt, C. (1993). A compilation of inventories of emissions to the atmosphere. *Global Biogeochem. Cycl.*, 7:1–26.
- Grell, G., Dudhia, J., and Stauffer, D. (1995). A Description of the Fifth-Generation Penn State/NCAR Mesoscale Model (MM5). NCAR Technical Note NCAR/TN-398+STR, Mesoscale and Microscale Meteorology Division. National Center for Atmospheric Research (NCAR), Boulder, Colorado. 122.
- Gryning, S. and Batchvarova, E. (1990). Analytical model for the growth of the coastal internal boundary layer during onshore flow. *Quarterly Journal of Meteorological Society*, 116:187–203.
- Guenther, A., Hewitt, C., Erickson, D., Fall, R., Geron, C., Graedel, T., Harley, P., Klinger, L., Lerdau, M., McKay, W., Pierce, T., Scholes, B., Steinbrecher, R., Tallamraju, R., Taylor, J., and Zimmerman, P. (1995). A global-model of natural volatile organic-compound emissions. *Journal of Geophysical Research*, 100 -Atmosphere:8873–8892.
- Hansen, K. (2006). *Transport of persistent organic pollutants into the Arctic*. PhD thesis, University of Copenhagen.
- Hansen, K., Christensen, J. H., Brandt, J., Frohn, L. M., and Geels, C. (2004). Modelling atmospheric transport of a α -hexachlorocyclohexane in the northern hemisphere with a 3-d dynamic model: Dehm-pop. *Atmospheric Chemistry and Physics*, 4:pp.1–13.
- Hertel, O., Berkowicz, R., Christensen, J., and Ø. Hov (1993). Test of two numerical schemes for use in atmospheric transport-chemistry models. *Atmospheric Environment*, 27A(16):2591–2611.
- Hesselbjerg Christensen, J., Christensen, O., Lopez, P., Meijgaard, E., and Botzet, M. (1996). The HIRHAM4 Regional Atmospheric Climate Model. Scientific Report 96-4, Danish Meteorological Institute, Copenhagen.
- Hjellbrekke, A. (2000). EMEP Co-operative Programme for Monitoring and Evaluation of the Long-range Transmission of Air Pollutants in Europe. Data report 1998, part 1: Annual summaries. EMEP/CCC-Report 3, EMEP.
- Hogrefe, C., Lynn, B., Civerolo, K., Ku, J.-Y., Rosenthal, J., Rosenzweig, C., Goldberg, R., Gaffin, S., Knowlton, K., and Kinney, P. (2004). Simulating changes in regional air pollution over the eastern United States due to changes in global and regional climate and emissions. *Journal of Geophysical Research*, 109:D22301, doi 10.1029/2004JD004690.

- Holton, J. (1992). *An introduction to Dynamic Meteorology*. Academic Press, third edition edition.
- Horowitz, L. (2003). Global simulation of tropospheric ozone related tracers: Description and evaluation of MOZART, version 2. *Journal of Geophysical Research*, 108:4784, doi:10.1029/2002JD002853.
- Houghton (2001). *Climate Change 2001: The Scientific Basis*. Cambridge University Press.
- Johns, T., Carnell, R., Crossley, J., Gregory, J., Mitchell, J., Senior, C., Tett, S., and Wood, R. (1997). The second hadley centre coupled ocean atmosphere gcm : model description, spinup and validation. *Climate dynamics*, 13(2):103–134.
- Johnson, C., Stevenson, D., Collins, W., and Derwent, R. (2001). Role of climate feedback on methane and ozone studied with a coupled ocean-atmosphere-chemistry model. *Geophysical Research Letter*, 28(9).
- Lambert, S. J. and Boer, G. (2001). Cmpi1 evaluation and intercomparison of coupled climate models. *Climate Dynamics*, (17):83–106.
- Langner, J., Bergström, R., and Foltescu, V. (2005). Impact of climate change on surface ozone and deposition of sulphur and nitrogen in Europe. *Atmospheric Environment*, 39:1129–1141.
- Mallet, V. and Sportisse, B. (2004). 3-d chemistry-transport model polair3d: numerical issues, validation and automatic-differentiation strategy. *Atmos. Chem. Phys.*, (Disc. 4):1371–1392.
- Malmberg, A. (1985). *Erlang S Statistiske tabeller*, volume 5. G E C GAD København.
- McGuffie, K. and Henderson-Sellers, A. (2001). Forty years of numerical climate modelling. *International Journal of Climatology*, 21:1067–1109.
- McRae, G., Goodin, W., and Seinfeld, J. (1984). Numerical solution of the atmospheric diffusion equations for chemical reacting flows. *Journal of Computational Physics*, 45:1–42.
- Meehl, A., Boer, J., Covey, C., Latif, M., and Stouffer, R. (2000). Meeting summary, the coupled model intercomparison project (cmip).
- Morcrette, J., Smith, L., and Fouquart, Y. (1986). Pressure and temperature dependence of the absorption in longwave radiation parameterizations. *Beitr. Phys. Atmos.*, 59:455–469.
- Mosca, S., Graziniani, G., Klug, W., Bellasio, R., and Bianconi, R. (1997). ATMES-II Evaluation of Long-range dispersion models using 1st ETEX release data. 2. Draft report VOL. 1 and VOL. 2, ETEX Symposium on Long-range Atmospheric Transport, Model Verification and Emergency Response, Vienna.
- Murazaki, K. and Hess, P. (2006). How does climate change contribute to surface ozone change over the united states. *Journal of Geophysical Research*, 111.
- Nakicenovic, N., Alcamo, J., Davis, G., de Vries, B., Fenham, J., Gaffin, S., Gregory, K., Grübler, A., Jung, T., Kram, T., Rovere, E. L., Michaelis, L., Mori, S., Morita, T., Pepper, W., Pitcher, H., Price, L., Riahi, K., Roehrl, A., Rogner, H.-H., Sankovski, A., Schlesinger,

- M., Shukla, P., Smith, S., Swart, R., van Rooijen, S., Victor, N., and Dadi, Z. (2000). *Special Report on Emission Scenarios*. Cambridge University Press.
- Nikovic, S., Mihailovic, D., Rajkovic, B., and Papadopoulos, A. (1998). The weather forecasting system SKIRON. Description of the model VOL 2, Athens.
- Oberhuber, J. (1993). Simulation of the atlantic circulation with a coupled sea ice-mixed layer-isopycnal general circulation model. part 1:model description. *Journal Physical Oceanography*, 23:808–829.
- Olivier, J., Bouwman, A., van der Maas, C., Berdowski, J., Veldt, C., Bloos, J., Visschedijk, A., Zandveld, P., and Haverlag, J. (1996). Description of EDGAR Version 2.0: A set of global emission inventories of greenhouse gases and ozone-depleting substances for all anthropogenic and most natural sources on a per country basis and on 1 degree x 1 degree grid. RIVM report, TNO MEP report R96/119, RIVM, Bilthoven.
- Pepper, D., Kern, C., and Long, J. P. (1979). Modelling the dispersion of atmospheric pollution using cubic splines and chapeau functions. *Atmospheric Environment*, 13:223–237.
- Peters, L., Berkowitz, C., Carmichael, G., Easter, R., Fairweather, G., Ghan, S., Hales, J., Leung, L., Pennell, W., Potra, F., Saylor, R., and Tsang, T. (1995). The current state and future direction of eulerian models in simulating the tropospheric chemistry and transport of trace species: a review. *Atmospheric Environment*, 29(2):189–222.
- Prather, M. and Ehhalt, D. (2001). *Climate Change 2001: The Scientific Basis*, chapter 4:Atmospheric Chemistry and Greenhouse Gases. Cambridge University Press.
- Prather, M., Gauss, M., Berntsen, T., Isaksen, I., Sundet, J., Bey, I., Brasseur, G., Dentener, F., Derwent, R., Stevenson, D., Grenfell, L., Hauglustaine, D., Horowitz, L., Jacob, D., Mickley, L., Lawrence, M., von Kuhlmann, R., Muller, J.-F., Pitari, G., Rogers, H., Johnson, M., Pyle, J., Law, K., van Weele, M., and Wild, O. (2003). Fresh air in the 21st century. *Geophysical Research Letters*, 30(2):1100.
- Richardson, L. F. (1922). *Weather prediction by numerical process*. Cambridge University Press. reprinted Dover, 1965.
- Roeckner, E., Arpe, K., Bengtsson, L., Christoph, M., Clausen, M., Dümenil, L., Giorgetta, M., Schlese, U., and Schulzweida, U. (1996). The atmospheric general circulation model ECHAM-4: Model description and simulation of present-day climate. Technical Report 218, Max-Planck-Institut für Meteorologie.
- Roeckner, E., Bengtsson, L., and Feichter, J. (1999). Transient climate change simulations with a coupled atmosphere-ocean GCM including the tropospheric sulfur cycle. *Journal of Climate*, 12:3004–3032.
- Roelofs, G. and Lelieveld, J. (1995). Distribution and budget of o_3 in the troposphere calculated with a chemistry general circulation model. *Journal of Geoph. Research*, 100:20983–20998.

- Schaap, M., Timmermans, R., Roemer, M., Boersen, G., and Builtjes, P. J. (2005). The LOTUS-EUROS model: description, validation and latest developments. *Int. J. Environment and Pollution*, in press.
- Schmidt, H., Derognat, C., Vautard, R., and Beekmann, M. (2001). A comparison of simulated and observed ozone mixing ratios for the summer of 1998 in western europe. *Atmospheric Environment*, (36):6277–6297.
- Seinfeld, J. H. and Pandis, S. N. (1998). *Atmospheric Chemistry and Physics*. John Wiley and Sons, Inc.
- Simpson, D., Fagerli, H., Jonson, J., Tsyro, S., and Wind, P. (2003). Transboundary Acidification, Eutrophication and Ground Level Ozone in Europe, Part 1. Technical report, Norwegian Meteorological Institute, available at www.emep.int.
- Smagorinsky, J., Manabe, S., and Holloway, J. (1965). Results from a nine-level general circulation model of the atmosphere. *Monthly Weather Review*, (93):727–768.
- Spiegel, M. R. (1992). *Theory and problems of Statistics, 2. edition*. Shaum's Outline Series, McGraw-Hill.
- Stendel, M., Schmidt, T., Roeckner, E., and Cubasch, U. (2002). The climate of the 21'st century: Transient simulations with a coupled atmosphere-ocean circulation model. Technical Report 02-1, Danish climate center.
- Stern, R., Yamartino, R., and Graff, A. (2003). Dispersion modelling within the european Community's air quality directives: Long term modelling of o3, pm10 and no2. In *26th ITM on Air Pollution Modelling and its Application*, Istanbul, Turkey.
- Taylor, J. (1997). *An Introduction to Error Analysis - The Study of Uncertainties in Physical Measurements*. University Science Books, Sausalito, California, second edition.
- Tilmes, S., Brandt, J., Flatøy, F., Bergström, R., Flemming, J., Langner, J., Christensen, J. H., Frohn, L. M., Ø. Hov, Jacobsen, I., Reimer, E., Stern, R., and Zimmermann, J. (2002). Comparison of Five Eulerian Air Pollution Forecasting Systems for the Summer of 1999 Using the German Ozone Monitoring Data. *Journal of Atmospheric Chemistry*, 42:91–121.
- Trenberth, K. E., editor (1992). *Climate System Modelling*. Cambridge University Press.
- Tuovinen, J., Simpson, D., Mayerhofer, P., Lindfors, V., and Laurila, T. (2002). Surface ozone exposures in northern europe in changing environmental conditions. In Hjort, J., Raes, F., and Angeletti, G., editors, *A Changing Atmosphere: Proceeding of the Eight European Commission*, AP61. DG Research, Joint Research Centre.
- van Loon, M., Roemer, M., Builtjes, P., Bessagnet, B., Rouill, L., Christensen, J., Brandt, J., Fagerli, H., Tarrason, L., Rodgers, I., R. Stern, Bergström, R., Langner, J., and Foltescu, V. (2004). Model inter-comparison. In the framework of the review of the Unified EMEP model. TNO-report, TNO-MEPO-R 282.

- van Loon, M., Vautard, R., Schaap, M., Bergström, R., Bessagnet, B., Brandt, J., Builtjes, P., Christensen, J., Cuvelier, K., Graff, A., Jonson, J., Krol, M., Langner, J., Roberts, P., Rouil, L., Stern, R., Tarrasón, L., Thunis, P., Vignati, E., White, L., and Wind, P. (2006). Evaluation of long-term ozone simulations from seven regional air quality models and their ensemble average. *Atmospheric Environment*, page pp.28. Accepted August 2006.
- Verwer, J., Blom, J., van Loon, M., and Spee, E. (1996). A comparison of stiff ODE solvers for atmospheric chemistry problems. *Atmospheric Environment*, 30(1):49–56.
- Vestreng, V. (2001). Emission data reported to UNECE/EMEP: Evaluation of the spatial distribution of emission. EMEP/MS-CW Note 1/01, EMEP.
- Williamson, D. and Rasch, P. (1994). Water vapor transport in the NCAR CCM2. *Tellus*, 46A:34–51.
- Zlatev, Z. and Brandt, J. (2005). Impact of Climate Changes in Europe on European pollution levels. *Proceedings from the First ACCENT Symposium, Urbino, Italy*, page 6.

NERI National Environmental Research Institute

DMU Danmarks Miljøundersøgelser

National Environmental Research Institute,
NERI, is a part of
University of Aarhus.

NERI's tasks are primarily to conduct
research, collect data, and give advice
on problems related to the environment
and nature.

At NERI's website www.neri.dk
you'll find information regarding ongoing
research and development projects.

Furthermore the website contains a database
of publications including scientific articles, reports,
conference contributions etc. produced by
NERI staff members.

Further information: www.neri.dk

National Environmental Research Institute
Frederiksborgvej 399
PO Box 358
DK-4000 Roskilde
Denmark
Tel: +45 4630 1200
Fax: +45 4630 1114

Management
Personnel and Economy Secretariat
Monitoring, Advice and Research Secretariat
Department of Policy Analysis
Department of Atmospheric Environment
Department of Marine Ecology
Department of Environmental Chemistry and Microbiology
Department of Arctic Environment

National Environmental Research Institute
Vejløvej 25
PO Box 314
DK-8600 Silkeborg
Denmark
Tel: +45 8920 1400
Fax: +45 8920 1414

Monitoring, Advice and Research Secretariat
Department of Marine Ecology
Department of Terrestrial Ecology
Department of Freshwater Ecology

National Environmental Research Institute
Grenåvej 14, Kalø
DK-8410 Rønde
Denmark
Tel: +45 8920 1700
Fax: +45 8920 1514

Department of Wildlife Ecology and Biodiversity

The fate of a selected number of chemical species is inspected with respect to climate change. The coupled Atmosphere-Ocean General Circulation Model ECHAM4-OPYC3 is providing future meteorology for the Chemical long-range Transport Model DEHM-REGINA. Three selected periods (1990s, 2040s and 2090s) are inspected. The 1990s are used as a control and validation period. In this decade the model results are tested against similar model simulations with MM5 meteorology and against observation from the EMEP monitoring sites in Europe. In the validation the emissions are held constant at the 1990 level in all simulations in order to separate out the effects from climate change. The overall performance of the ECHAM4-OPYC3 setup as meteorological input to the DEHM-REGINA model is acceptable according to the ranking method. It is concluded that running a chemical long-range transport model on data from a "free run" climate model is scientifically sound!

The absolute dominating impact from climate change on a large number of chemical species is found to be the predicted temperature increase. The temperature is by the ECHAM4-OPYC3 model predicted to increase 2-3 Kelvin on a global average with local maxima in the Arctic of 11 Kelvin. As a consequence of this temperature increase, the temperature dependent biogenic emission of isoprene is predicted to increase significantly in concentration over land in the DEHM-REGINA chemistry-transport model. This leads to an increase in the ozone production and in the number of free OH radicals. This again leads to a significant change in the typical life times of many species, since the hydroxyl radicals are participating in a large number of chemical reactions. It is e.g. found that more sulphate will be present in the future over the already polluted areas and this increase can be explained by an enhancement in the conversion of sulphur to sulphate.